UNIVERSITÀ
DEGLI STUDI
FIRENZE

DOTTORATO DI RICERCA IN

SCIENZE DELLA TERRA

CICLO XXXI

COORDINATORE Prof.ssa Lorella Francalanci

Analysis and monitoring of geohazards in cultural heritage sites

Settore Scientifico Disciplinare GEO/05

Dottorando

Dott.ssa Laura Pastonchi

Laura Pastonchi

Tutore

Dott.ssa Veronica Tofani

Veronica Tofani

Coordinatore

Prof.ssa Lorella Francalanci

Anni 2015/2018

Table of contents

Abstract

The traces that humans have left in the world are guarded by historical and cultural heritage, which, for this reason, has an unestimable value. This public good is currently a variegated reality, composed of, e.g, churches, monuments, archaeological sites, natural and industrial landscapes. The importance of this heritage makes its maintenance and its protection particularly onerous and economically expensive. However, the problem of its conservation is not only due to the lack of economic resources, but also to the more and more frequent geohazards caused by the current climate change. Unfortunately, local and government authorities tend to underestimate the effects that such phenomena could have on sites of cultural interest. For example, within the United Nations Educational, Scientific and Cultural Organization (UNESCO) management system, only "sudden geological events" are considered as factors that undermine the protection of World Heritage Sites (WHS), although it is well known that also slow-kinematic phenomena can threaten cultural and natural heritage.

The aim of this thesis has therefore been to promote good cultural heritage management practices through the recent technological innovations and the knowledge of past geological disasters. Among the current technological developments there are remote sensing systems that, if compared to traditional techniques (e.g. inclinometer, total station), allow making investigations to take place without any physical contact with the object of interest (i.e. non-invasiveness). Furthermore, they guarantee a reduction of time needed for data acquisition in wide areas, in addition to a great cost-benefit ratio. Due to these advantages, these technologies have all the characteristics to improve the preservation of cultural heritage. Therefore, both at regional and local scale, three of these innovative systems have been exploited in order to analyze and monitor some geological instabilities.

At regional scale, a procedure based on the satellite Interferometric Synthetic Aperture Radar (InSAR) technique has been proposed in order to identify, characterize and monitor the temporal and spatial evolution of ground deformation related to slow-kinematic geohazards (i.e. slow-moving landslides and ground-subsidences). This operative choice has been done to improve the knowledge of these geohazards within the UNESCO safeguarding system. In fact, the proposed methodology, applied for the first time on the WHS in Tuscany (Italy), simplify the InSAR products interpretation, making them easily exploitable by the local WHS managers for long-term geohazards monitoring and conservation strategies. These activities, thanks to the main

characteristics of the recent Sentinel-1 data (short revisit time, free availability without any restrictions and worldwide coverage), can be defined for each UNESCO site of the world.

At local scale, the joint use of historical research and innovative remote sensing techniques (the latter chosen according to the characteristics of both the cultural site and the investigated phenomenon), has proved to be a productive choice to assess the geological instabilities.

In the case of the landslide that occurred along the Arno artificial riverbank (Florence, Italy) on 25 May 2016, the monitoring through a Ground-Based Synthetic Aperture Radar Interferometry (GBInSAR) system has been essential in managing the emergency that put at risk both the Historic Center of Florence (UNESCO site) and human lives. Furthermore, the historical research has served to reconstruct the dynamics of this disastrous event.

In a second case study, the main geological instability processes localized through a historical research in the cultural site of Canossa (Emilia Romagna Region, Italy), have been analyzed and monitored through a Terrestrial Laser Scanning (TLS) system. This allowed the observation of changes that occurred over time on the cliff and the castle of Canossa and on its surrounding landscape, that are due to the rockfall phenomenon and the badlands evolution.

The aforementioned case studies are intended as examples to show that, currently, the developments in the technology field allow accurate assessments of geological risks that threaten cultural heritage sites, both at regional and local scale.

The results obtained in this thesis are preliminary but they represent a first important step to plan, for example, long-term geohazards monitoring and conservation strategies in order to safeguard this unestimable worldwide heritage.

Riassunto (In italian)

Le tracce che gli uomini hanno lasciato nel mondo sono custodite dal patrimonio storico e culturale, che, per questo motivo, ha un valore inestimabile. Questo bene pubblico è attualmente una realtà variegata, composta, ad esempio, da chiese, monumenti, siti archeologici, paesaggi naturali e industriali. L'importanza di questo patrimonio rende la sua manutenzione e la sua protezione particolarmente onerose ed economicamente costose. Tuttavia, il problema della sua conservazione non è dovuto solo alla mancanza di risorse economiche, ma anche ai sempre più frequenti disastri geologici causati dall'attuale cambiamento climatico. Sfortunatamente, le autorità locali e governative tendono a sottovalutare gli effetti che tali fenomeni potrebbero avere sui siti di interesse culturale. Ad esempio, nell'ambito del sistema di gestione dell'Organizzazione delle Nazioni Unite per l'Educazione, la Scienza e la cultura (UNESCO), solo gli "eventi geologici improvvisi" sono considerati fattori che minano la protezione dei Siti Patrimonio dell'Umanità (WHS), sebbene sia noto che anche i fenomeni a cinematica lenta possono minacciare il patrimonio culturale e naturale.

Lo scopo di questo lavoro di tesi è quindi stato quello di promuovere buone pratiche di gestione del patrimonio culturale attraverso le recenti innovazioni tecnologiche e la conoscenza dei disastri geologici del passato. Tra i recenti sviluppi tecnologici vi sono i sistemi di telerilevamento che, se confrontati con le tecniche tradizionali (ad es. inclinometro, stazione totale), consentono di effettuare indagini senza un contatto fisico con l'oggetto di interesse (cioè non invasività); inoltre, garantiscono una riduzione del tempo necessario per l'acquisizione dei dati in vaste aree, oltre a un ottimo rapporto costi-benefici. Per tutte queste peculiarità, queste tecnologie hanno le caratteristiche per migliorare la conservazione del patrimonio culturale. Pertanto, sia a scala regionale che locale, tre di questi sistemi innovativi sono stati sfruttati al fine di analizzare e monitorare alcune instabilità geologiche.

A scala regionale, è stata proposta una procedura basata sulla tecnica dell'Interferometria Radar satellitare ad Apertura Sintetica (space-borne InSAR) al fine di identificare, caratterizzare e monitorare l'evoluzione temporale e spaziale delle deformazioni del terreno relative ai rischi geologici a cinematica lenta (frane lente e subsidenze). Questa scelta operativa è stata fatta per migliorare la conoscenza di questi rischi all'interno del sistema di salvaguardia dell'UNESCO. Infatti, la metodologia proposta, applicata per la prima volta in questo lavoro ai siti UNESCO della Regione Toscana (Italia), semplifica l'interpretazione dei prodotti InSAR, rendendoli facilmente sfruttabili dai gestori locali dei siti UNESCO per il monitoraggio a lungo termine dei

rischi geologici e per strategie di conservazione. Queste attività, grazie alle principali caratteristiche dei recenti dati Sentinel-1 (tempi di rivisitazione brevi, disponibilità gratuita senza restrizioni e copertura mondiale), possono essere definite per ciascun sito UNESCO del mondo.

A scala locale, l'uso congiunto di ricerche storiche e di tecniche innovative di telerilevamento (queste ultime scelte in base alle caratteristiche del sito culturale e del fenomeno indagato), si è dimostrato una scelta produttiva per valutare le instabilità geologiche.
Nel caso della frana avvenuta lungo un tratto del muraglione d’argine dell'Arno (Firenze, Italia) il 25 maggio 2016, il monitoraggio svolto attraverso un sistema di Interferometria Radar ad Apertura Sintetica basato a terra (GBInSAR) è stato essenziale per gestire l'emergenza che ha messo a rischio sia il centro storico di Firenze (sito UNESCO) che le vite umane. Inoltre, una ricerca storica è servita a ricostruire le dinamiche di questo evento disastroso.
Nel secondo caso, invece, i principali processi di instabilità geologica localizzati attraverso una ricerca storica nel sito culturale di Canossa (Regione Emilia Romagna, Italia), sono stati analizzati e monitorati attraverso il sistema Laser Scanner Terrestre (TLS). Ciò ha permesso di osservare i cambiamenti nel tempo dovuti al fenomeno della caduta massi e all'evoluzione dei calanchi, sia sulla rupe e sul castello di Canossa che sul paesaggio circostante.

I casi di studio citati sono da intendersi come esempi per dimostrare che, attualmente, gli sviluppi nel campo della tecnologia consentono di effettuare valutazioni accurate dei rischi geologici che minacciano i siti del patrimonio culturale, sia a livello regionale che locale.
I risultati ottenuti in questa tesi sono preliminari ma rappresentano un primo passo importante per pianificare, ad esempio, il monitoraggio a lungo termine dei rischi geologici e le strategie di conservazione, al fine di salvaguardare questo patrimonio mondiale inestimabile.

Glossary of frequently-used acronyms

ACRONYMS	MEANING
ADA	Active Deformation Area/s
AP	Active Point
GBInSAR	Ground-Based Synthetic Aperture Radar Interferometry
GIS	Geographic Information System
ICA	Identity Card of ADA
InSAR	Interferometric Synthetic Aperture Radar
LOS	Line Of Sight
OUV	Outstanding Universal Value
PS	Persistent/Permanent Scatterer
PSI	Persistent Scatterer Interferometry
PSInSAR	Permanent Scatterer Interferometry
SAR	Synthetic Aperture Radar
TLS	Terrestrial Laser Scanning
UNESCO	United Nations Educational, Scientific and Cultural Organization
WHL	World Heritage List
WHS	World Heritage Site/s

1. Introduction

1.1 Background

The cultural heritage is the memory of humanity as it represents the exceptional diversity of cultures, religions, and traditions that have coexisted over the centuries in the Planet Earth. The concept of cultural heritage has significantly expanded over the last half-century; previously, only those monuments or buildings that reflected the identity of a community were recognized as cultural property, excluding any relationship with the surrounding landscape. Today, the remarkable changes on the environment due to the ever-increasing interaction with man are evident to everyone. For this reason, the cultural heritage is no longer only made up of historical and cultural buildings, monuments, churches, archaeological sites, and other artifacts created by man in different eras, but it also includes, e.g., natural and industrial landscapes. This variegated heritage, for its inestimable value, is considered as a public good, in the same way as natural heritage. Unfortunately, being a public good, it provides little incentives for consumers and businesses to develop a market. As a result, the resources to manage and safeguard public goods are usually insufficient, as they come mainly from taxation and public program (Navrud and Ready, 2002; Spennemann and Graham, 2007). The lack of economic resources is just one of the negative aspects that affect the cultural heritage sites (Allen, 2016; Kriesi, 2012), because they are everyday exposed to further threats that undermine their integrity: the main ones are urban development, social/cultural uses of heritage (tourism/visitor/recreational activities), and natural/geological disasters (Galland et al., 2016). Among these threats, those that have left a lasting mark on cultural history are natural disasters (Gizzi and Lazzari, 2012). The destruction of Pompei (south of Italy), following the eruption of Vesuvius in 79 a.d.; the flooding of some protected historic centers during the floods occurred in 1966 in Florence (Italy) and in 2002 in the Czech Republic; the irreparable damages to several religious buildings that occurred in 1997 in the Center of Italy, owing to a three-month earthquake swarm; or the demolition in 2005 of some historic centers of the Southeastern parts of USA due to the hurricane Katrina (Figure 1), are some examples of the consequence of the most devastating natural disasters that come to mind (Principe and Sica, 1967; Will and Meier, 2007; Taboroff, 2000).

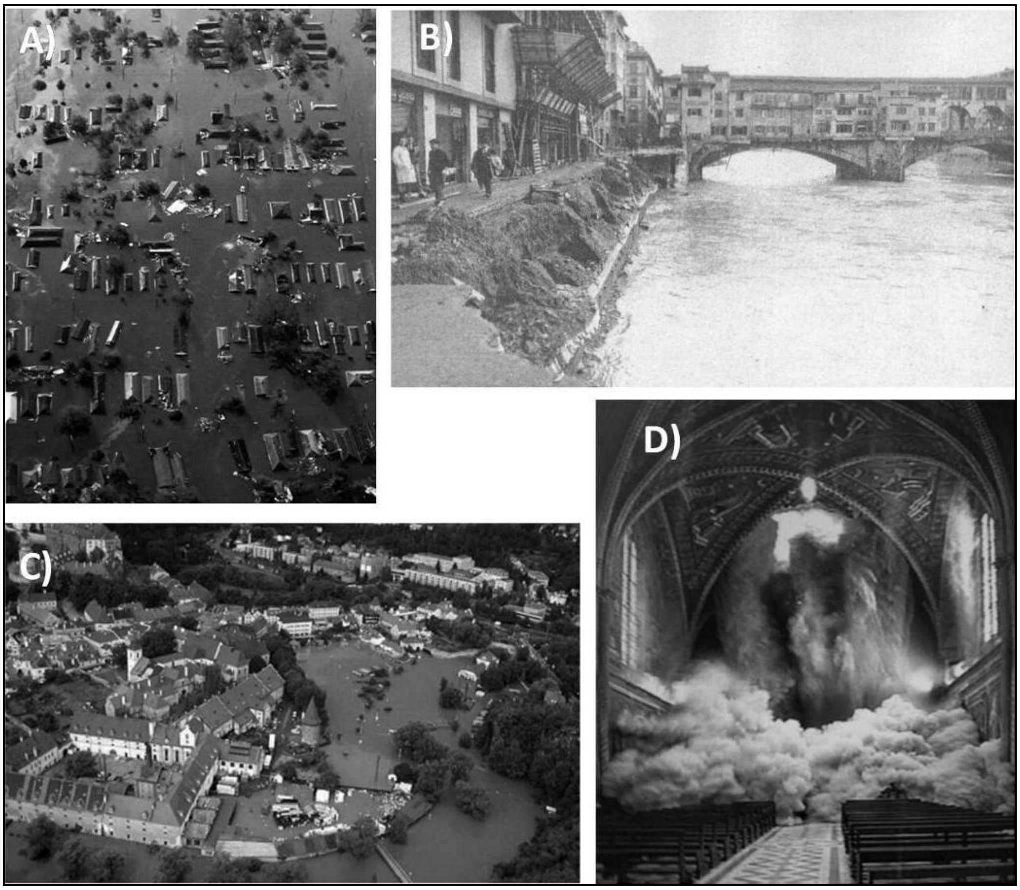

Figure 1. Some of the greatest natural disasters that have affected: A) New Orleans (USA); B) Lungarno Acciaioli (Historic Center of Florence); C) historic core of Ceský Krumlov (Czech Republic); D) the upper basilica of San Francesco in Assisi (Italy). Pictures A, C and D from Will and Meier, 2007; picture B from Principe and Sica, 1967.

Unfortunately, not only these catastrophes have threatened and currently threaten cultural heritage, but there are also other phenomena that act at different spatial and temporal scale, such as landslides, ground-subsidences, rockfalls, and other instability mechanisms. Some examples are: the collapse of the rock massif occurred on 27 February 2014 in the historic town of San Leo (Emilia Romagna Region; Frodella et al., 2016); the several landslides that are progressively reducing the urban area of Civita di Bagnoregio (Central Italy), for this defined the “dying city” (Delmonaco et al., 2009); the damages to the bastions and buildings of Mdina, the former capital of Malta, mainly associated with the differential movements produced by the contrasting mechanical behavior of the underlying lithologies (Gigli et al., 2012); or the ground-subsidence phenomenon which led to the progressive tilt of the Tower of Pisa (Figure 2).

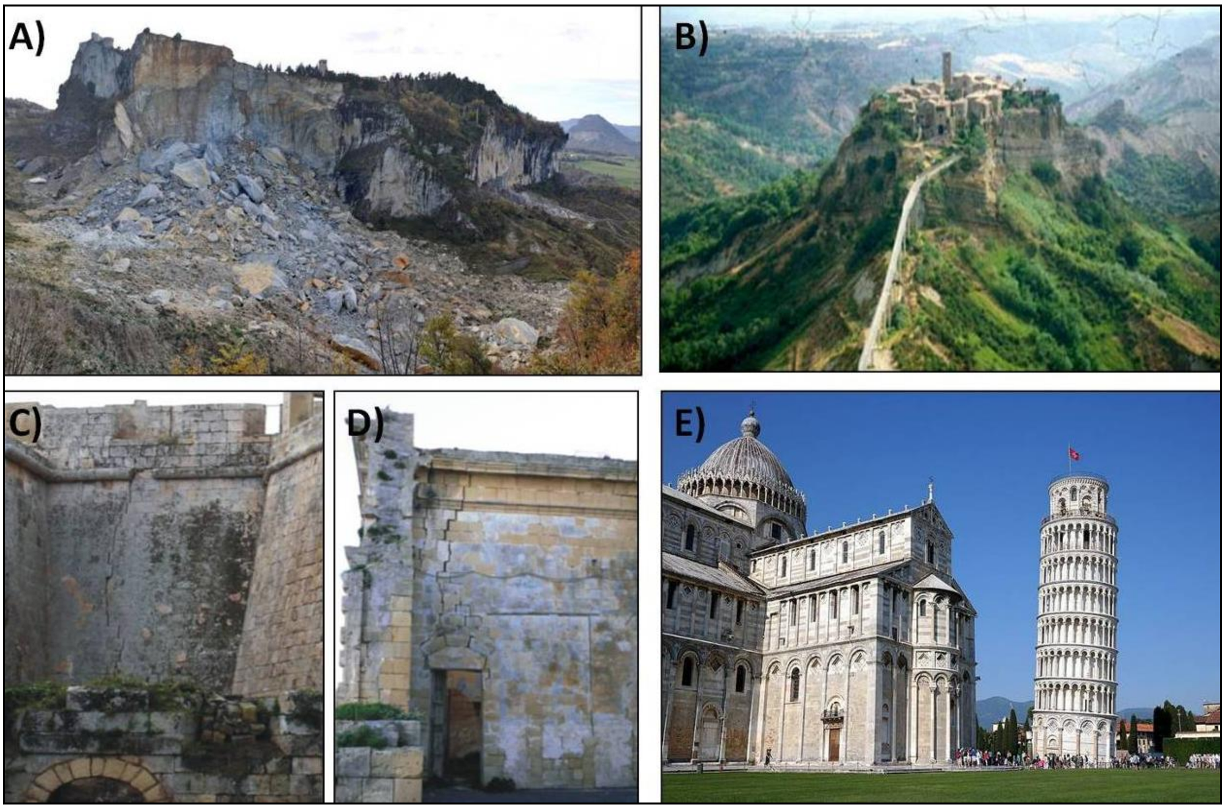

Figure 2. A) Rockfall occurred on 2014 in the historic town of San Leo (Italy), from Frodella et al., 2016; B) Civita of Bagnoregio (Italy) threatened by several landslides, from Delmonaco et al., 2009; C) damages to the bastions and D) buildings of Mdina (Malta), modified from Gigli et al., 2012; E) the leaning tower of Pisa, from Wikimedia Commons.

A further negative note consists in the fact that in the past natural disasters were sporadic and localized phenomena, whereas, in recent years, the climate change has led to a new dimension of disasters: worldwide transformations that takes many forms and evolve over an extended period of time (Will and Meier, 2007). Given the current and projected trends in global environmental change, the exposure to natural risks in cultural heritage sites is expected to increase in the coming decades. The consequences of this uncontrolled phenomenon will be, as expected, further damage, destruction, death, and economic losses.

In the protection and conservation of cultural heritage field, much has been done since 16 November 1945, when the representatives of 37 countries meet in London to sign the UNESCO Constitution (UNESCO, 2010).

In 1972, the General Conference of UNESCO adopted the Convention concerning the Protection of World Cultural and Natural Heritage (UNESCO, 1972), and subsequently, in 1978, the first sites were inscribed on the World Heritage List (WHL) (UNESCO, 2010). After 40 years, at the beginning of 2018, this list, made up of cultural, natural and mixed sites, contains 1073 inscribed proprieties (http://whc.unesco.org/en/list/stat). The 77,5% of these properties are cultural sites (832 proprieties), most of which are localized in Europe and North America Region (Figure 3).

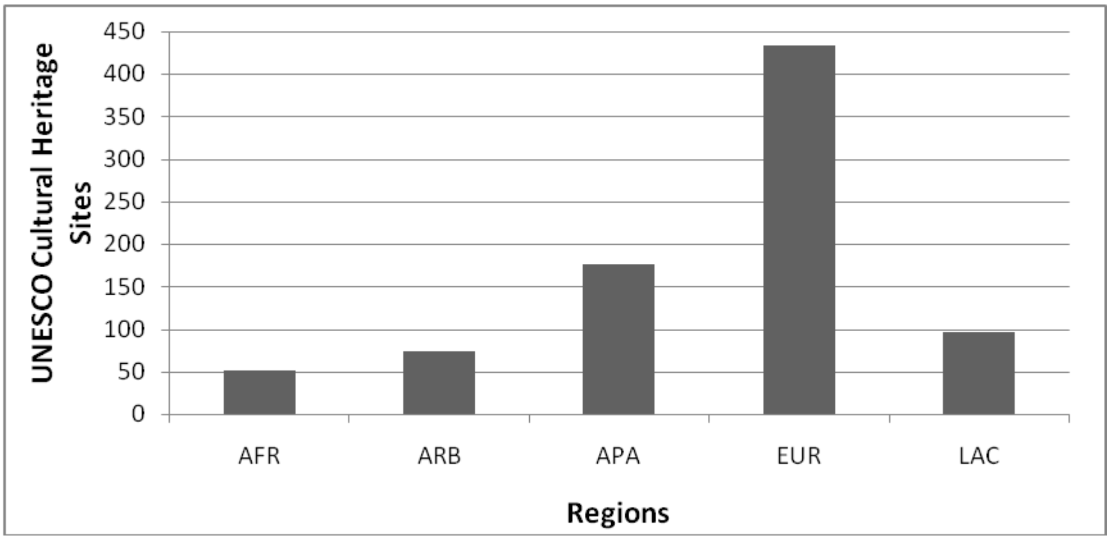

Figure 3. Number of Cultural Heritage Properties by Region. The Regions presented here are defined by UNESCO. AFR = Africa; ARB = Arab States; APA = Asia and the Pacific; EUR = Europe and North America; LAC = Latin America and the Carribean. Modified after, http://whc.unesco.org/en/list/stat.

Italy, with 48 proprieties, has the largest number of cultural assets belonging to the World Heritage (see for example the Basilica of San Francesco in Assisi or the leaning tower of Pisa, respectively at Figure 1 and Figure 2), followed by Spain, with 40 sites, and France and Germany with both 39 sites (http://whc.unesco.org/en/list/stat).

To be registered on this list, that is updated every year by the WH Committee, the proprieties must reflect the characteristics of Outstanding Universal Value (OUV), i.e. represent a priceless and irreplaceable heritage belonging to the entire humanity. Indeed, "the belief that World Heritage Sites belong to everyone and should be preserved for future generations is the very principle on which the World Heritage Convention is based" (Pedersen A., 2002). Furthermore, World Heritage Sites are selected on the basis of 10 strict criteria, e.g.: "(i) represent a masterpiece of human creative genius"; "(iv) be an outstanding example of a type of building, architectural or technological ensemble or landscape which illustrates (a) significant stage(s) in human history", and they also must be safeguarded with an adequate protection and management system to guarantee their integrity and authenticity during the years (UNESCO, 2017).

The World Heritage system requires to States Parties to engage in the management of Cultural Properties in two different and significant stages: 1) a State Party must first demonstrate, during the inscription process, that it will guarantee the OUV of the property through a protection plan; 2) after the inscription, a State Party must respect its commitment to safeguarding the property through effective long-term management, and through a series of procedures which allow this protection to be verified (UNESCO, 2013). By virtue of this system, the State Parties submit every six years a Periodic Reporting to the World Heritage Committee in order to provide "up-dated information about the World Heritage properties to record the changing circumstances and state of conservation of the properties" (http://whc.unesco.org/en/periodicreporting/).

Unfortunately, despite the extensive protection and safeguard measures implemented over the years by the UNESCO International Agency, the level at which natural risks, particularly geological risks, threaten World Heritage Sites is quite high. The scientific community, recently, has cross-compared the UNESCO proprieties with different geological databases to provide a statistical estimation of UNESCO WHS affected by geological risks. From the work of Pavlova et al., 2017, emerges that ~60% of all the sites registered in the WHL are exposed to at least one geological hazard and that the most frequent ones are earthquakes and landslides. At European scale, Spizzichino et al., 2016, claim that 16% of the WH properties belong to high seismic hazard category, 12% and 14% have very high and high landslide susceptibility, respectively, and, at least 7% of them have high volcanic hazard. At National scale, 45% of the Italian UNESCO sites are affected by landslides (Spizzichino et al., 2016). Subsidences and landslides, instead, are the geohazards that mainly threaten the stability of United Kingdom World Heritage Sites (18.6% and 11.5% of the total susceptible land, respectively; Cigna et al., 2018).

The aforementioned framework shows that a great part of World Heritage, that consists mainly of cultural sites, is seriously threatened by geohazards. However, it is important to underline that geohazards, together with the previously mentioned lack of economic resources, tourism and urban development, are concrete threats that can generate emergency situations in cultural sites, but they are not the only ones. There is also a "dangerous attitude" of the ordinary administration in underestimating or not using too much effort to effectively asses the natural risks; this could lead to improper conservation policies of cultural heritage sites (Margottini and Vilímek, 2014; Cuca, 2017). For example, within the UNESCO safeguarding system, only "sudden geological events" are considered as factors that undermine the protection of WHS, although it is well known that also slow-kinematic phenomena can threaten cultural and natural heritage.

It is therefore necessary a close collaboration between the scientific community and the institutional governance in order to improve the knowledge and the awareness of geohazards both in UNESCO and not-UNESCO sites. This can be obtained through useful procedures and methodologies that allow identifying and monitoring the geological instabilities.

Historically, the monitoring of monuments or cultural buildings was performed through in situ observations, which included field surveying, ground-based data collection, and periodical

observations through the installation of monitoring devices, such as optical targets, GPS (Global Positioning System) stations, or inclinometers. These methodologies, in addition to being expensive, also require a considerable amount of time for the operator and can lead to aesthetic and functional impacts to the heritage (Spizzichino et al., 2016).
Nowadays, these limits have been overcome by the advent of a variety of new remote sensing technologies that, in a short period of time and with a great cost-benefit ratio, allow investigating extended areas of the Earth surface at high resolution. In particular, space-borne and Ground-Based InSAR technologies and Terrestrial Laser Scanning technique are some of the innovations in the scientific field that, starting from the last years of the past century, have given remarkable results in the analysis and monitoring of some geological risks on cultural sites (Tarchi et al., 2000; Evans and Farr, 2006; Canuti et al., 2009; Gigli et al., 2012; Tapete and Cigna, 2012; Tapete et al., 2012; Vacca et al., 2012; Fanti et al., 2013; Tapete et al., 2013; Alfarè et al., 2014; Montuori et al., 2014; Zhou et al., 2015; Pratesi et al., 2015; Frodella et al., 2016; Themistocleous et al., 2016; Tapete and Cigna, 2017a).
The first Earth surface imagines acquired from Synthetic Aperture Radars (SAR) installed onboard a satellite have given a significant impulse to the Earth observation field and opened new unimaginable perspectives on the analysis and monitoring of slow-kinematic geohazards.
The GBInSAR technique exploits the same interferometric principle used in the space-borne InSAR technique to obtain displacement measurements but, having different characteristics and acquisition geometries, it guarantees better performance for landslides real-time monitoring and for early warning systems.
A high resolution 3D reproduction of the investigated scene is instead the result obtained through the Terrestrial Laser Scanning technique, which has been widely exploited in different application such as the characterization of rock masses or the monitoring campaigns of cliffs evolution.
This range of currently survey techniques allows analyzing several geohazards within different cultural heritage sites, choosing time after time the most suitable methodology to the single scenario.

1.2 Project approach

The main aim of this research has been to exploit the aforementioned new technologies potential in order to safeguard different types of historical and cultural sites from the increasingly frequent geological processes that threaten them. In fact, remote surveys are one of the actions that can guarantee the conservation and, therefore, the transmission of man-made assets over the centuries to the future generations.

This work has been organized into two different analysis scales: regional and local (Figure 4).

The analysis scale, together with the typology and kinematics of the investigated instability phenomenon, is one of the parameters that has influenced on the choice of the different technologies exploited in this study, because each technology has quality and characteristics that make it suitable for certain surveys.

At regional scale, the Persistent Scatterer Interferometry (PSI) has been exploited to propose a simple and repeatable procedure that could improve the current knowledge and awareness of slow-kinematic geohazards (slow-moving landslides and ground-subsidences) within the boundaries of WHS. The choice to operate with this technique is due to the fact that it is the most advanced InSAR technique, and it is a powerful tool for large-scale investigations, as it allows monitoring wide areas in a short time. To illustrate the proposed procedure, 7 UNESCO proprieties of Tuscany Region (Italy), have been chosen as test sites.

At local scale, a multidisciplinary approach, composed of a combined use of past instability knowledge and remote sensing surveys, has been developed with the aim of better localize and characterize the geohazards that threaten a cultural site.

Two test sites have been chosen as cases of study:

- The Historic Center of Florence (Tuscany Region), where on 25 May 2016 a GBInSAR system was installed for a real-time monitoring of a landslide occurred along the Arno riverbank.

- The Canossa Cliff (Emilia Romagna Region), where the main geological instability processes have been analyzed and monitored through the most suitable technology for the geological and geomorphological characteristics of this site: the TLS technology.

The final goal of this project has been to develop an innovative approach to geological risks, in order to enhance cultural heritage management practices and to reinforce institutional and government support through the knowledge of the past instabilities and the technological innovation.

The skills in this area were acquired since November 2015, both at the Department of Earth Sciences of the University of Florence and during a six months research period at the Centre Tecnològic Telecomunicacions Catalunya (CTTC) of Castelldefels (Barcelona).

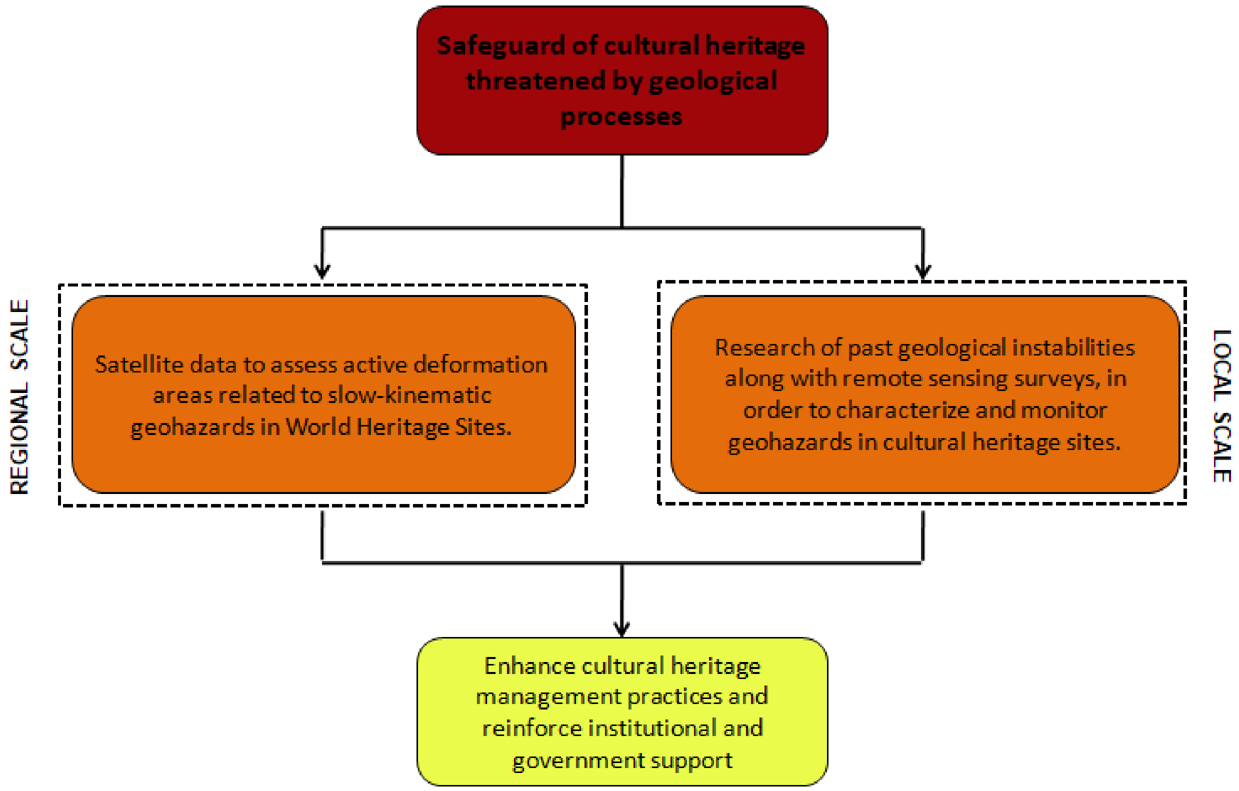

Figure 4. Scheme of the research activity.

2. Analysis at Regional Scale

A new satellite data analysis procedure to identify, characterize and monitor the temporal and spatial evolution of ground deformation related to slow-moving landslides and ground-subsidences has been developed following an investigation conducted on the current state of geohazards knowledge by the UNESCO Agency. It emerged that the level of UNESCO attention placed on geohazards is poor (Pavlova et al., 2017), especially if compared with the others potential threatening factors, such as wars, uncontrolled urban development or arsons (Canuti et al., 2009). This unawareness can be found within the Periodic Reporting that the State Parties submit every six years to the World Heritage Committee, in order to provide “up-dated information about the World Heritage properties to record the changing circumstances and state of conservation of the properties” (http://whc.unesco.org/en/periodicreporting/). Particularly, within the II Cycle of UNESCO reports (2008-2015), where a standard list of factors affecting the OUV of WHS is present (http://whc.unesco.org/en/factors/), only some “sudden ecological and geological events” are included: volcanic eruption, earthquake, tsunami/tidal wave, avalanche/landslide, erosion and siltation/deposition, and wildfire. It is well known that, unfortunately, not only these geological factors can threaten cultural heritage sites, but also slow-moving landslides (as defined by Cruden and Varnes 1996), and ground-subsidences (Jamiolkowski et al., 1993; Bromhead et al., 2006; Canuti et al., 2009; Cigna et al., 2012; Vlcko, 2004; Alfarè et al., 2014). A greater knowledge of the potential impact of such phenomena has been obtained through the geoinformation that the space-borne InSAR techniques allow acquiring (Tapete and Cigna, 2017b). To illustrate the proposed procedure, 7 UNESCO proprieties of Tuscany Region (Italy), have been chosen as test sites. Envisat (2003–2010) and Sentinel-1 (2014–2017) C-band datasets, processed with different PSI techniques, have been analyzed.

2.1 Space-borne InSAR technique and the PSI product

The launches on the space, since 1992, of satellites equipped with active radar sensors have allowed acquiring several images of the Earth’s surface over the years. The Synthetic Aperture Radar (SAR) technique is a recently developed methodology that, using the Doppler Effect, allows synthesizing large antennas with the use of only very small antennas. The SAR sensor is defined an active sensor because it emits electromagnetic waves that “illuminates” the target on the ground at a certain frequency and wavelength depending on the type of sensor (X-, C- and L-bands are the most common bands for satellite sensors), and itself receives the echo (backscattering phenomenon). Moreover, the potentiality of this sensor also includes the ability to acquire both day and night, in all the weather conditions and at high geometric resolution (i.e. the minimum distance that must exist between two objects in order that they are distinguishable in the acquired image), that improve with increasing bandwidth. A spaceborne SAR sensor travels along two predefined polar orbits: a descending orbit, when the satellite travels from the North Pole towards the South Pole for half of its trajectory, and an ascending orbit when satellite travels from the South Pole towards the North Pole. The same area is thus revisited along this two orbits (Figure 5a). Furthermore, a SAR satellite acquires data along its Line Of Sight (LOS), which is the connection line between the sensor and the monitored object. The satellite inclination with respect to the Earth’s surface is called incidence angle or off-nadir angle (Figure 5b). The off-nadir angle ranges from values of 20° to 45° according to the type of satellite platform (Henderson and Lewis, 1998; Franceschetti and Lanari, 1999; Hanssen, 2001; Colesanti, 2006; Solari, 2017). Because of these rather small incidence angles, the sensor is much more sensitive to the vertical component of the movement than the horizontal one. Hence, the radar sensor can estimate only a small component of the 3D real motion of the landslide, i.e., the projection along the satellite LOS (Tofani et al., 2013).

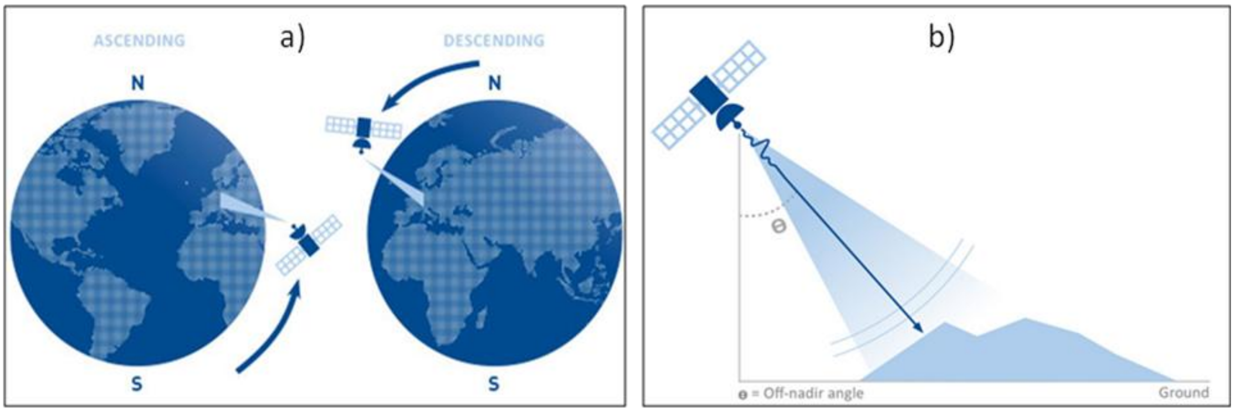

Figure 5. a) Ascending and descending orbit of satellite (http://tre-altamira.com/technology/#sar-imagery); b) SAR image acquisition (https://site.tre-altamira.com/company/our-technology/#insar-and-dinsar).

The product acquired by a SAR sensor is an image called interferogram, which is composed of a matrix of cells (pixels). Each pixel value corresponds to both amplitude and phase information about the backscattered microwave signal. Amplitude is related to the energy of the backscattered signal, while the phase is related to the sensor-to-target distance, and this latter property is used in estimating displacement with millimetric precision in interferometric applications (Bamler and Hartl, 1998). The conventional technique for the study of SAR data is the Differential Interferometric SAR (DInSAR) (Crosetto et al., 2011), which is based on the analysis of changes in the phase value between two distinct acquisitions in order to highlight differences due to any range displacement of the radar target, topographic distortion arising from slightly different viewing angles of the two satellite passes, atmospheric disturbances or noise (decorrelation effects) (Massonnet e Feigl, 1998, Rosen et al., 2000). The DInSAR technique allows isolating the effective change of signal phase related only to a variation of the distance between the sensor and the object and, therefore, to a displacement of the latter (Figure 6).

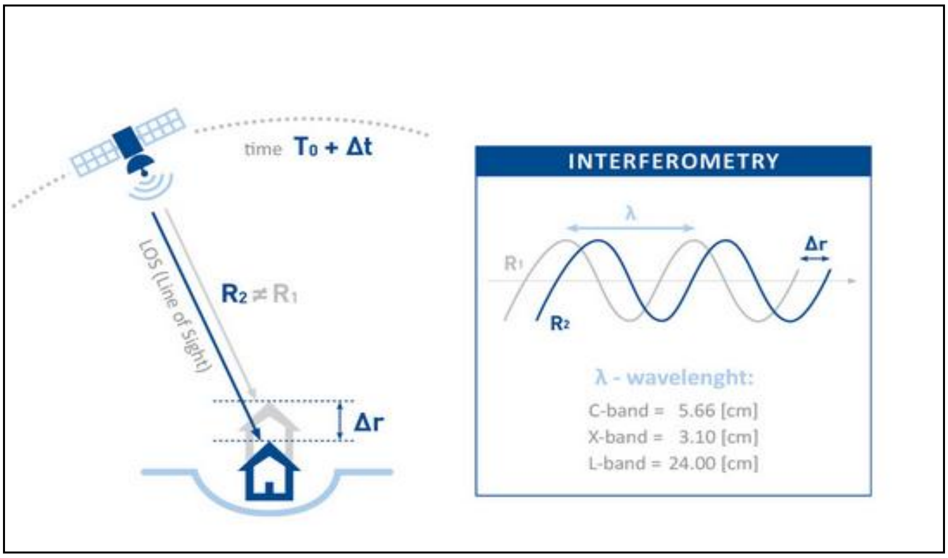

Figure 6. Representative scheme of the DInSAR technique (https://site.tre-altamira.com/company/our-technology/#insar-and-dinsar).

The different satellites that have continuously circumnavigated the globe since 1992 (with ERS/1-2 satellites), has allowed the creation of a large data archives. In Figure 7, these satellites, with their main characteristics (e.g., time of launch, revisiting time, that is the time needed to acquire data on the same area, and resolution), are shown.

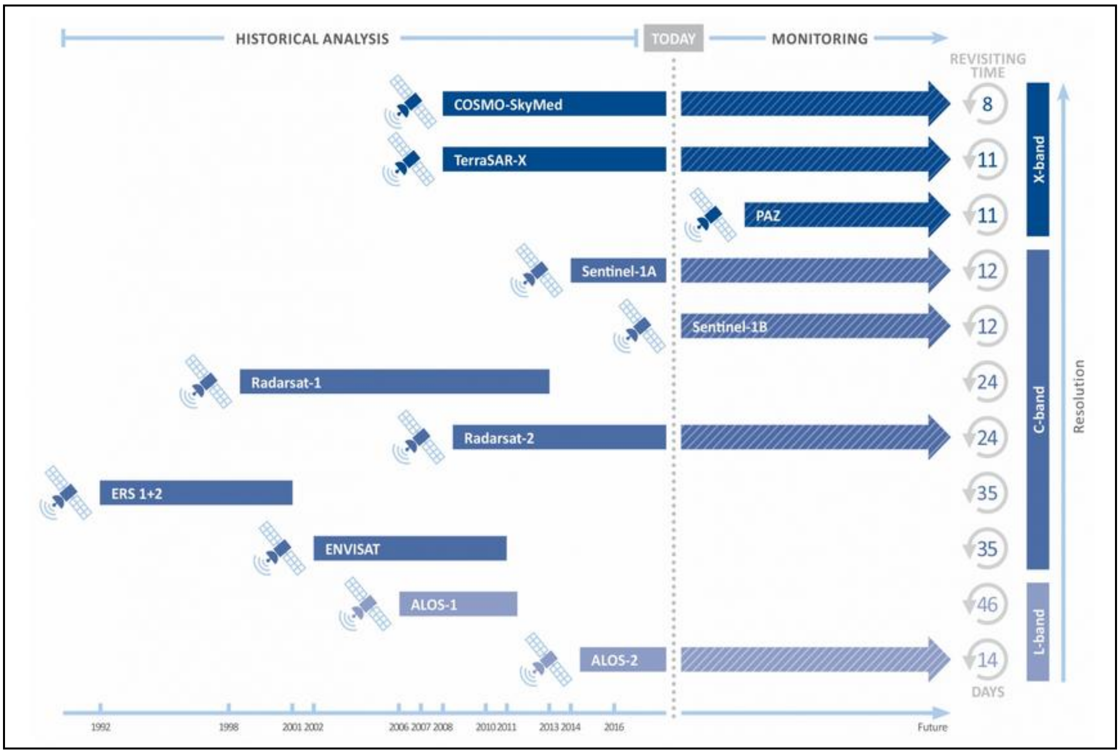

Figure 7. Satellites launched on the space and their main characteristic (http://tre-altamira.com/technology/#insar-and-dinsar).

In recent years, a significant evolution of the common InSAR technique has led to a multi-interferogram or multi-image approach. This was done in order to overcome the main limitations of the single-pair interferometry (difficulty in removing atmospheric and decorrelation phenomena). The Persistent Scatterer Interferometry (PSI; Ferretti et al., 2001; Crosetto et al., 2016a), is one of these new approaches, and it allows detecting some targets called PS, which are mainly stable elements on the ground, e.g. rocks, buildings or roads. For this reason, the PSI analysis is optimal in urban centers, while in the densely vegetated areas no data are recognized. Recently, new significant improvements in remote investigations are guaranteed by the SqueeSAR technique (Ferretti et al., 2011). This technique jointly detects PS and DS (Distributed Scatterers), which are principally pastures, debris areas or uncultivated fields (Figure 8). Thus, SqueeSAR technique allows an excellent ground deformation monitoring, not only in strongly anthropized areas but also in non-urban areas, where the number of PS is limited (Bianchini et al., 2015; Tang et al., 2016).

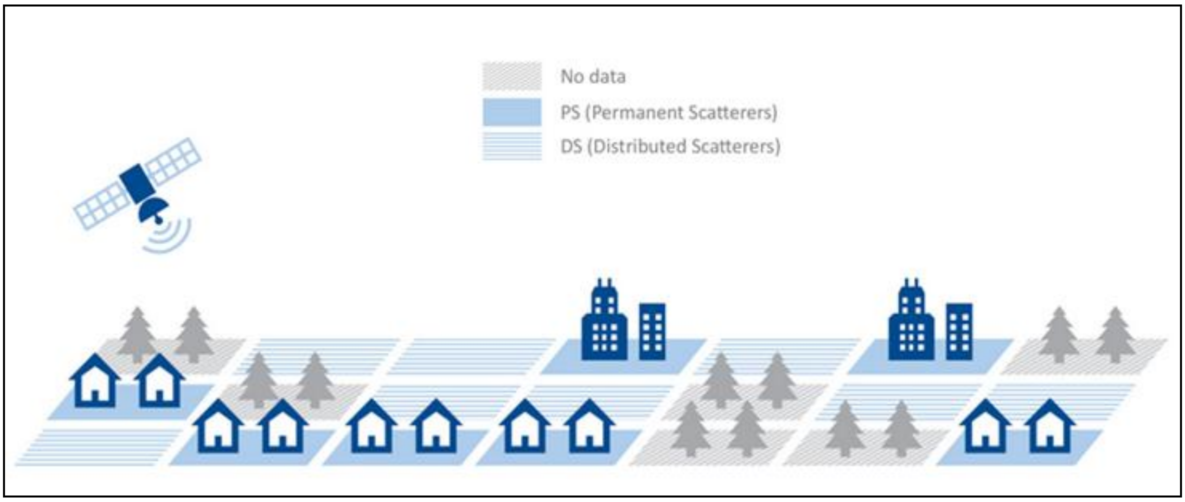

Figure 8. Comparison between PSInSAR (Permanent Scatterers Interferometry) and SqueeSAR techniques (modified after, http://tre-altamira.com/technology/#insar-and-dinsar).

Only ground deformation related to slow-kinematic geohazards (e.g., ground-subsidences and slow-moving landslide as defined by Cruden and Varnes, 1996), can be successfully detected by PSInSAR (Permanent Scatterers Interferometry) and SqueeSAR techniques (Bonforte et al., 2011; Lu et al., 2012; Tofani et al., 2013; Ciampalini et al., 2016; Nolesini et al., 2016; Raspini et al., 2016; Rosi et al., 2016; Rosi et al., 2018; Solari et al., 2018). This is due to the major limitation of this technique: the maximum displacement measurable between two acquisitions is equal to $\lambda/4$, where λ is the wavelength of the radar signal (e.g., 1.4 cm for C-band sensors). Considering not only the wavelength but also the revisiting time, the maximum deformation rate detectable for example by the Sentinel-1 sensors is 42.6 cm/yr (Crosetto et al. 2016; Solari et al., 2018). For this reason, the slow-kinematic geohazards that have deformation rates generally below these thresholds can be successfully detected.

PSInSAR and SqueeSAR techniques have also been successfully exploited for conservation strategies in cultural and natural heritage, mainly for their non-invasiveness in the investigated assets (Tapete and Cigna, 2012; Tapete et al., 2012).

The launch in 2014 of the Sentinel-1 constellation has drastically increased the possible applications of PSI for mapping and monitoring geohazards. These new generation satellites, with C-band sensor, acquire on the same area with a 12 days revisiting time and their images are freely available with a worldwide coverage. All these characteristics, in addition to a regular acquisition plan, are fundamental to design long-term geohazards monitoring strategies (Barra et al., 2016; Crosetto et al., 2016b; Devanthéry et al., 2016a). An excellent procedure based on Sentinel-1 data has been proposed in a recent study of Barra et al., 2017, which allows identifying the most critical ground deformation, named Active Deformation Areas (ADA), in the investigated area.

2.2 A new procedure to improve the knowledge of slow-kinematic geohazards in UNESCO sites

Within this section, a new procedure to assess the main critical ground movements triggered by slow-kinematic geohazards (slow-moving landslides and ground-subsidences) within the boundaries of UNESCO sites is described. The general organization of this procedure, broadly illustrated in the subsequent sections, is divided into three main blocks (Figure 9):

1. Identification: this is the first step of the proposed procedure that allows localizing the most critical ground deformation through the management of satellite data with the Active Deformation Areas methodology (Barra et al., 2017), here adapted for the specific aims of this work (Pastonchi et al., 2018).
2. Characterization: through an intersection in a Geographic Information System (GIS) platform of previously created ADA databases with geohazards inventories (slow-moving landslides and ground-subsidences inventories) and, subsequently, through the compilation of a checklist called "Identity Card of ADA (ICA)", it is possible to characterize the typology of slow-kinematic movement of Active Deformation Areas and detect their impact on the cultural heritage site.
3. Monitoring: in this final step, a comparison between ADA extracted from satellite datasets acquired at different times is made. It is thus possible to monitor the temporal and spatial evolution of the main ground deformation previously characterized (Pastonchi et al., 2018).

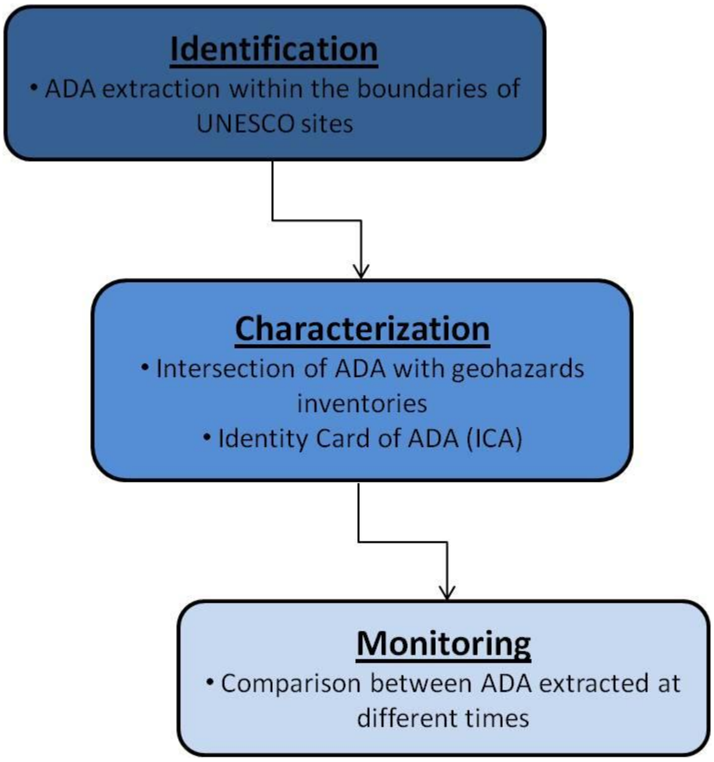

Figure 9. The three main steps of the procedure proposed in this study.

This procedure has been designed to be periodically updated with new satellite datasets. It can be applied to any satellite SAR data, however, thanks to the main characteristics of the recent Sentinel-1 data (short revisit time, free availability without any restrictions and worldwide coverage) it provides the best performances with Sentinel-1 regional datasets.

These product could be used by the local institutions responsible for each WHS as a tool to update the UNESCO periodic reports (updated every six years by the State Parties), and perform an assessment of the slow-kinematic geohazards (slow-moving landslides and ground-subsidences) that actually are not present in these reports (see Section 2).

2.2.1 Identification of Active Deformation Areas (ADA)

The identification of reliable moving areas within the boundaries of UNESCO sites that could be due to potential geohazards (slow-moving landslides and ground-subsidences), is based on the simple, fast and repeatable methodology proposed by (Barra et al., 2017). Figure 10 shows a scheme of this approach.

The huge amount of data contained in the satellite datasets (millions of PS), is managed on a Geographic Information System (GIS) platform, through the following steps. First, all the PS velocity measurements acquired along the satellite line of sight (V_{LOS}) are filtered, with a threshold value that is twice the standard deviation (2σ) of all the velocity measurements. At this stage, "active" points ($|V_{LOS}|>2\sigma$), are distinguished from those in which a movement has not been detected ($|V_{LOS}|\leq 2\sigma$). Subsequently, for each "active" point (AP), a circular area of influence is defined on the basis of the size of the ground resolution cell of the SAR images. Among all the buffered APs only those intersecting each other and forming a polygon with at least 3 APs inside are considered an ADA (Figure 11). This choice, that is new with respect to the steps of the original ADA methodology, was made to perform a local scale analysis on a regional dataset (downscale process). This allowed identifying even small active deformation that may compromise the conservation of the UNESCO proprieties (Pastonchi et al., 2018). Finally, to obtain the magnitude of each ADA, the average of the APs velocities (in absolute value) included in the ADA has been calculated.

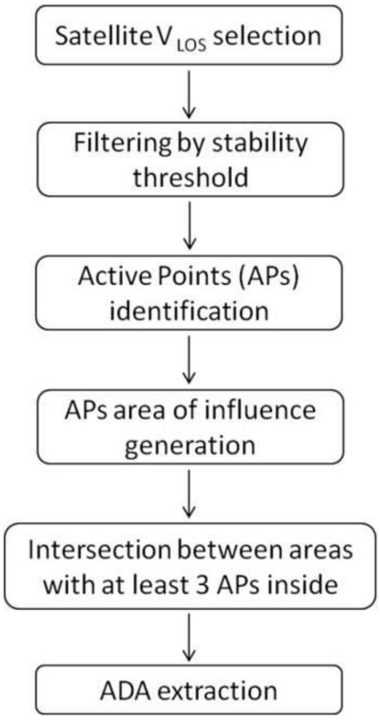

Figure 10. Flowchart of the methodology. From Pastonchi et al., 2018.

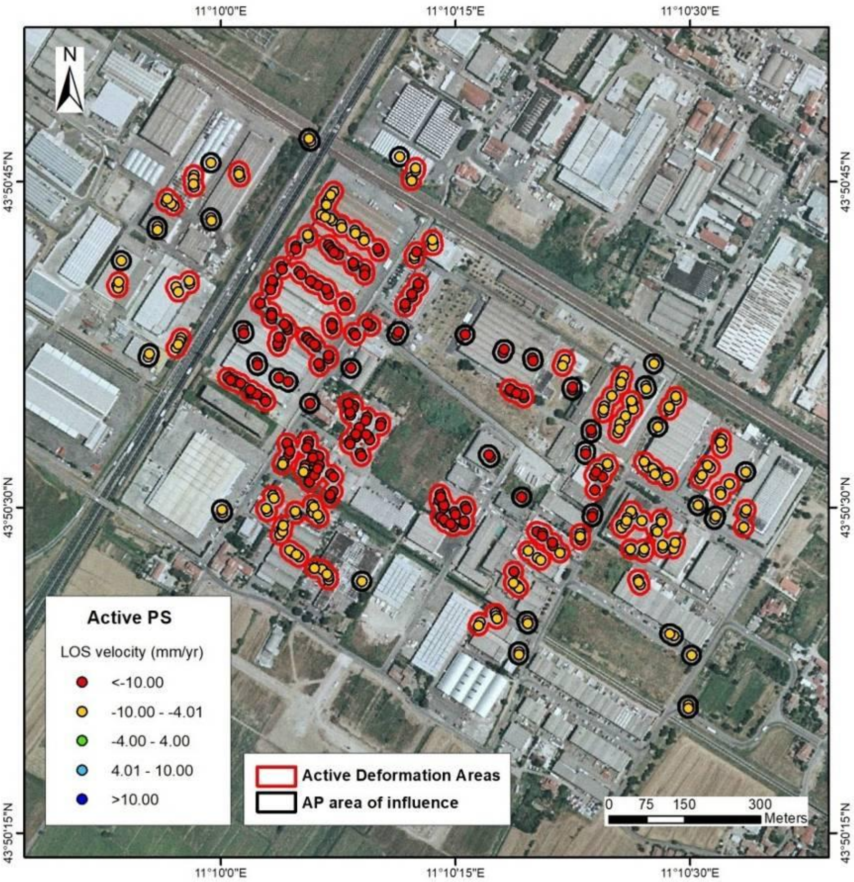

Figure 11. ADA extraction from the Active Points (APs) of Envisat dataset (ascending orbit), in the urban area of Florence. In this map only the active PS are visualized. From Pastonchi et al., 2018.

2.2.2 Characterization of ADA

In order to unequivocally discriminate the typology of slow-kinematic movement that characterizes the identified ADA, it is necessary an intersection between the ADA polygons and the available geohazards inventories (landslides and ground-subsidences inventories). This is a first screening, useful to recognize the geohazard that affects the area where the ADA have been identified.

For a better characterization of the active motion and for an evaluation of its impact on the cultural heritage sites, a simple check-list, here called ICA, has been expressly created (Table 1).

This table is a simple tool and it could be used by the competent authorities to better characterize the ADA that, according to the criteria that will be considered most appropriate, require in situ investigations. The ICA is mostly useful to analyze the ADA that do not intersect any inventory and whose main characteristics, through the only office analysis, can not be identified. These unclassified areas are due to the fact that between the drafting of the inventory and the used satellite dataset, few months or years may have elapsed, and, therefore, some newly formed areas can be identified.

Table 1. "Identity card of ADA"- ICA

ICA - IDENTITY CARD of ADA					
Date:			Operator:		
1. LOCATION AND FEATURES OF ADA					
Name of WHS:				ID number:	
Nation:		Province:		Municipality:	
Governmental Institution responsible for the Property:			Property manager / Coordinator, Local Institution / Agency:		
ADA coordinate (WGS-84): Latitude, Longitude		ADA situated in: Core zone, Buffer zone, Influence zone		Satellite characteristic: Sensor, Orbit, Time Period	
ADA velocity (mm/yr):			ADA areal extension (m²):		
2. INTERSECTION OF ADA WITH OTHER DATA					
With other ADA from previous update	Yes ☐: Satellite sensor, Satellite orbit, Satellite time period, ADA velocity (mm/yr), ADA areal extension (m²)				No ☐
With geohazards inventory	Yes ☐	Landslides inventory ☐ Inventory name .... Description of phenomenon........		Ground-subsidences inventory ☐ Inventory name .... Description of phenomenon........	No ☐
With geological cartography	Name/Number .... Description of Outcropping lithologies.........				
3. ELEMENTS AT RISK					
Buildings ☐	Transport or service infrastructures ☐	Agricultural territories ☐	Wooded areas and natural environments ☐	Water bodies ☐	
Category*:	Category*:	Category*:	Category*:	Category*:	
*Examples: Private habitation; hospital, cultural asset	*Examples: Main street; highway; hydraulic channel	*Examples: Pasture, protected area, arable land	*Examples: Sparse vegetated area; protected area, outcrop	*Examples: River, lake, lagoon	
4. IN SITU OBSERVATIONS					
☐ Damages on buildings and infrastructures			☐ No damages	Notes:	
Observations*:		Picture n°			
Observations*:		Picture n°			
Observations*:		Picture n°			
*Examples: cracks; distortions; partial collapses					
☐ Damages on natural ground surface and on water bodies			☐ No damages	Notes:	
Observations*:		Picture n°			
Observations*:		Picture n°			
Observations*:		Picture n°			
*Examples: depressions; clefts; Inclined trees					

The ICA has been organized in 4 subsections: 1- location and feature of ADA; 2- intersection of ADA with other data; 3- elements put at risk by ADA and 4- in situ observations to identify any damage caused by the active phenomenon (Table 1). The 1st session is characterized by some simple information regarding the UNESCO site where the ADA is and by the main parameters of the latter (e.g., velocity, areal extension and coordinate of ADA). The 2nd section, highlighting the intersection of ADA with other ADA derived from previous updates and with geohazards inventories and geological cartographies, is useful to discriminate/characterize the phenomenon that has triggered the ADA. Regarding sections n°3 and n°4, given the wide range of classifications of elements at risk and damages due to slow-moving landslides and ground-subsidences (Cardinali et al., 2002; Dai et al. 2002; Fell et al. 2005; Cooper, 2008; Fell et al. 2008; Mansour et al., 2011; Figueroa-Miranda et al., 2018), it was decided to design them in a very simple and quick way, in order to qualitatively collect information regarding the impact of slow movements in UNESCO sites. In the 3rd section, the elements at risk are divided into: buildings; transport or service infrastructures; agricultural and industrial territories; natural environments and water bodies. Furthermore, some examples to help the operator to fill in the table are shown. In section n°4, finally, it is possible to write notes, observations, and references to photos of detected damages on buildings, infrastructures and on natural ground surface or water bodies. The choice of this simplification is also due to the fact that the effects of such movements are generally revealed by little evidence within man-made structures or on natural ground surfaces, despite their high potential to limit a structural functionality and induce a total or partial disruption of an environment (Del Soldato et al., 2017). At last, the human life has not been included among the elements at risk because the "slow" and "extremely slow" phenomena, like those analyzed in this study, are not considered a threat to human life (Alexander, 1993).

2.2.3 Monitoring of ADA

Comparing the main characteristics of ADA extracted from two satellite datasets acquired at different times within the UNESCO sites boundaries, it is possible to identify the spatial and temporal evolution of the most critical ground deformation associated with geohazards (Pastonchi et al., 2018). In Figure 12 a scheme of the monitoring procedure is shown.

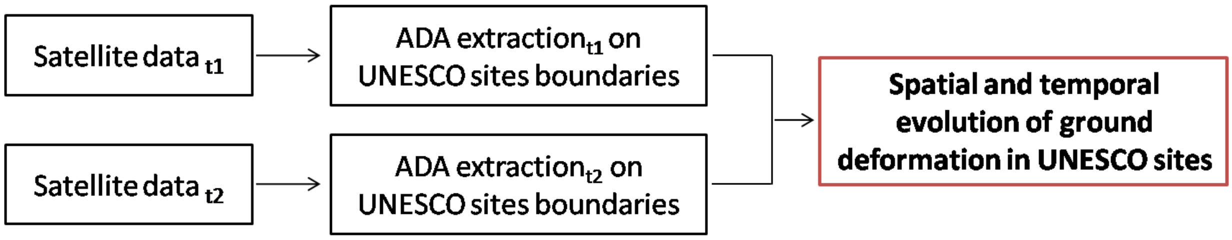

Figure 12. Procedure to identify the temporal and spatial evolution of critical ground deformation within the UNESCO sites boundaries (t_1= time1; t_2= time2). From Pastonchi et al., 2018.

This monitoring procedure can be updated with a new satellite dataset whenever necessary (the recent Sentinel-1 data, characterized by short revisit time, free availability and worldwide coverage, make this possible), and it could be useful for evaluating also the trend of the phenomenon that characterized the identified ADA.

2.3 Test sites

2.3.1 An overview on the UNESCO sites in Tuscany

At the beginning of 2018, Italy, with a total of 53 proprieties, is the nation with the highest number of sites inscribed in WHL (http://whc.unesco.org/en/list/stat).
Eight of these 53 proprieties, both cultural and natural sites, are located in the Tuscany Region and they have been inscribed in WHL in different years (Table 2), on the base of different criteria assumed in https://whc.unesco.org/en/criteria/.
The cultural heritage sites of Tuscany, on which this thesis work has been focused, are: the Historic Center of Florence; Piazza del Duomo, Pisa; the Historic Center of San Gimignano; the Historic Center of Siena; the Historic Center of Pienza; Medici Villas and Gardens in Tuscany (14 proprieties), and Val d'Orcia. A map indicating the location of these sites is shown in Figure 13 (Pastonchi et al., 2018).

Table 2. Main features of the UNESCO Tuscan sites and their boundaries (Core zone and Buffer zone), from Pastonchi et al., 2018. The inscription criteria shown in this table can be consulted in https://whc.unesco.org/en/criteria/.

UNESCO TUSCAN SITES	COORDINATES (Latitude/Longitude)	INSCRIPTION YEAR	INSCRIPTION CRITERIA	TYPE OF PROPERTY			BOUNDARIES (ha)	
				CULTURAL	NATURAL	MIXED	CORE ZONE	BUFFER ZONE
Historic Center of Florence	43.773 / 11.256	1982	(i)(ii)(iii)(iv)(vi)	X			505	10.480
Historic Center of Siena	43.319 / 11.332	1995	(i)(ii)(iv)	X			170	9.907
Medici Villas and Gardens in Tuscany								
Cafaggiolo Villa	43.965 / 11.295	2013	(ii)(iv)(vi)	X			2.35	649.56
Il Trebbio Villa	43.953 / 11.287	2013	(ii)(iv)(vi)	X			16	650.31
Careggi Villa	43.809 / 11.249	2013	(ii)(iv)(vi)	X			3.6	55.71
Medici of Fiesole Villa	43.806 / 11.289	2013	(ii)(iv)(vi)	X			2.11	44.88
Castello Villa	43.819 / 11.228	2013	(ii)(iv)(vi)	X			8.33	289.31
Poggio a Caiano Villa	43.818 / 11.056	2013	(ii)(iv)(vi)	X			9.31	135.63
La Petraia Villa	43.819 / 11.237	2013	(ii)(iv)(vi)	X			21.31	276.33
Boboli Garden	43.762 / 11.248	2013	(ii)(iv)(vi)	X			40	132
Cerreto Guidi Villa	43.759 / 10.879	2013	(ii)(iv)(vi)	X			0.76	4.12
Seravezza Palace	43.994 / 10.232	2013	(ii)(iv)(vi)	X			1.01	50.14
Pratolino Garden	43.858 / 11.304	2013	(ii)(iv)(vi)	X			26.53	210.35
La Magia Villa	43.852 / 10.973	2013	(ii)(iv)(vi)	X			2.1	103.65
Artimino Villa	43.782 / 11.044	2013	(ii)(iv)(vi)	X			1.04	701.66
Poggio Imperiale Villa	43.749 / 11.248	2013	(ii)(iv)(vi)	X			5.35	235.43
Historic Center of San Gimignano	43.468 / 11.042	1990	(i)(iii)(iv)	X			13.88	/
Piazza del Duomo, Pisa	43.723 / 10.396	1987	(i)(ii)(iv)(vi)	X			8.87	254
Historic Center of the City of Pienza	43.077 / 11.679	1996	(i)(ii)(iv)	X			4.41	/
Val d'Orcia	43.067 / 11.55	2004	(iv)(vi)	X			61.187.961	5.660.077
Sasso Fratino	43.844 / 11.803	2017	(ix)		X		781.43	6.936.64

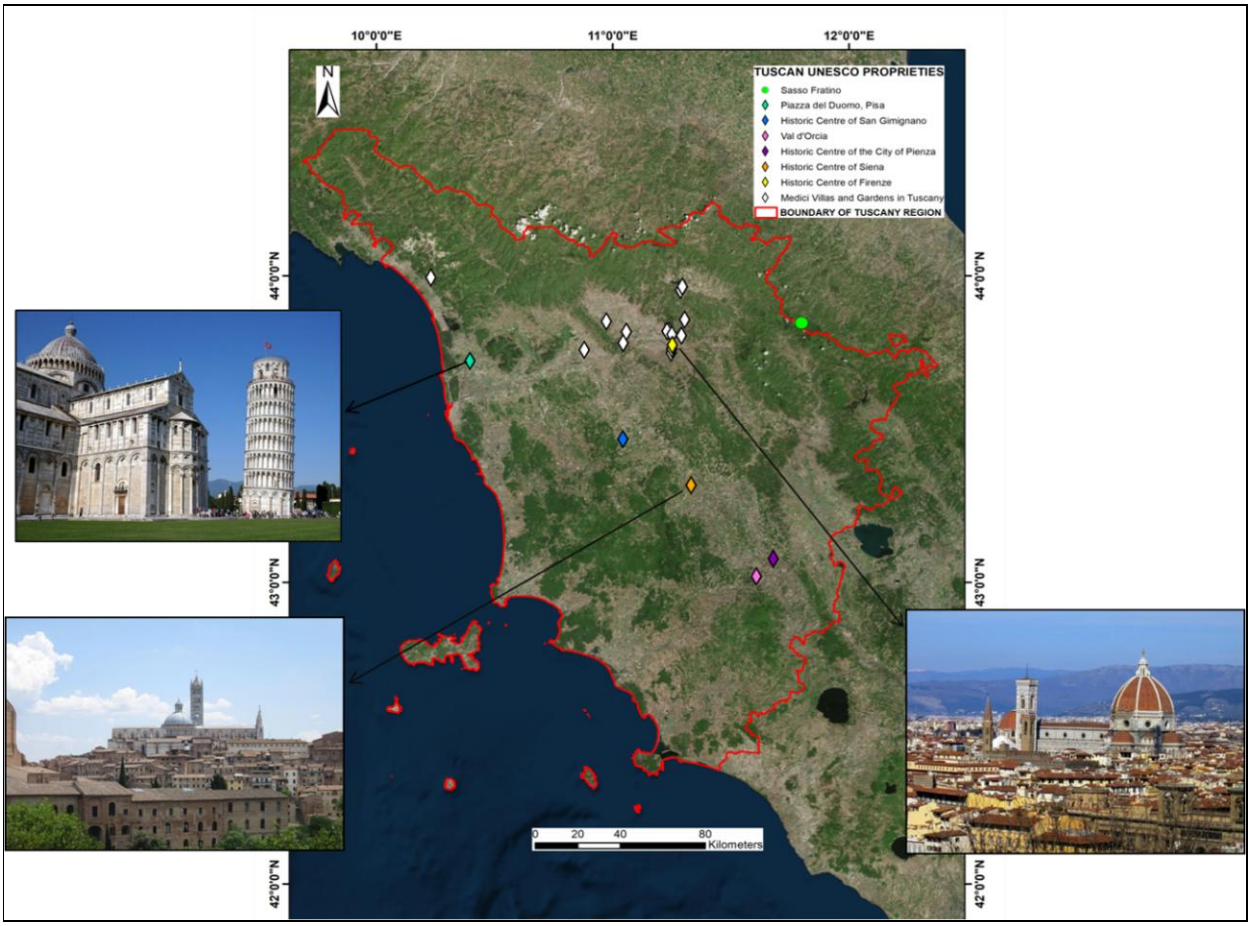

Figure 13. Location of the UNESCO Tuscan sites, from Pastonchi et al., 2018. Some Medici Villas and Gardens, due to their proximity, are not visible at this scale. Photos source: Luca Aless - Wikimedia Commons.

The 20 aforementioned cultural sites (14 Medicean proprieties plus the other six sites) are the symbol of the flourishing economic, cultural and social development that has involved the Tuscan territory over several centuries of history. Each property has a specific boundary formally called Core Zone, and another boundary called Buffer Zone. A Buffer Zone is an area surrounding the Core Zone, where only activities compatible with the conservation objectives of UNESCO proprieties can take place. In other words a Buffer Zone plays a fundamental role in guaranteeing the Outstanding Universal Value of a Core Zone (Martin and Piatti, 2009). As shown in Table 2, only the Historic Centers of San Gimignano and Pienza are not currently provided with a Buffer Zone.

In order to understand the degree of knowledge of geological risks in each of the aforementioned UNESCO sites, the most updated cycle of UNESCO reports (II Cycle - 2008/2015) has been analyzed (Pastonchi et al., 2018). Within these reports, a "Factors Summary Table" that threatens the World Heritage proprieties is shown. At this table, some "sudden ecological or geological events” are listed. At the Historic Centers of Siena and San Gimignano, the Medicean proprieties, and Piazza del Duomo (Pisa), the earthquake is the most recognized geohazard, and it is indicated as negative and potential. Only at the San Gimignano UNESCO site, the landslide has also been identified as a current and negative geohazard (Table 3). At the Historic Center of San Gimignano and at the Medici Villas and Gardens, the origin of the threats is both inside and outside of the proprieties; at the Historic Center of Siena it is inside the Core Zone while at Piazza del Duomo it is outside. Only for the current and negative factors the UNESCO agency provides an assessment**.** Therefore, for the landside factor that affects the Historical Center of San Gimignano, the following parameters have been analyzed: spatial and temporal scale, impact, management response and trend. It is important to underline that no further information is provided in this table, e.g. the used methods to identify the factors or more details about their assessment.

Table 3. Sudden geological events listed in the UNESCO reports (II Cycle) of the Tuscan sites, modified from Pastonchi et al., 2018. A factors assessment is performed only for the current and negative ones.

UNESCO TUSCAN SITES	FACTORS SUMMARY TABLE							ASSESSMENT OF CURRENT NEGATIVE FACTORS				
	SUDDEN GEOLOGICAL EVENTS	IMPACT				ORIGIN		SPATIAL SCALE	TEMPORAL SCALE	IMPACT	MANAGMENT RESPONSE	TREND
		POSITIVE	NEGATIVE	CURRENT	POTENTIAL	INSIDE	OUTSIDE					
Historic Center of Siena	Earthquake		X		X	X						
Medici Villas and Gardens in Tuscany	Earthquake		X		X	X	X					
Historic Center of San Gimignano	Earthquake		X		X	X	X					
	Landslide		X	X		X	X	Restricted	Intermittent or sporadic	Significant	High capacity	Static
Piazza del Duomo, Pisa	Earthquake		X		X		X					

2.3.2 Geological setting

Tuscany has an extension of 22.994 km^2 including an island archipelago. Its territory is mainly hilly (66.5%), with mountainous areas (25.1%) and few plains (8.4%) (Rosi et al., 2012).

The geological setting of the Tuscany region is directly connected with the stacking process that formed, during the Tertiary, the Northern Apennines, developed following the closure of the

Ligurian Ocean (Figure 14). The emplacement of this mountain chain includes three main geological units: the Ligurian Unit that overlaps the Tuscan Unit, in turn overlaid by the Umbro-Marchigian Unit (Vai and Martini, 2001). These units belong to different paleo-geographic domains (Sub-Ligurian, Tuscan and Umbro-Marchigian), depending on their relative position in the pre-orogen Ligurian-Piedmontese Jurassic ocean (Bortolotti, 1992). The Tuscan Unit is subdivided into the Metamorphic Tuscan Unit and the Non-Metamorphic Tuscan Unit (Carmignani et al., 2001). The compression phase, which has defined the architecture of the Northern Apennines, was followed by an extensional regime. This led to a series of basins (Miocene-Pleistocene) subsequently filled by Neogene-Quaternary deposits. The extension was also accompanied by widespread Late Miocene-Quaternary magmatism. For an exhaustive explanation of these units see (Carmignani et al., 2013).

The peculiar geological setting makes the Tuscany Region prone to ground instability phenomena. In particular, this region is a very landslide-prone area (Lu et al., 2012), with ca. 91,700 landslides recognized. They are mainly slides (39%), followed by flows (14%) and fall (1%) and 46% of unclassified landslides (Rosi et al., 2018). In addition, several subsidence phenomena have been recognized in some areas of the Tuscany (Rosi et al., 2016).

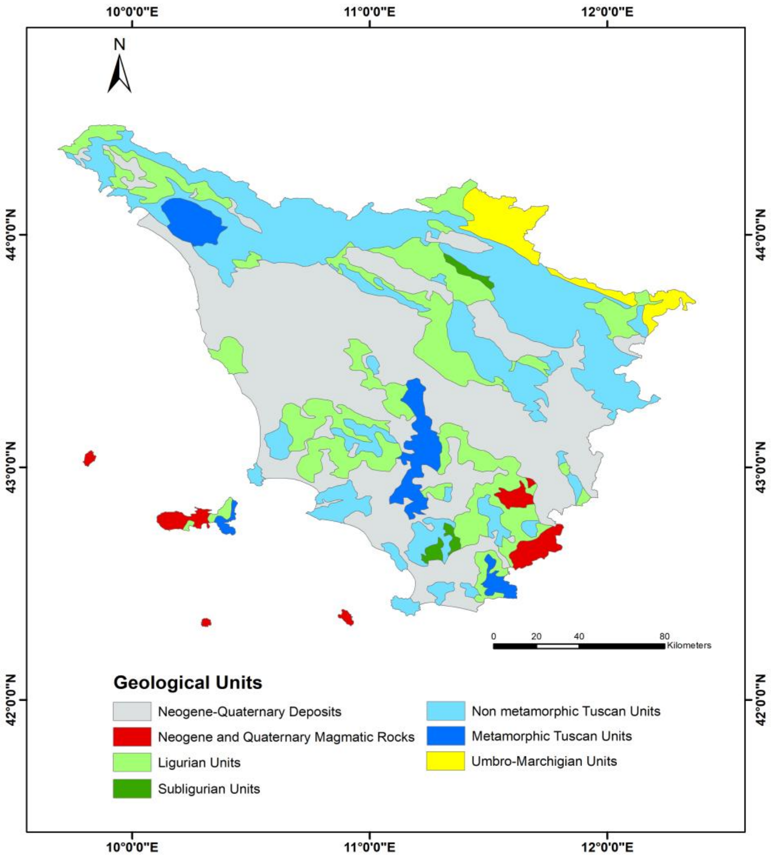

Figure 14. Lithostratigraphic units in the Tuscany Region. Modified from Fratini et al., 2014.

2.4 Data collection

2.4.1 UNESCO boundaries

Each World Heritage Site is characterized by a Core and a Buffer Zone, available at the UNESCO website (http://whc.unesco.org/en/list). These boundaries have been digitized in a GIS platform, in order to integrate them with the ADA.

The Historic Centers of San Gimignano and Pienza, unlike the other sites, are not currently provided with a Buffer Zone (see Table 2). By virtue of the fact that a Buffer Zone is necessary to guarantee the integrity of the Core Zone, new Buffer Zones for these two sites have been identified.

The project for the Buffer Zone of the Historic Center of Florence, proposed by Capitanio et al., 2017, approved by UNESCO on July 2015, was taken as example to define the new Buffer Zones. It is important to underline that this work has been done in a qualitative way, collecting all the necessary material in digital format, without carrying out on-site investigations. As indicated by Capitanio et al., 2017, in order to demarcate a Buffer Zone, it is necessary to analyze both the anthropic and natural system, as they are components potentially capable of altering the identity of a place, or, in case of a UNESCO site, of changing its Outstanding Universal Value. In this study, the following information and databases has been collected: use and land cover; infrastructure; hydrography and morphology; Sites of Regional Interest (Siti di Interesse Regionale-SIR); Protected Areas and Digital Terrain Models (DTM). Through the intersection of all these information in a GIS environment, considering that the new Buffer Zones must have a manageable and realistic dimension, i.e. with borders unambiguously recognizable on digital cartography (Martin and Piatti, 2009), two possible Buffer Zones for Historic Center of Pienza and San Gimignano, have been identified (4.569 ha and 5.800 ha, respectively).

According to Capitanio et al., 2017, between the natural and anthropic elements analyzed for the identification of the new Buffer Zone of the Historic Center of San Gimignano, the Castelvecchio Regional Protected Area stands out for its importance and, being very close to the San Gimignano Core Zone, has been included in its new Buffer Zone (see Figure 15).

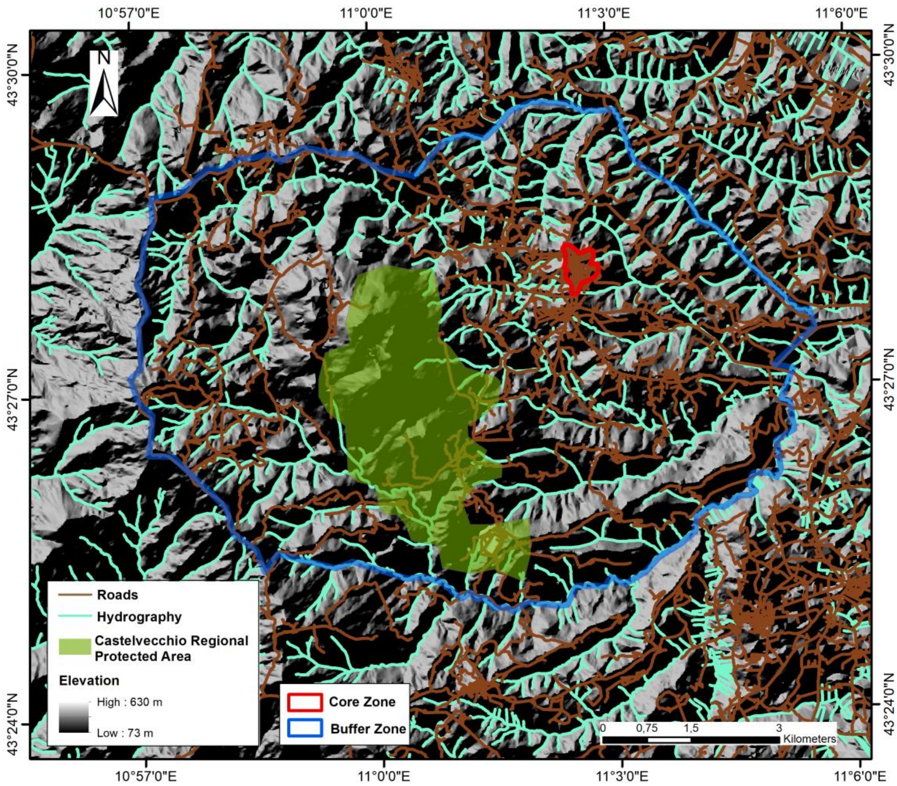

Figure 15. Buffer Zone for the Historic Center of San Gimignano (Pastonchi et al., 2018), identified in a qualitative way taking into account the following elements: Digital Terrain Model (DTM) in shaded relief, Roads, Hydrography and Protected Areas (downloaded from http://www502.regione.toscana.it/geoscopio/cartoteca.html).

2.4.2 The Influence Zones: new boundaries

For a more reliable protection of the UNESCO sites, the territory outside the Buffer Zones has also been analyzed through the creation of new areas: the Influence Zones (Pastonchi et al., 2018). This innovative idea arises from the awareness that a territory is no longer a static reality, but the continuous evolution of the environment by the hand of man and nature, makes it a dynamic and more vulnerable system. Within such a dynamic reality, it is necessary to extend the monitoring of geological risks also to the territory immediately close to the Buffer Zones. The safeguard of this territory play a fundamental role in guaranteeing the Outstanding Universal Value of UNESCO sites. The new Influence Zones have been therefore created according to the following criteria. For the Medici Villas and Gardens, that have smaller Buffer Zones with respect to the other cultural sites (See Table 2), the Influence Zones surround the Buffer Zones within a 500 m range, whereas for the others proprieties, a distance of 1 km has been used. Only the distance from the Buffer Zones was considered in this phase since natural and anthropic factors, which can considerably modify the stability of cultural sites, have been analyzed by the UNESCO for the delimitation of Buffer Zones (see Section 2.4.1).

2.4.3 Satellite datasets

In this study, the proposed procedure has been applied over the entire Tuscany Region by using as input-data two PSI-derived velocity maps (Pastonchi et al., 2018). The original datasets are C-band SAR datasets, acquired by the satellites Envisat and Sentinel-1 covering a total period of 10 years (Table 4). These datasets have been chosen in order to obtain a monitored period similar to the one chosen by UNESCO to update its reports (every six years). Envisat data have been processed in the framework of the PST-A Project (Piano Straordinario di Telerilevamento), thanks to the combined effort of the private companies Telespazio and Tre-Europa. This project aimed at covering the entire national territory with interferometric products; the goal was achieved by combining PSP (Persistent Scatterer Pairs) and PSInSAR algorithms (Costantini et al., 2017). The reliability of these interferometric datasets has successfully been proven by other authors in other Italian case studies (e.g., Peduto et al., 2015; Pratesi et al., 2015). Sentinel-1 data have been recently analyzed with the SqueeSAR algorithm (Ferretti et al., 2015), in the framework of a regional project aimed at frequently updating the knowledge of active ground motions over Tuscany by means of interferometric products (Raspini et al., 2018). Both datasets have been processed in ascending and descending orbits (see Table 4 for details), guaranteeing a better "radar interpretation" of the obtained results (Farina et al., 2007).

Table 4. Time period, spatial resolution cell of the SAR datasets used to extrapolate PS, and standard deviation of all the velocity measurements for each satellite datasets. From Pastonchi et al., 2018.

Dataset	Satellite	Orbit	Time Period	Spatial resolution (m)	Standard deviation (mm/yr)
1	Sentinel-1	Ascending	2014 - 2017	14 x 4	1.6
2	Sentinel-1	Descending	2014 - 2017	14 x 4	1.5
3	Envisat	Ascending	2003 - 2010	20 x 20	2.0
4	Envisat	Descending	2003 - 2010	20 x 20	2.2

2.4.4 Landslides and ground-subsidences inventories

In order to discriminate and characterize the slow-kinematic geohazard that triggered the deformation areas, it is necessary to intersect the ADA databases with the most updated geohazards inventories. For this purpose, the maps of hydrogeological instabilities of Tuscany Region (with regard to landslides and ground-subsidences), made starting from 2009 and completed in 2013 by the Earth Science Department of the University of Florence (Casagli et al., 2009; Casagli et al., 2013), have been used. These maps have been performed through the interpretation of PSI data (ERS ½ and Envisat data, which cover the 1992-2000 and 2003-2010 time intervals, respectively, and are freely distributed by the Italian government), and several environmental ancillary data (e.g., DTM, lithological and topographic map).

Around 91.700 landslides on the entire Tuscany Region were thus localized (Figure 16), indicating furthermore their average velocity, type of movement and activity status.

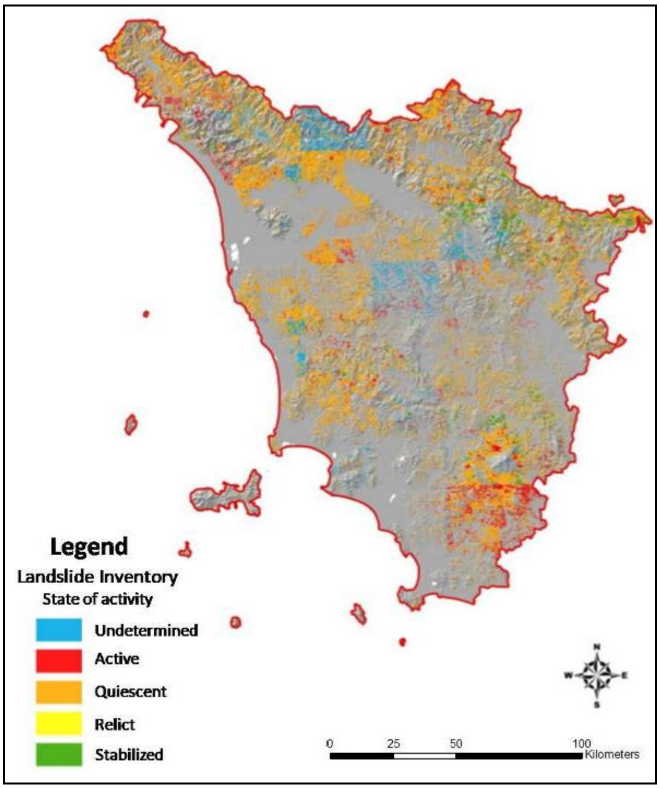

Figure 16. Landslides inventory of Tuscany Region, modified from Casagli et al., 2013.

Regarding the ground-subsidence phenomena, some moving areas have been identified over the region, as shown in Figure 17a. In this picture, it is possible to recognize clearly that the major displacements are localized in the western part of the region. The only significant uplift was identified in the city of Prato (North of Tuscany).

In addition to these areas, a series of local ground-subsidences have been recognized. Their dimensions turned out to be too small to be mapped on a regional scale, so, they have been organized in another database. In total, 100 areas affected by local subsidences have been recognized, and they are mainly located, as expected, in flat areas (Figure 17b).

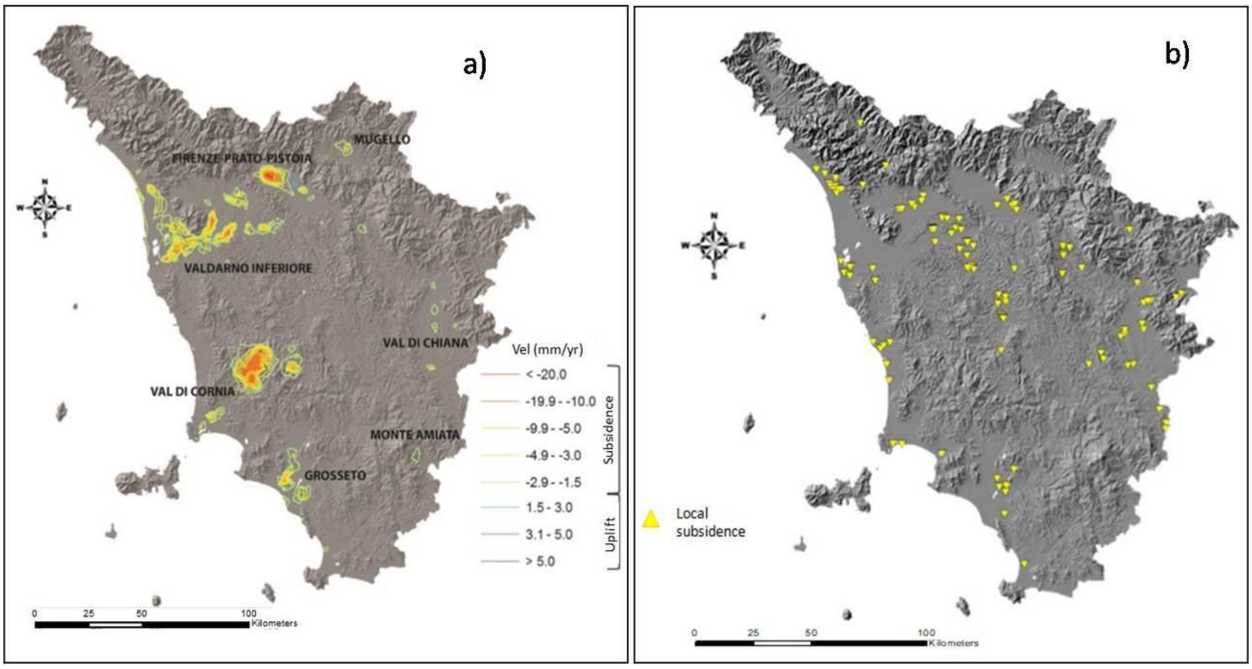

Figure 17. Ground-subsidences inventories of Tuscany Region: a) regional scale; b) local scale. Modified from Casagli et al., 2013.

2.5 Results

2.5.1 The first step of ADA identification

Table 5 reports some basic information regarding the PSI datasets within each UNESCO Tuscan heritage site, in terms of mean and maximum velocity, and number of Active Points (APs) (Pastonchi et al., 2018). These points have been identified through the workflow illustrated at Section 2.2.1 (Figure 10). The obtained results are clearly influenced by the type and dimension of the UNESCO contour analyzed. In fact, the Villas of Il Trebbio, Cafaggiolo and Careggi, and the Seravezza Palace do not register PS for some datasets within the contour of their Core Zone. It’s important to underline that the maximum velocity value is sometimes less representative of an active motion, i.e., being included or not into an ADA, because it can be related to deformation outliers, not triggered by a geohazard. The most important parameter shown in Table 5 is the number of APs; it is a proxy for a-priori knowledge of the potential presence of ADA. In fact, if the number of APs is high, especially within small contours, it is more probable that the moving points will be grouped in one or more ADA. The variation of this number can be an index of a temporal variation of a certain phenomenon; for example a strong reduction or increment of APs have been found in the case of the Buffer and Transition Zones of the Historic Centers of Pisa and Florence, and in all the three zones of the Val d'Orcia UNESCO heritage.

Table 5. Mean, max velocities and number of APs for each UNESCO heritage site in Tuscany. The velocity fields units are mm/year in absolute value. nd = no data. From Pastonchi et al., 2018.

UNESCO SITE	CORE ZONE				BUFFER ZONE				INFLUENCE ZONE			
	Satellite	|Vel max|	|Mean vel|	APs	Satellite	|Vel max|	|Mean vel|	APs	Satellite	|Vel max|	|Mean vel|	APs
Historic Center of Florence	Env Asc	4.5	0.44	13	Env Asc	9.3	0.59	314	Env Asc	17.3	1.05	455
	Env Desc	5.2	0.42	10	Env Desc	13.4	0.64	622	Env Desc	17.6	0.95	527
	SNT Asc	2.9	0.98	0	SNT Asc	7.2	0.71	75	SNT Asc	8.7	0.98	437
	SNT Desc	2,0	0.35	0	SNT Desc	7,0	0.44	64	SNT Desc	7.9	0.8	205
Historic Center of Siena	Env Asc	4.9	0.58	6	Env Asc	7.7	0.74	144	Env Asc	7.2	0.73	94
	Env Desc	5,0	0.48	5	Env Desc	5.4	0.56	42	Env Desc	6.8	0.67	40
	SNT Asc	2.4	0.75	0	SNT Asc	8.3	0.62	45	SNT Asc	8.7	0.64	17
	SNT Desc	2.3	0.54	0	SNT Desc	5.4	0.54	35	SNT Desc	8.4	0.64	27
Cafaggiolo Villa	Env Asc	0.7	0.41	0	Env Asc	3.7	0.5	0	Env Asc	5.1	0.78	2
	Env Desc	nd	nd	nd	Env Desc	1.4	0.37	0	Env Desc	3.8	0.52	0
	SNT Asc	1.5	1.5	0	SNT Asc	2.3	1.18	0	SNT Asc	10.6	1.14	2
	SNT Desc	nd	nd	nd	SNT Desc	2.3	0.81	0	SNT Desc	2.2	0.56	0
Il Trebbio Villa	Env Asc	nd	nd	nd	Env Asc	3.7	0.5	0	Env Asc	5.1	0.77	2
	Env Desc	nd	nd	nd	Env Desc	1.4	0.37	0	Env Desc	3.8	0.53	0
	SNT Asc	0.8	0.8	0	SNT Asc	2.3	1.18	0	SNT Asc	10.6	1.14	2
	SNT Desc	0.7	0.35	0	SNT Desc	1.5	0.6	0	SNT Desc	2.3	0.57	0
Careggi Villa	Env Asc	1.9	0.62	0	Env Asc	3.9	0.61	0	Env Asc	4.5	0.41	2
	Env Desc	nd	nd	nd	Env Desc	3.9	0.64	0	Env Desc	4.6	0.58	4
	SNT Asc	1.8	0.66	0	SNT Asc	1.8	0.5	0	SNT Asc	3.1	0.48	1
	SNT Desc	0.6	0.31	0	SNT Desc	1.5	0.4	0	SNT Desc	2.9	0.47	0
Medici of Fiesole Villa	Env Asc	1.2	0.5	0	Env Asc	1.8	0.44	0	Env Asc	4,0	0.44	0
	Env Desc	1.1	0.57	0	Env Desc	2.5	0.46	0	Env Desc	4,0	0.46	1
	SNT Asc	0.9	0.35	0	SNT Asc	1.7	0.42	0	SNT Asc	2.5	0.62	0
	SNT Desc	1.4	0.92	0	SNT Desc	1.6	0.52	0	SNT Desc	2,0	0.46	0
Castello Villa	Env Asc	0.7	0.31	0	Env Asc	5.2	0.62	6	Env Asc	4.6	0.6	7

	Env Desc	0.7	0.32	0	Env Desc	4.8	0.69	4	Env Desc	5.2	0.57	5
	SNT Asc	1.7	0.55	0	SNT Asc	2.6	0.56	0	SNT Asc	3.6	0.66	2
	SNT Desc	0.6	0.22	0	SNT Desc	1.9	0.43	0	SNT Desc	4.3	0.52	1
Poggio a Caiano Villa	Env Asc	1.2	0.37	0	Env Asc	4.4	0.44	3	Env Asc	4.2	0.47	3
	Env Desc	2.1	0.48	0	Env Desc	4.2	0.7	6	Env Desc	4.1	0.58	1
	SNT Asc	1.2	0.69	0	SNT Asc	1.8	0.79	0	SNT Asc	5.4	0.9	1
	SNT Desc	1.6	0.66	0	SNT Desc	1.7	0.73	0	SNT Desc	2,0	0.79	0
La Petraia Villa	Env Asc	1.5	0.29	0	Env Asc	5.2	0.62	6	Env Asc	4.6	0.6	7
	Env Desc	1.5	0.55	0	Env Desc	4.8	0.69	4	Env Desc	5.2	0.57	5
	SNT Asc	1.5	0.36	0	SNT Asc	2.6	0.56	0	SNT Asc	3.6	0.66	2
	SNT Desc	0.7	0.14	0	SNT Desc	1.9	0.43	0	SNT Desc	4.3	0.52	1
Boboli Garden	Env Asc	2.9	0.47	0	Env Asc	3.3	0.55	0	Env Asc	4.7	0.5	3
	Env Desc	4,0	0.34	0	Env Desc	4,0	0.65	2	Env Desc	6.5	0.51	4
	SNT Asc	1.3	0.54	0	SNT Asc	2.3	0.73	0	SNT Asc	3.1	0.91	1
	SNT Desc	1.3	0.4	0	SNT Desc	2,0	0.43	0	SNT Desc	2.9	0,0	0
Cerreto Guidi Villa	Env Asc	0.7	0.42	0	Env Asc	4.6	0.73	6	Env Asc	5.2	0.53	1
	Env Desc	0.7	0.32	0	Env Desc	1.5	0.47	0	Env Desc	2.6	0.51	0
	SNT Asc	1.7	1.51	0	SNT Asc	1.7	1,0	0	SNT Asc	5.4	1.09	3
	SNT Desc	1,0	0.82	0	SNT Desc	1,0	0.58	0	SNT Desc	2.9	0.73	0
Seravezza Palace	Env Asc	nd	nd	nd	Env Asc	2.4	0.38	0	Env Asc	5.1	0.54	2
	Env Desc	nd	nd	nd	Env Desc	1.33	0.29	0	Env Desc	4.1	1,0	6
	SNT Asc	0.6	0.42	0	SNT Asc	2.2	1.07	0	SNT Asc	5.3	0.8	1
	SNT Desc	1.3	1.1	0	SNT Desc	2.3	1.5	0	SNT Desc	7.5	1.11	18
Pratolino Garden	Env Asc	0.8	0.3	0	Env Asc	3.4	1.2	0	Env Asc	7.5	0.97	12
	Env Desc	3.1	1.19	0	Env Desc	3.1	0.51	0	Env Desc	4.8	0.64	3
	SNT Asc	0.3	0.3	0	SNT Asc	0.7	0.42	0	SNT Asc	4.4	0.6	2
	SNT Desc	0.9	0.52	0	SNT Desc	1.4	0.55	0	SNT Desc	2.2	0.62	0
La Magia Villa	Env Asc	0.9	0.28	0	Env Asc	1.9	0.41	0	Env Asc	4.7	0.42	1
	Env Desc	1.1	nd	0	Env Desc	2.8	0.85	0	Env Desc	5.4	0.5	2
	SNT Asc	1.5	1.22	0	SNT Asc	2.6	1.68	0	SNT Asc	3.3	1.55	3
	SNT Desc	1.2	0.78	0	SNT Desc	2.5	1.31	0	SNT Desc	4.1	1.21	8
Artimino	Env Asc	0.2	0.2	0	Env Asc	3.2	0.8	0	Env Asc	4.4	0.67	1

Villa												
	Env Desc	0.9	0.43	0	Env Desc	5.4	0.59	3	Env Desc	5.6	0.66	4
	SNT Asc	1,0	1,0	0	SNT Asc	2.6	0.79	0	SNT Asc	2.3	0.58	0
	SNT Desc	0.3	0.2	0	SNT Desc	3.2	0.59	0	SNT Desc	3.3	0,0	2
Poggio Imperiale Villa	Env Asc	2.3	0.86	0	Env Asc	5.9	0.61	5	Env Asc	6.1	0.61	4
	Env Desc	0.4	0.25	0	Env Desc	6.5	0.52	4	Env Desc	4.2	0.57	1
	SNT Asc	0.9	0.44	0	SNT Asc	2.4	0.49	0	SNT Asc	3.9	0.58	3
	SNT Desc	1.3	0.61	0	SNT Desc	1.8	0.41	0	SNT Desc	2.9	0.74	0
Historic Center of San Gimignano	Env Asc	2.1	0.46	0	Env Asc	5.2	0.61	4	Env Asc	8.2	0.95	47
	Env Desc	2.9	0.39	0	Env Desc	6.5	0.63	5	Env Desc	7.3	1.13	50
	SNT Asc	1.4	0.69	0	SNT Asc	6.2	0.89	29	SNT Asc	11.1	1,0	12
	SNT Desc	1,0	0.37	0	SNT Desc	5.1	0.78	22	SNT Desc	5.4	0.77	8
Piazza del Duomo, Pisa	Env Asc	3.2	0.87	0	Env Asc	6.4	1.41	27	Env Asc	19,0	3.16	1687
	Env Desc	4,0	1.02	2	Env Desc	6.4	1.69	34	Env Desc	13.4	3.3	1742
	SNT Asc	2.2	1.56	0	SNT Asc	2.7	0.88	0	SNT Asc	7.1	0.97	213
	SNT Desc	2.1	1.21	0	SNT Desc	2.9	0.93	0	SNT Desc	7.1	0.92	164
Historic Center of the City of Pienza	Env Asc	1.1	0.25	0	Env Asc	3.7	0.55	0	Env Asc	5.5	0.74	1
	Env Desc	1.2	0.55	0	Env Desc	5.7	0.69	15	Env Desc	6.2	0.88	8
	SNT Asc	0.9	0.58	0	SNT Asc	6.9	0.9	13	SNT Asc	5.6	0.98	9
	SNT Desc	1.1	0.5	0	SNT Desc	3.9	0.72	4	SNT Desc	3.4	0.83	1
Val d'Orcia	Env Asc	6,0	0.76	226	Env Asc	5.6	10025,0	9	Env Asc	5.3	5017,0	8
	Env Desc	7.9	0.78	158	Env Desc	6.2	11325,0	38	Env Desc	6.2	5681,5	16
	SNT Asc	19.2	1.28	468	SNT Asc	15.2	7025,0	102	SNT Asc	11.7	3563,5	96
	SNT Desc	29.4	1.11	416	SNT Desc	8.9	4.45	74	SNT Desc	7,0	40,5	99

2.5.2 Identification of ADA within the UNESCO Tuscan sites

The extraction of ADA has been performed on each boundary (Core, Buffer and Influence Zones) of every UNESCO heritage site, in order to create simple databases of this data. Thus, the PS datasets considered are the ones reported in Table 5 (Pastonchi et al., 2018). Each result, shown in Table 6, includes the number of ADA extracted both in ascending and descending orbit for each of the two datasets. As visible from Table 6, ADA have been extracted only in some of the 20 UNESCO Tuscan sites and, particularly, the only Core Zone in which ADA are present is in Val d'Orcia. The greatest number of ADA has been identified through the Envisat dataset in the Buffer and Influence Zones of the Historic Center of Florence, with 82 ADA and 96 ADA respectively, and in the Influence Zone of Piazza del Duomo, where 411 ADA, have been extracted. Furthermore, it is important to underline that the lack of ADA does not univocally mean the absence of movement, but it could be due to satellite information unavailability (Barra et al., 2017).

Table 6. Number of ADA extracted from Envisat and Sentinel-1 datasets within the boundaries of the UNESCO Tuscan sites. N° = number of ADA. Modified from Pastonchi et al., 2018.

UNESCO TUSCAN SITES	N° OF ADA EXTRACTED FROM ENVISAT DATA			N° OF ADA EXTRACTED FROM SENTINEL-1 DATA		
	CORE ZONE	BUFFER ZONE	INFLUENCE ZONE	CORE ZONE	BUFFER ZONE	INFLUENCE ZONE
Historic Center of Florence		82	96		7	56
Historic Center of Siena		11	15		2	1
Cerreto Guidi Villa						1
Seravezza Palace			2			2
Pratolino Garden			1			
La Magia Villa						1
Poggio Imperiale Villa			1			
Historic Center of San Gimignano			6			
Piazza del Duomo, Pisa		8	411			34
Historic Center of Pienza			2		2	1
Val d'Orcia	21	2		30	6	2

2.5.3 Characterization of ADA within the UNESCO Tuscan sites

Trough the previous step, it has been possible only to identify the number of critical movements that threaten and have threatened the Tuscan cultural sites, but this practice does not allow unequivocally recognizing the typology of slow-kinematic geohazard that triggered the ADA. In order to overcome this limit, the ADA databases have been intersected with the available ground-subsidences and landslides inventories of Tuscany Region (Casagli et al., 2013; see Section 2.4.4) on a GIS environment. The intersections between these data are shown in Table 7, where it can be observed that they are present only in five cultural sites.

Table 7. Number of ADA extracted from Envisat and Sentinel-1 datasets that intersect the landslides (LI) and the ground-subsidence (GSI) inventories.

UNESCO TUSCAN SITES	INTERSECTION OF ENVISAT ADA WITH GEOHAZARDS INVENTORIES						INTERSECTION OF SENTINEL-1 ADA WITH GEOHAZARDS INVENTORIES					
	CORE ZONE		BUFFER ZONE		INFLUENCE ZONE		CORE ZONE		BUFFER ZONE		INFLUENCE ZONE	
	LI	GSI	LI	GSI	LI	GSI	LI	GSI	LI	GSI	LI	GSI
Historic Center of Florence				70		90			1	1		46
Seravezza Palace					1						2	
Piazza del Duomo, Pisa				8		411						34
Historic Center of Pienza					2							
Val d'Orcia	11						4					

Regarding the Envisat dataset, at the cultural site of Piazza del Duomo (Pisa), all the ADA extracted in the previous step intersect a wide ground-subsidence zone cataloged in the inventory at regional scale (Figure 18a, Table 6 and Table 7), as well as most of the ADA identified within the NW part of the Florence Buffer and Influence Zone (intersection with the inventory both at regional and local scale, Figure 18b).

Within Seravezza Palace and Val d'Orcia sites, some ADA intersect the landslides inventory, as well as the only two ADA identified in the Influence Zone of Pienza. All these ADA intersect an active landslide, except four of them, localized in Val d'Orcia, that intersect quiescent landslides.

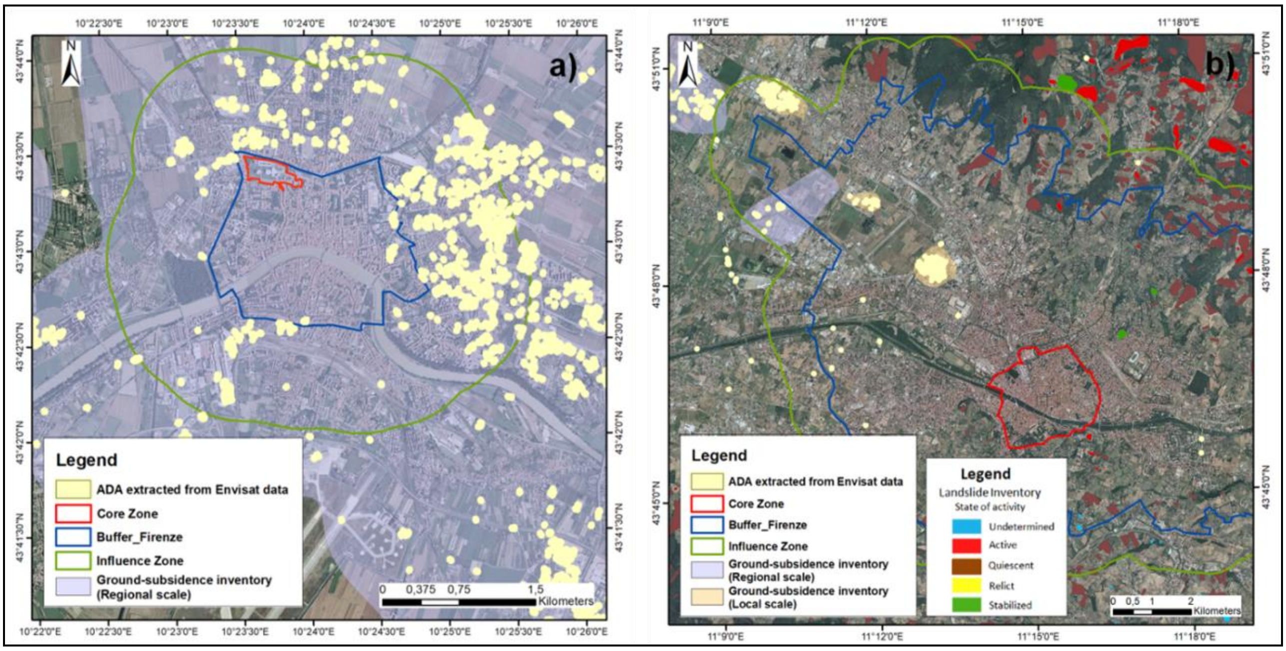

Figure 18. Overlap of ADA extracted from Envisat dataset with the geohazards inventory (Casagli et al., 2013), at Piazza del Duomo, Pisa (a), and Historic Center of Florence (b). ADA that do not intersect any inventory are also visible.

Through the intersection of geohazards inventory with the ADA extracted from Sentinel-1 data, only within Piazza del Duomo of Pisa and Seravezza Palace, all the ADA are cataloged: they intersect ground-subsidences (regional scale; Figure 19a) and landslides inventory, respectively. In Florence, within its Buffer Zone, one ADA is associated with a landslide (quiescent landslide), and another one with ground-subsidence phenomenon (identified at local scale), while within its Influence Zone most of the identified ADA intersect ground-subsidences inventory (both at local and regional scale, Figure 19b).

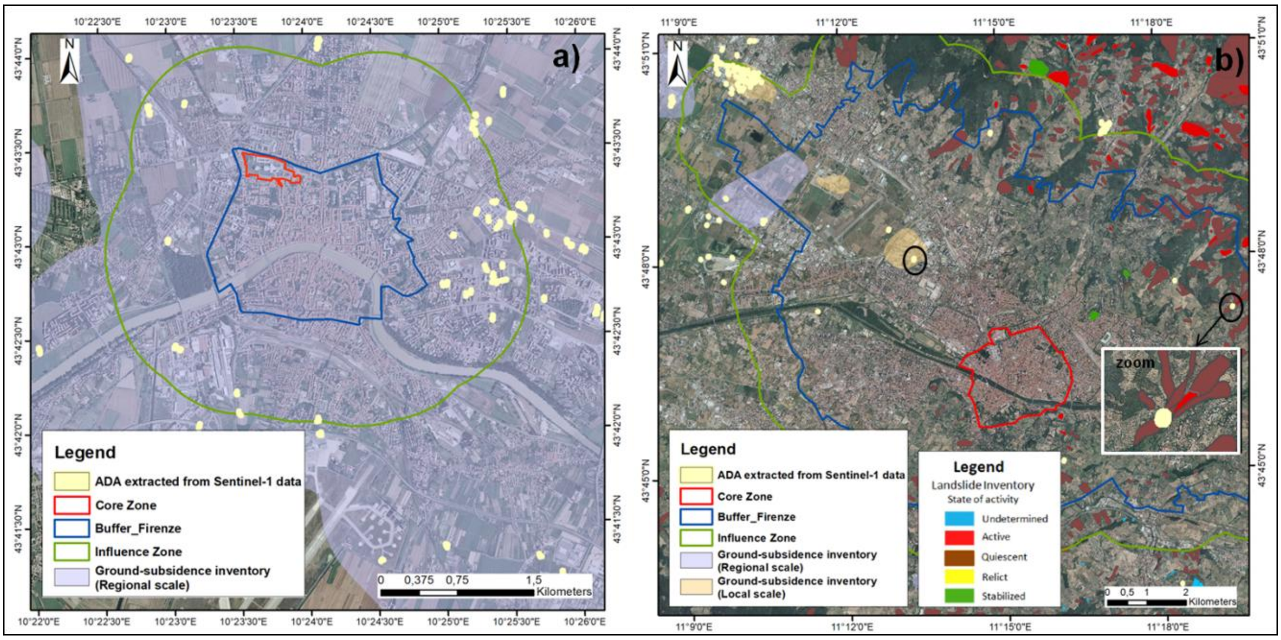

Figure 19. Overlap of ADA extracted from Sentinel-1 dataset with the geohazards inventory (Casagli et al., 2013), at Piazza del Duomo, Pisa (a), and Historic Center of Florence (b). The black circles in picture b highlight the ADA that intersect a ground-subsidence (local scale) and a quiescent landslide. ADA that do not intersect any inventory are also visible.

Within the Core Zone of Val d'Orcia, only 4 of the 30 identified ADA are localized on cataloged landslides: 2 of them are active landslides while the other 2 are quiescent landslides (Figure 20). Finally, at the cultural site of Seravezza, the two identified landslides phenomena are active.

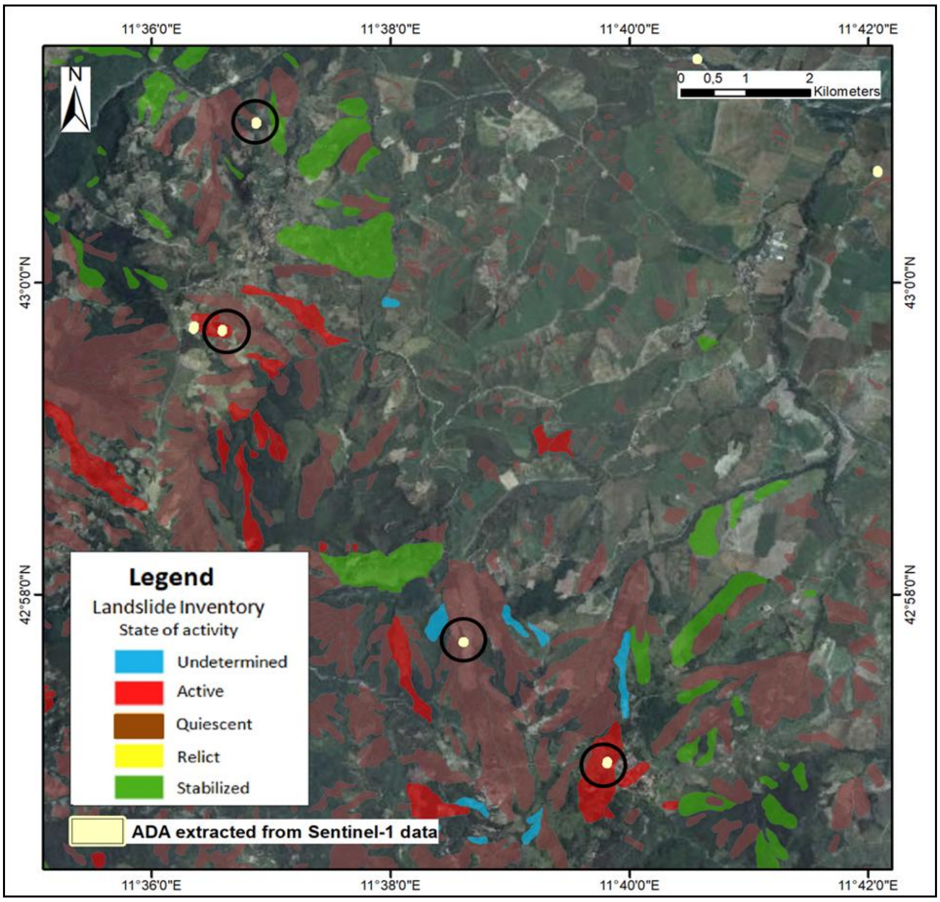

Figure 20. Overlap of ADA extracted from Sentinel-1 dataset with landslides inventory (Casagli et al., 2013) at the Core Zone of Val d'Orcia. The black circles highlight the ADA that intersect quiescent and active landslides. One ADA that does not intersect the inventory is also visible.

As visible from the comparison between Table 6, Table 7, and in Figure 18, Figure 19, and Figure 20, not all the identified ADA intersect the geohazards inventories. Furthermore, the ADA, that are active movements, in some cases intersect quiescent landslides. All of these can be attributed to the fact that the used inventory was drawn up both through a satellite dataset (ERS ½ data) whose time interval is previous to the ones here used to extract the ADA, and through the additional use of several ancillary data that has allowed identifying geohazards also where, with the use of the only satellite data, is impossible (e.g., vegetated areas).

Therefore, in order to better characterize all the ADA and evaluate in situ their impact on the cultural heritage sites, a simple check-list, called ICA, has been expressly created, also with the aim of simplifying the surveys to the UNESCO operators (see Section 2.2.2).

Not being possible to characterize all the Envisat ADA, as these areas indicate where the movements were active in the past, the ICA of the most critical ADA extracted from Sentinel-1 database (current update) in the Core Zone of Val d'Orcia are later shown as examples.

The choice fell on the Core Zone of Val d’Orcia because it is the only Core Zone where some ADA have been extracted.

The Val d’Orcia has been named a cultural heritage site on 2004, by virtue of the remodeling of its landscape made by man in the 14th and 15th centuries, in order to reflect an idealized model of good governance and to create an aesthetically pleasing image that has inspired many painters and artists (Figure 21).

Figure 21. Val d’Orcia UNESCO site landscape.

From a geological point of view, most part of the Val d’Orcia site is located within a NW – SE elongated tectonic depression, filled with Plio-Pleistocene marine and continental deposits predominantly made of clays and silty clays. The Quaternary tectonic uplift has subsequently led to deep valley downcutting and intensive slope denudation. This area, furthermore, is currently affected by recent and active landslides, solifluction, and creep (Vergari et al., 2011; Aucelli et al., 2016).

Most of the ADA extracted in the Core Zone of Val d’Orcia are located in not accessible private properties or industrial buildings and along the bed of the Ombrone and Orcia Rivers. These latter active movements have been attributed to the fluvial dynamics and therefore they have not been investigated in this study.

Thus, because of these limitations, the two ADA located in active landslides (those situated in quiescent landslides are in not accessible areas), and three of the ADA with the highest absolute velocity values (Figure 22), have been chosen to be analyzed through in situ surveys (carried out on 3 and 22 July 2018).

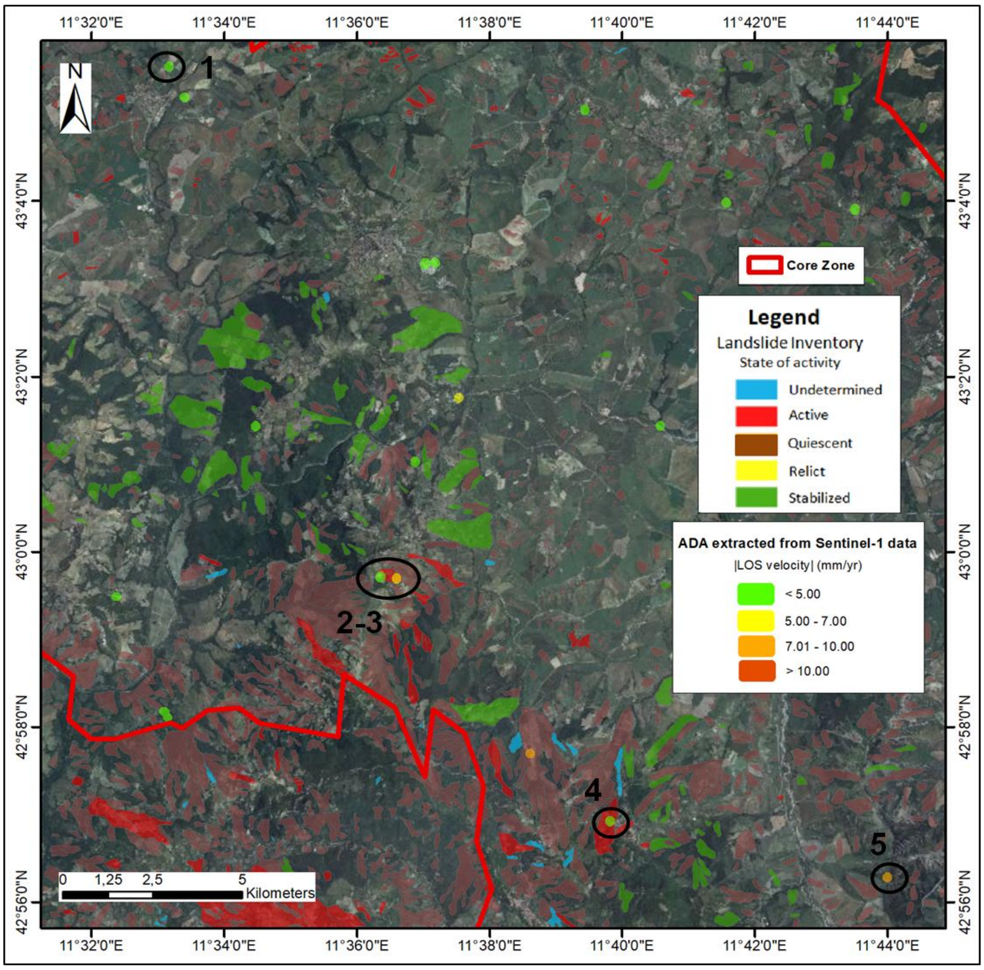

Figure 22. Localization of the ADA where in situ investigations were carried out (circled in balck).

The northernmost ADA (n°1 in Figure 22) is located in Montalcino Municipality, and it covers an accessible private building used for agricultural activity, a country road and a portion of the adjacent olive grove (Figure 23a). The on-site observations made in these areas have shown the presence of some deformations on the structure (Figure 23b-c), in addition to the presence of consolidation works implemented through the use of metal chains (Figure 23d).

No damage is currently present on the road but, in the nearby fields, a landslide has been identified through the misalignment of some olive trees and, as reported by the owner of the land, this phenomenon has occurred slowly over the years (Figure 23e). From the analysis of Sentinel-1 data through the ADA methodology, it is therefore clear that this movement is still active with a velocity value of 4.7 mm/yr. This ground movement is more evident from satellite images (Figure 23f), where it is possible to observe two rows of olive trees that no longer follow the classic straight line layout. All of these informations have been noted on the ICA of this area (Table 8).

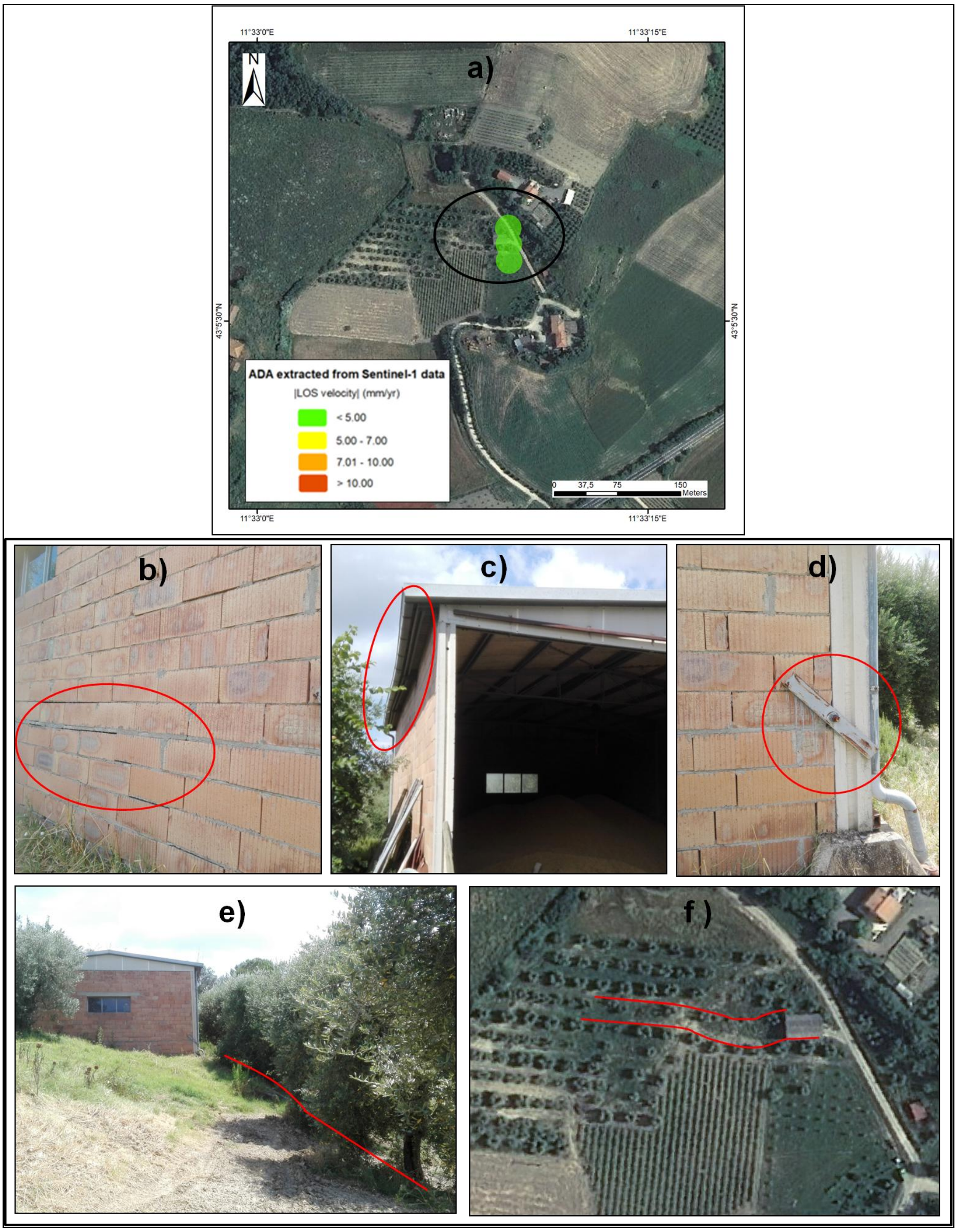

Figure 23. a) Localization of the northernmost ADA; b-c) damages on the structure (circled in red); d) consolidation works (circled in red); e-f) misalignment of some olive trees highlighted by red lines.

Table 8. ICA of the ADA n°1 in Figure 22.

ICA - IDENTITY CARD of ADA							
Date: 22/07/2018				Operator: Laura Pastonchi			
1. LOCATION AND FEATURES OF ADA							
Name of WHS: ***VAL D'ORCIA***					ID number: **1026rev**		
Nation: ***ITALY***		Province: ***SIENA***			Municipality: ***MONTALCINO***		
Governmental Institution responsible for the Property: ***Ministry for Cultural Heritage and Activities***				Property manager / Coordinator, Local Institution / Agency: ***SRL Val d'Orcia***			
ADA coordinate (WGS-84)		ADA situated in			Satellite characteristic		
Latitude	Longitude	Core zone	Buffer zone	Influence zone	Sensor	Orbit	Time Period
43°5' 33"	*11°33' 10"*	***X***			***Sentinel-1***	***Ascending***	***2014-2017***
ADA velocity: ***4.7 mm/yr***				ADA areal extension: ***715 m²***			

2. INTERSECTION OF ADA WITH OTHER DATA						
With other ADA from previous update	Yes ☐					No ☒
	Satellite sensor	Satellite orbit	Satellite time period	ADA velocity (mm/yr)	ADA areal extension (m²)	
With geohazards inventory	Yes ☐					No ☒
	Landslides Inventory ☐ Inventory name: Description of Phenomenon:			Subsidence Inventory ☐ Inventory name:........ Description of Phenomenon:........		
With geological cartography	Name/Number: ***Section n° 308110 (CARG Project)*** Outcropping lithologies: ***Clays and silty clays***					

3. ELEMENTS AT RISK				
Buildings ☒	Transport or service infrastructures ☒	Agricultural and industrial territories ☒	Natural environments ☐	Water bodies ☐
Category:	Category: ***Country road***	Category: ***Olive grove***	Category:	Category:

4. DAMAGES ASSESSMENT				
☒ Damages on buildings and infrastructures			☐ No damages	Notes: **Consolidation works Picture n°23d**
Observations: ***Deformation on the masonry structure***		Picture n° **23b-c**		
☒ Damages on natural ground surface and on water bodies			☐ No damages	Notes:
Observations: ***Landslide on the olive grove***		Picture n° **23e-f**		

The ADA n°2, with an absolute velocity value of 6.9 mm/yr, has been identified in an active landslide at the Castiglione d'Orcia Municipality (see Figure 22). This ground deformation currently threatens a private building and the adjacent agricultural territory used as olive grove (Figure 24a). The field surveys carried out in proximity to the building, have highlighted the presence of thin cracks under the roof and some open and perpendicular fractures within the sidewalk (Figure 24b-c).

The agricultural territory, being strongly reshaped by the hand of man, did not show evidence attributable to active landslides (Table 9).

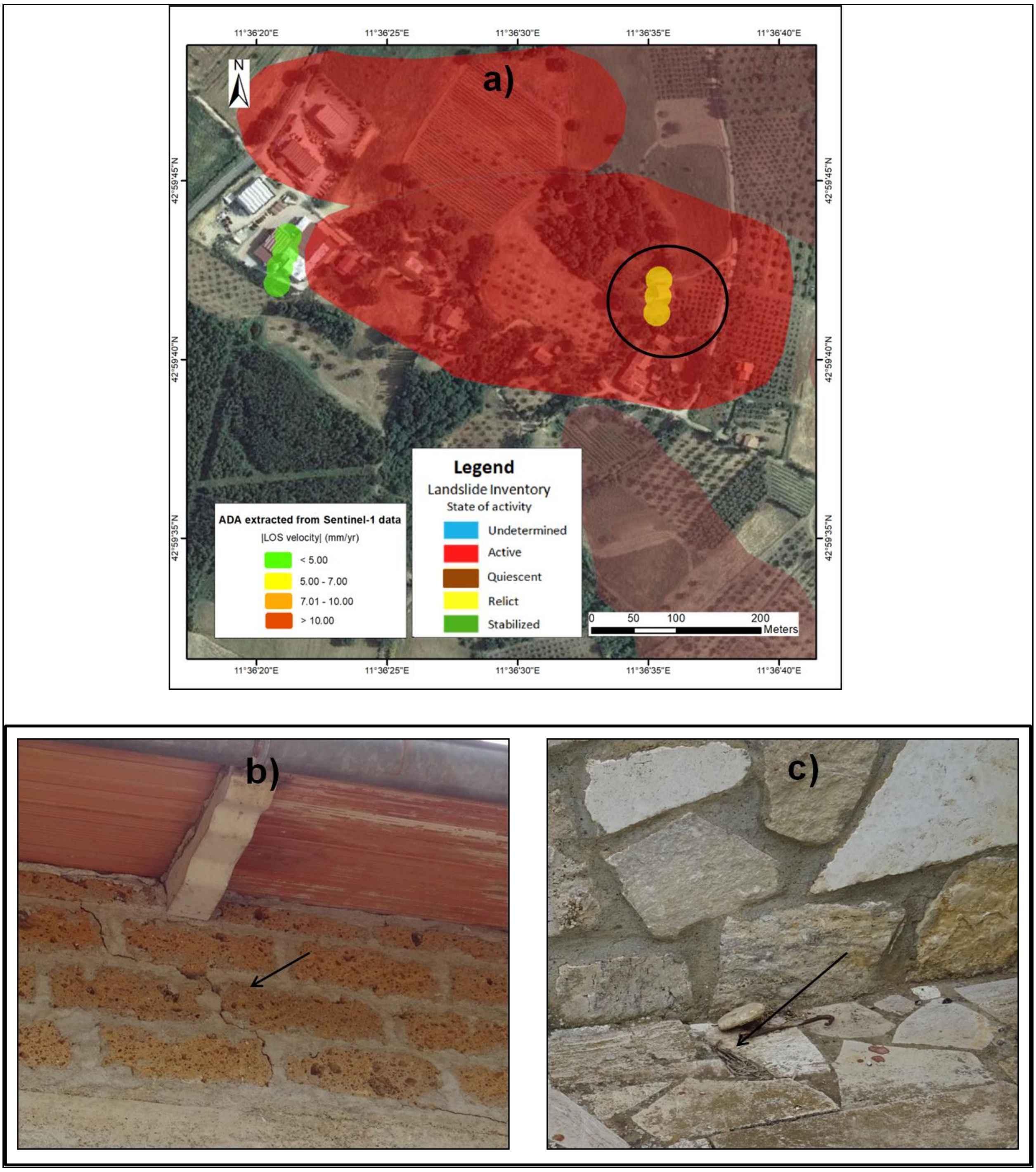

Figure 24. a) Localization of the second surveyed ADA (see Figure 22); b-c) Damages found on the private building threatened by the ADA.

Table 9. ICA of the ADA n°2 (see Figure 22), localized in an active landslide.

ICA - IDENTITY CARD of ADA	
Date: 03/07/2018	Operator: Laura Pastonchi

1. LOCATION AND FEATURES OF ADA

Name of WHS: ***VAL D'ORCIA***		ID number: **1026rev**
Nation: ***ITALY***	Province: ***SIENA***	Municipality: ***CASTIGLIONE D'ORCIA***
Governmental Institution responsible for the Property: ***Ministry for Cultural Heritage and Activities***		Property manager / Coordinator, Local Institution / Agency: ***SRL Val d'Orcia***

ADA coordinate (WGS-84)		ADA situated in			Satellite characteristic		
Latitude	Longitude	Core zone	Buffer zone	Influence zone	Sensor	Orbit	Time Period
42° 59' 42''	***11° 36' 35''***	***X***			***Sentinel-1***	***Ascending***	***2014-2017***

ADA velocity: **6.9** ***mm/yr***	ADA areal extension: ***720 m²***

2. INTERSECTION OF ADA WITH OTHER DATA

With other ADA from previous update	Yes [ ]					No [X]
	Satellite sensor	Satellite orbit	Satellite time period	ADA velocity (mm/yr)	ADA Areal extension (m²)	

With geohazards inventory	Yes [X]		No [ ]
	Landslides Inventory [X] Inventory: ***Landslides inventory of Tuscany (Casagli et al., 2013)*** Description of Phenomenon: ***Active landslide (6,6 ha) with an indeterminate movement (vel 2,9 mm/yr)***	Subsidence Inventory [ ] Inventory name:........ Description of Phenomenon:........	
With geological cartography	Name/Number: ***Section n° 320040 (CARG Project)*** Outcropping lithologies: ***Santa Fiora Formation (claystones)***		

3. ELEMENTS AT RISK

Buildings [X]	Transport or service infrastructures [ ]	Agricultural and industrial territories [X]	Natural environments [ ]	Water bodies [ ]
Category: ***Private building***	Category:	Category: ***Olive grove***	Category:	Category:

4. DAMAGES ASSESSMENT

[X] Damages on buildings and infrastructures		[ ] No damages	Notes:
Observations: ***Thin cracks under the roof***	Picture n° **24b**		
Observations: ***Open and thin perpendicular fractures within the sidewalk***	Picture n° **24c**		
[ ] Damages on natural ground surface and on water bodies		[X] No damages	Notes: ***Land strongly reshaped by agriculture; damages not visible***
Observations:	Picture n°		
Observations:	Picture n°		

As shown in Figure 24a, few meters upstream of the active landslide there is another ADA with a velocity value of 5.0 mm/yr. Therefore, by virtue of the proximity of this ADA to the active landslide, the surveys were carried out also in this area. The ADA is located in an industrial building (Figure 25a) and, through a field survey, a severe open crack was found on this building (Figure 25b-c); no damages instead are currently present in the nearest territory (Table 10).

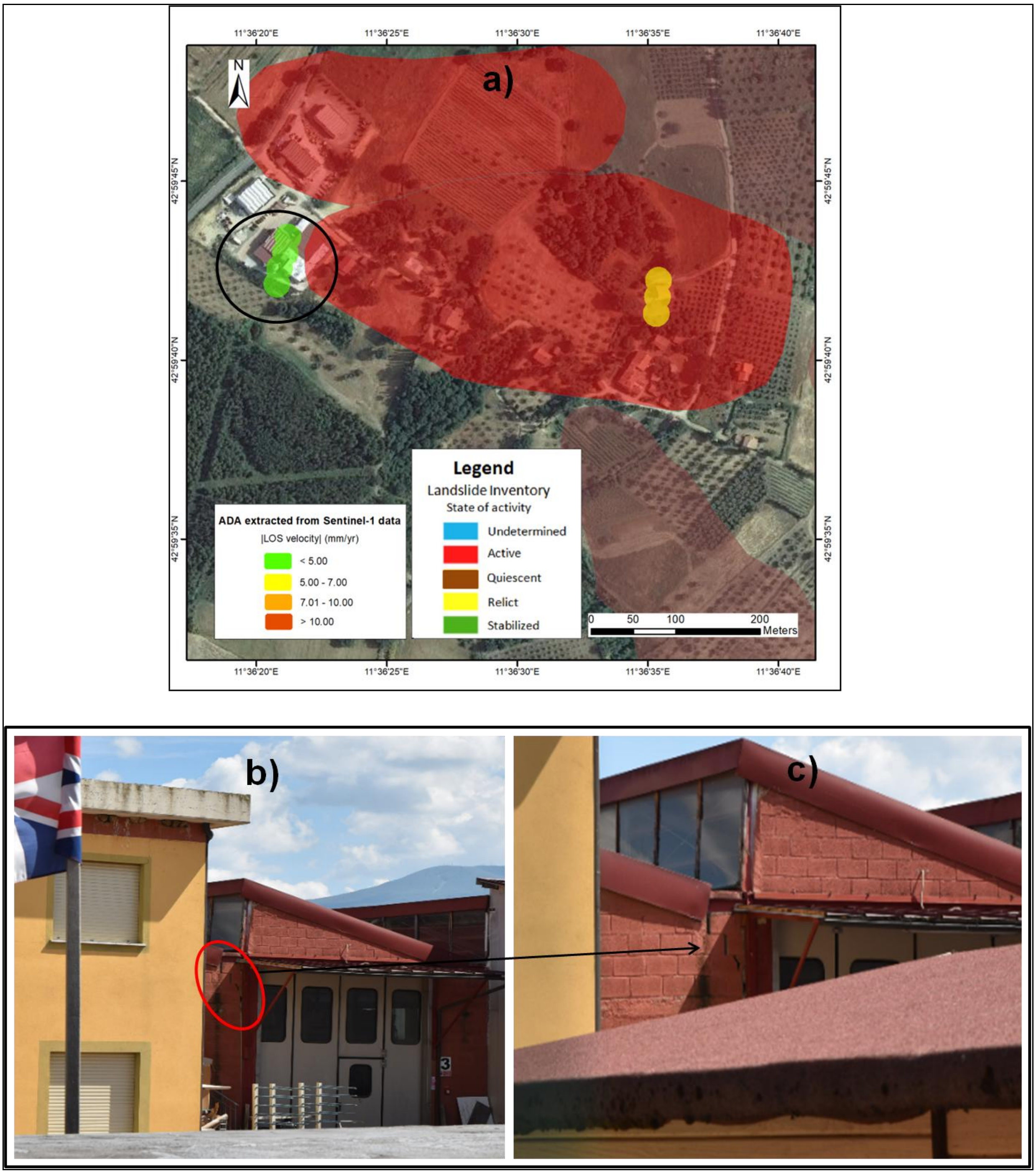

Figure 25. a) Localization of the ADA upstream of the active landslide; b-c) Open crack on the industrial building.

Table 10. ICA of the ADA localized upstream of the active landslide.

ICA - IDENTITY CARD of ADA	
Date: 03/07/2018	Operator: Laura Pastonchi

1. LOCATION AND FEATURES OF ADA		
Name of WHS: *VAL D'ORCIA*		ID number: **1026rev**
Nation: *ITALY*	Province: *SIENA*	Municipality: *CASTIGLIONE D'ORCIA*
Governmental Institution responsible for the Property: ***Ministry for Cultural Heritage and Activities***	Property manager / Coordinator, Local Institution / Agency: ***SRL Val d'Orcia***	

ADA coordinate (WGS-84)		ADA situated in			Satellite characteristic		
Latitude	Longitude	Core zone	Buffer zone	Influence zone	Sensor	Orbit	Time Period
42°59' 43"	*11°36' 20"*	***X***			*Sentinel-1*	*Descending*	*2014-2017*

ADA velocity: *5.0 mm/yr*	ADA areal extension: *940 m²*

2. INTERSECTION OF ADA WITH OTHER DATA						
With other ADA from previous update	Yes ☐					No ☒
	Satellite sensor	Satellite orbit	Satellite time period	ADA velocity (mm/yr)	ADA Areal extension (m²)	
With geohazards inventory	Yes ☐					No ☒ ***But near an active landslide***
	Landslides Inventory ☐ Inventory name: .... Description of Phenomenon:........			Subsidence Inventory ☐ Inventory name:........ Description of Phenomenon:........		
With geological cartography	Name/Number: ***Section n° 320040 (CARG Project)*** Outcropping lithologies: ***Conglomeratic lithofacies***					

3. ELEMENTS AT RISK				
Buildings ☒	Transport or service infrastructures ☐	Agricultural and industrial territories ☐	Natural environments ☐	Water bodies ☐
Category:	Category:	Category:	Category:	Category:

4. DAMAGES ASSESSMENT			
☒ Damages on buildings and infrastructures		☐ No damages	Notes:
Observations: **Severe open crack**	Picture n° *25b-c*		
☐ Damages on natural ground surface and on water bodies		☒ No damages	Notes:
Observations:	Picture n°		

By virtue of the fact that two nearby moving areas were extracted on an active landslide, it was decided to observe also the territory between them, in order to better understand the degree of instability. During this survey more damages have been identified in this area, which is located at the turn of the Santa Fiora Formation (claystone) and the Conglomeratic lithofacies. The natural environment, as explained above, is currently reshaped by agricultural activity and therefore no damages on the ground surface are present. In one private building, instead, a lot of thin cracks and losses of plaster have been observed (building n° 2 in Figure 26), whereas, in another building, some severe and open fractures have compromised the integrity of the structure (building n° 1 in Figure 26).

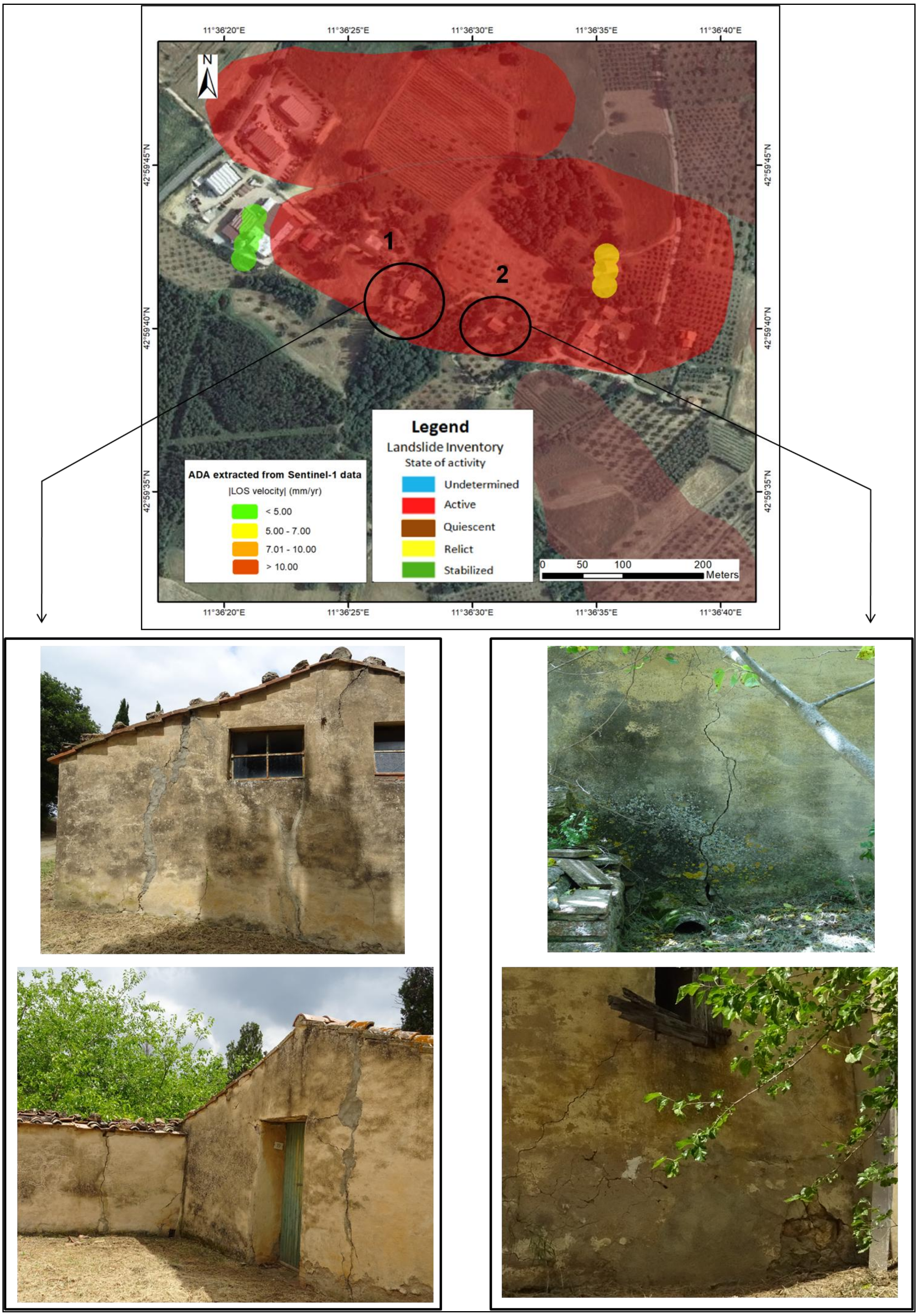

Figure 26. Field surveys carried out on two building within the active landslide body.

The second ADA extracted on an active landslide (ADA n°4 in Figure 22), is located on a cemetery and a provincial road in the Castiglione d'Orcia Municipality, and it has a velocity value of 3.2 mm/yr (Figure 27a). The field survey has revealed the presence of vertical cracks both inside and outside the building (Figure 27b-c) and many depressions on the ground, mostly visible from the subsidences of the tombs (Table 11 and Figure 27d-e). The area external to the cemetery is characterized by sparse vegetation and no damages have been identified, as well as on the Provincial road.

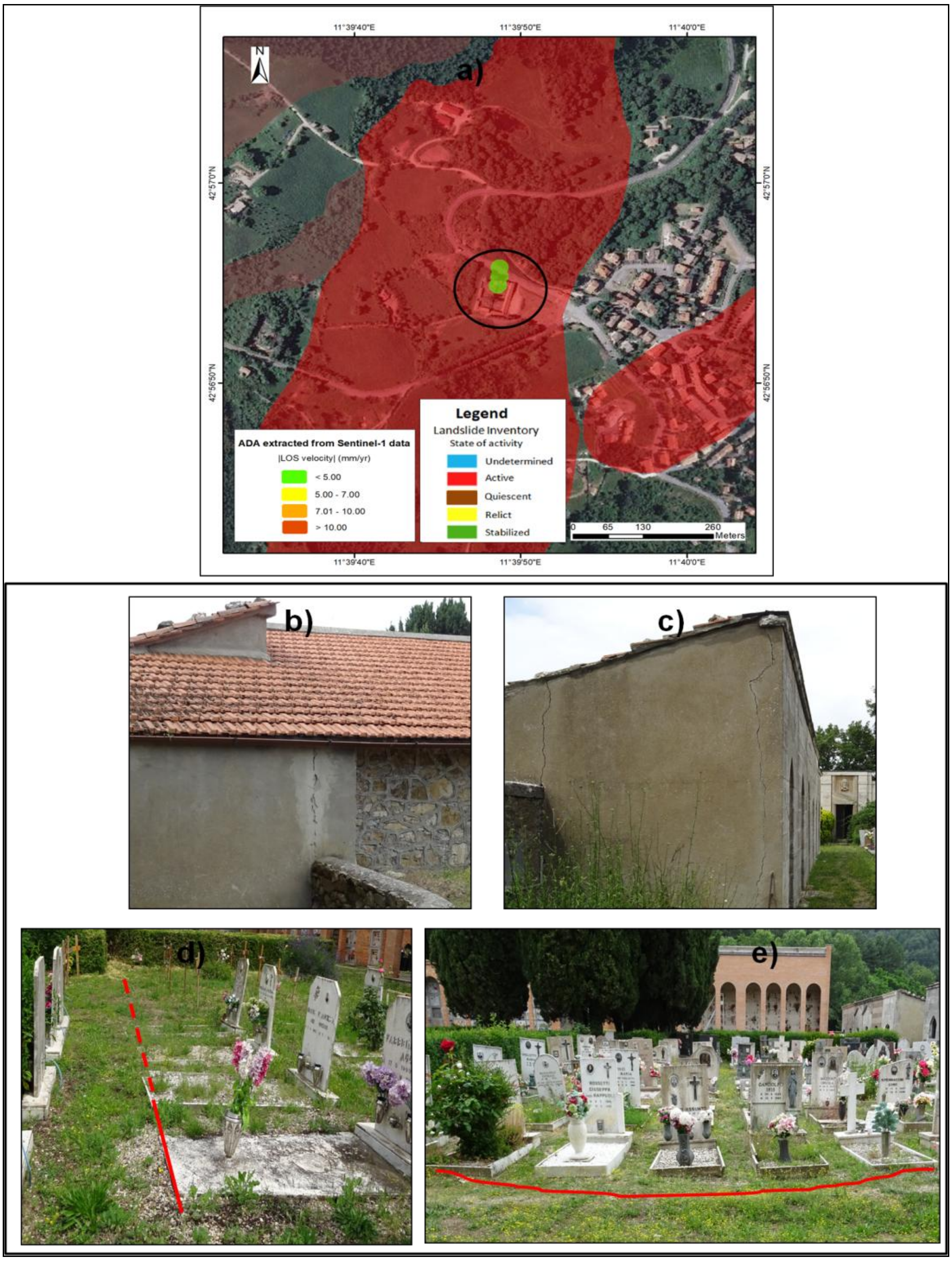

Figure 27. a) Localization of ADA; b-c) damages found on the structure; d-e) damages found on the ground inside the cemetery. The red lines highlights the subsidences of the ground.

Table 11. ICA of the southernmost ADA localized on an active landslide.

ICA - IDENTITY CARD OF ADA	
Date: 03/07/2018	Operator: Laura Pastonchi

1. LOCATION AND FEATURES OF ADA		
Name of WHS: *VAL D'ORCIA*		ID number: **1026rev**
Nation: *ITALY*	Province: *SIENA*	Municipality: *CASTIGLIONE D'ORCIA*
Governmental Institution responsible for the Property: *Ministry for Cultural Heritage and Activities*	Property manager / Coordinator, Local Institution / Agency: *SRL Val d'Orcia*	

ADA coordinate (WGS-84)		ADA situated in			Satellite characteristic		
Latitude	Longitude	Core zone	Buffer zone	Influence zone	Sensor	Orbit	Time Period
42° 56′ 55″	*11° 39′ 49″*	**X**			*Sentinel-1*	*Descending*	*2014-2017*

ADA velocity: *3.2 mm/yr*	ADA areal extension: *713 m²*

2. INTERSECTION OF ADA WITH OTHER DATA		
With other ADA from previous update	Yes ☐ — Satellite sensor: ; Satellite orbit: ; Satellite time period: ; ADA velocity (mm/yr): ; ADA Areal extension (m²):	No ☒
With geohazards inventory	Yes ☒ — Landslides Inventory ☒; Inventory name: *Landslide inventory of Tuscany (Casagli et al., 2013)*; Description of Phenomenon: *Active landslide (37.2 ha) with an indeterminate movement (vel 4.0 mm/yr)*; Subsidence Inventory ☐; Inventory name:……..; Description of Phenomenon:……..	No ☐
With geological cartography	Name/Number: *Section n° 320040 (CARG Project)*; Outcropping lithologies: *Landslide with an indeterminate movement*	

3. ELEMENTS AT RISK				
Buildings ☒	Transport or service infrastructures ☒	Agricultural and industrial territories ☐	Natural environments ☒	Water bodies ☐
Category:	Category: *Provincial road*	Category:	Category: *Sparse vegetated area*	Category:

4. DAMAGES ASSESSMENT			
☒ Damages on buildings and infrastructures		☐ No damages	Notes:
Observations: *Open and vertical cracks both inside and outside the cemetery*	Picture n° 27b-c		
☒ Damages on natural ground surface and on water bodies		☐ No damages	Notes:
Observations: *Many depressions visible through the subsidences of the tombs*	Picture n° 27d-e		

The southernmost ADA is localized in the Radicofani Municipality and it turned out to be the ADA with the highest velocity value (8.9 mm/yr) registered in the Val d'Orcia cultural site. This active movement threatens a Provincial road, partially surrounded by a badlands landscape (Figure 28a and Table 12). Before reaching the place of ADA, a warning sign indicating the presence of a landslide was seen along the road (Figure 28b). Few meters ahead, in the place where ADA has been extracted, a stretch of an untarmacked road that interrupts the asphalt was observed (Figure 28c). Moreover, a misalignment of the posts placed in the hill above the road is a further sign of a past movement of the ground, which, by virtue of the presence of the Sentinel-1 ADA, is still in progress.

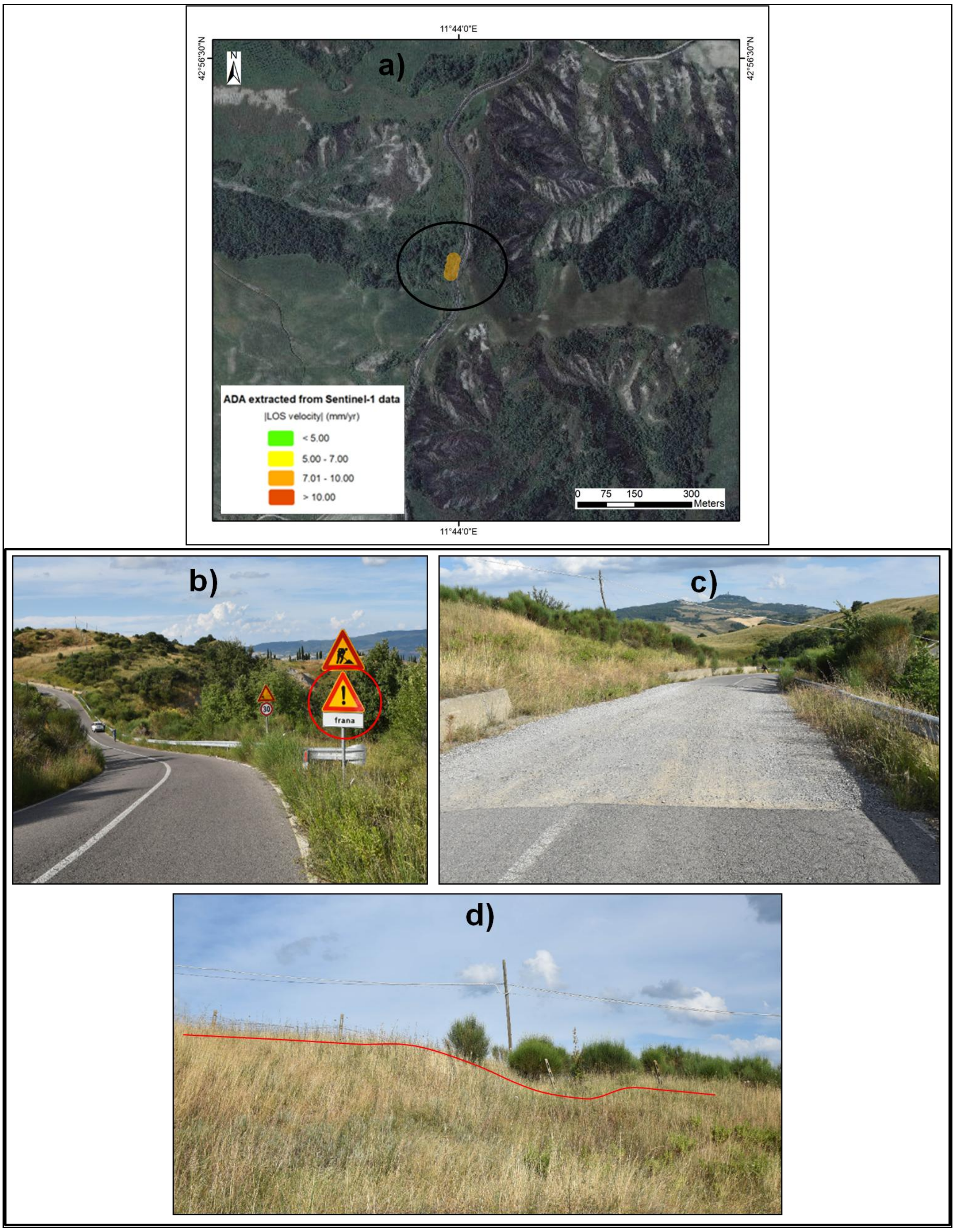

Figure 28. a) Localization of the southernmost ADA; b) warning sign indicating the presence of a landslide; c) stretch of a untarmacked road that interrupts the asphalt; d) misalignment of the posts placed in the hill above the road.

Table 12. ICA of the ADA with the highest velocity value.

ICA - IDENTITY CARD of ADA

Date: 22/07/2018	Operator: Laura Pastonchi

1. LOCATION AND FEATURES OF ADA

Name of WHS: ***VAL D'ORCIA***		ID number: **1026rev**
Nation: ***ITALY***	Province: ***SIENA***	Municipality: ***RADICOFANI***
Governmental Institution responsible for the Property: ***Ministry for Cultural Heritage and Activities***	Property manager / Coordinator, Local Institution / Agency: ***SRL Val d'Orcia***	

ADA coordinate (WGS-84)		ADA situated in			Satellite characteristic		
Latitude	Longitude	Core zone	Buffer zone	Influence zone	Sensor	Orbit	Time Period
42° 56' 15"	***11° 44' 0"***	***X***			***Sentinel-1***	***Descending***	***2014-2017***

ADA velocity: ***8.9 mm/yr***	ADA areal extension: ***711 m²***

2. INTERSECTION OF ADA WITH OTHER DATA

	Yes ☐					No
With other ADA from previous update	Satellite sensor	Satellite orbit	Satellite time period	ADA velocity (mm/yr)	ADA areal extension (m²)	☒

	Yes ☐		No
With geohazards inventory	Landslides Inventory ☐ Inventory name: Description of Phenomenon:	Subsidence Inventory ☐ Inventory name:........ Description of Phenomenon:........	☒
With geological cartography	Name/Number: ***Section n° 321050 (CARG Project)*** Outcropping lithologies: ***Clays and silty clays***		

3. ELEMENTS AT RISK

Buildings ☐	Transport or service infrastructures ☒	Agricultural and industrial territories ☐	Natural environments ☐	Water bodies ☐
Category:	Category: ***Provincial road***	Category:	Category:	Category:

4. DAMAGES ASSESSMENT

☒ Damages on buildings and infrastructures		☐ No damages	Notes: **Warning sign indicating the presence of a landslide**
Observations: ***Stretch of a untarmacked road that interrupts the asphalt***	Picture n° **28c**		
☒ Damages on natural ground surface and on water bodies		☐ No damages	Notes:
Observations: ***Misalignment of the posts placed in the hill above the road***	Picture n° **28d**		

2.5.4 Monitoring of ADA within the UNESCO Tuscan sites

In this section, a simple comparison between the main attributes of ADA is shown. It was not possible to illustrate the results in terms of geohazards because, for the reason explained in the previous section, only in Piazza del Duomo of Pisa, to every ADA has been associated a slow-kinematic phenomenon (ground-subsidence).

Inside Core, Buffer and Influence Zones of each propriety, we have collected the following information regarding the ADA (Table 13): number of ADA (N°); maximum velocity ($|v_{max}|$), minimum velocity ($|v_{min}|$), and the percentage of the areal coverage of ADA (%). Each result, shown in Table 13, includes the values of ADA extracted both in ascending and descending orbit for each of the two satellite datasets (Pastonchi et al., 2018).

Table 13. Main attributes of ADA extracted from Envisat and Sentinel-1 datasets, within the boundaries of the UNESCO Tuscan sites. N° = number of ADA; $|v_{max}|$ = maximum velocity (mm/year); $|v_{min}|$ = minimum velocity (mm/year); % = percentage of the areal coverage of ADA; NEGL = negligible (% < 0.1). All the velocities are in absolute value. From Pastonchi et al., 2018.

UNESCO TUSCAN SITES	ADA EXTRACTED FROM ENVISAT DATA												ADA EXTRACTED FROM SENTINEL-1 DATA											
	CORE ZONE				BUFFER ZONE				INFLUENCE ZONE				CORE ZONE				BUFFER ZONE				INFLUENCE ZONE			
	N°	|Vmax|	|Vmin|	%	N°	|Vmax|	|Vmin|	%	N°	|Vmax|	|Vmin|	%	N°	|Vmax|	|Vmin|	%	N°	|Vmax|	|Vmin|	%	N°	|Vmax|	|Vmin|	%
Historic Center of Florence					82	8.4	4.1	0.2	96	16.8	4.0	0.3					7	4.3	3.2	NEGL	56	8.3	3.1	0.1
Historic Center of Siena					11	6.3	4.5	NEGL	15	6.6	4.2	NEGL					2	4.7	3.8	NEGL	1	3.7	3.7	NEGL
Cerreto Guidi Villa																					1	5.1	5.1	0.1
Seravezza Palace									2	4.1	4.1	NEGL									2	5.1	4.7	0.1
Pratolino Garden									1	5.6	5.6	NEGL												
La Magia Villa																					1	3.2	3.2	NEGL
Poggio Imperiale Villa									1	5.1	5.1	NEGL												
Historic Center of S. Gimignano									6	6.2	5.4	0.1												
Piazza del Duomo. Pisa					8	5.9	4.2	0.5	411	19.8	4.0	7.0									34	6.1	3.0	0.3
Historic Center of Pienza									2	5.2	4.3	NEGL					2	4.2	4.1	NEGL	1	3.9	3.9	NEGL
Val d'Orcia	21	7.0	4.1	NEGL	2	5.6	4.8	NEGL					30	9.0	3.1	NEGL	6	4.9	3.2	NEGL	2	6.8	6.2	NEGL

As previously shown in Table 6, ADA have been extracted only in some of the 20 UNESCO Tuscan sites, and some differences both among the three boundaries and between the two satellite acquisitions are present. The only Core Zone with ADA is located in Val d'Orcia (Figure 29): 21 ADA have been identified through Envisat data, with $|v_{max}|$ = 7.0 mm/yr and

$|v_{min}|$ = 4.1 mm/yr, while 30 ADA have been extracted from Sentinel-1 dataset, with a slight increase in the maximum velocity ($|v_{max}|$ = 9.0 mm/yr).

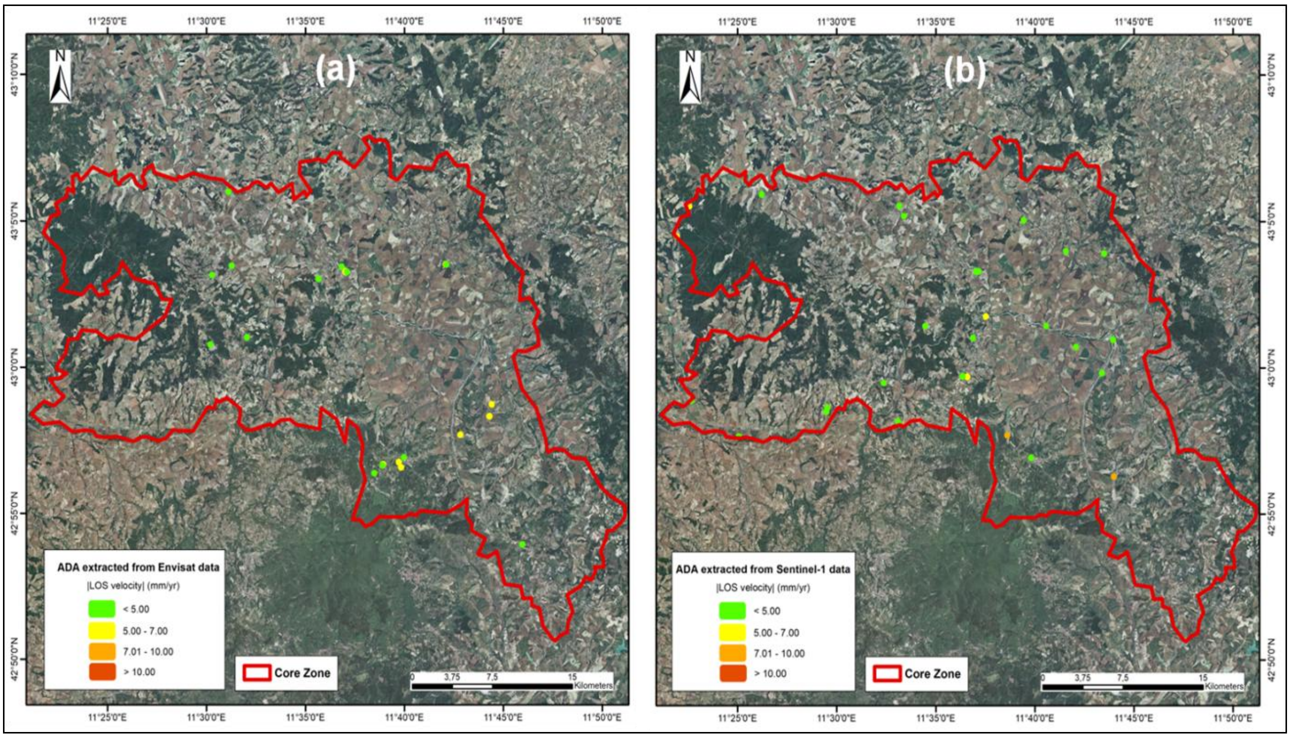

Figure 29. LOS velocities (absolute value) of ADA extracted in the Core Zone of Val d'Orcia, from a) Envisat data, and b) Sentinel-1 data, both in ascending and descending orbit. From Pastonchi et al., 2018.

Few ADA have been identified in both satellite acquisitions in the Buffer Zone of Val d'Orcia with similar velocity values, whereas in the Influence Zone, 2 ADA with $|v_{max}|$ = 6.8 mm/yr have been extracted through the newest dataset (Table 13).

The greatest number of ADA has been identified in the Influence Zone of Piazza del Duomo (Pisa), where 411 ADA, with the highest percentage of the areal coverage detected (7%), have been extracted through the Envisat dataset (Figure 30c and Table 13). Few ADA have been extracted, instead, in the Buffer Zone, whereas, considering Sentinel-1 dataset, no ADA have been detected in this area. At the Influence Zone, an evident decrease in the number of ADA (from 411 to 34) and in the $|v_{max}|$ value (from 19.8 mm/yr to 6.1 mm/yr) can be observed (Figure 30c-d and Table 13).

In the Florence area, a decrease in the number of ADA and in all the other detected values has been identified over time (Figure 30a-b; the maximum velocity in the Influence Zone is halved).

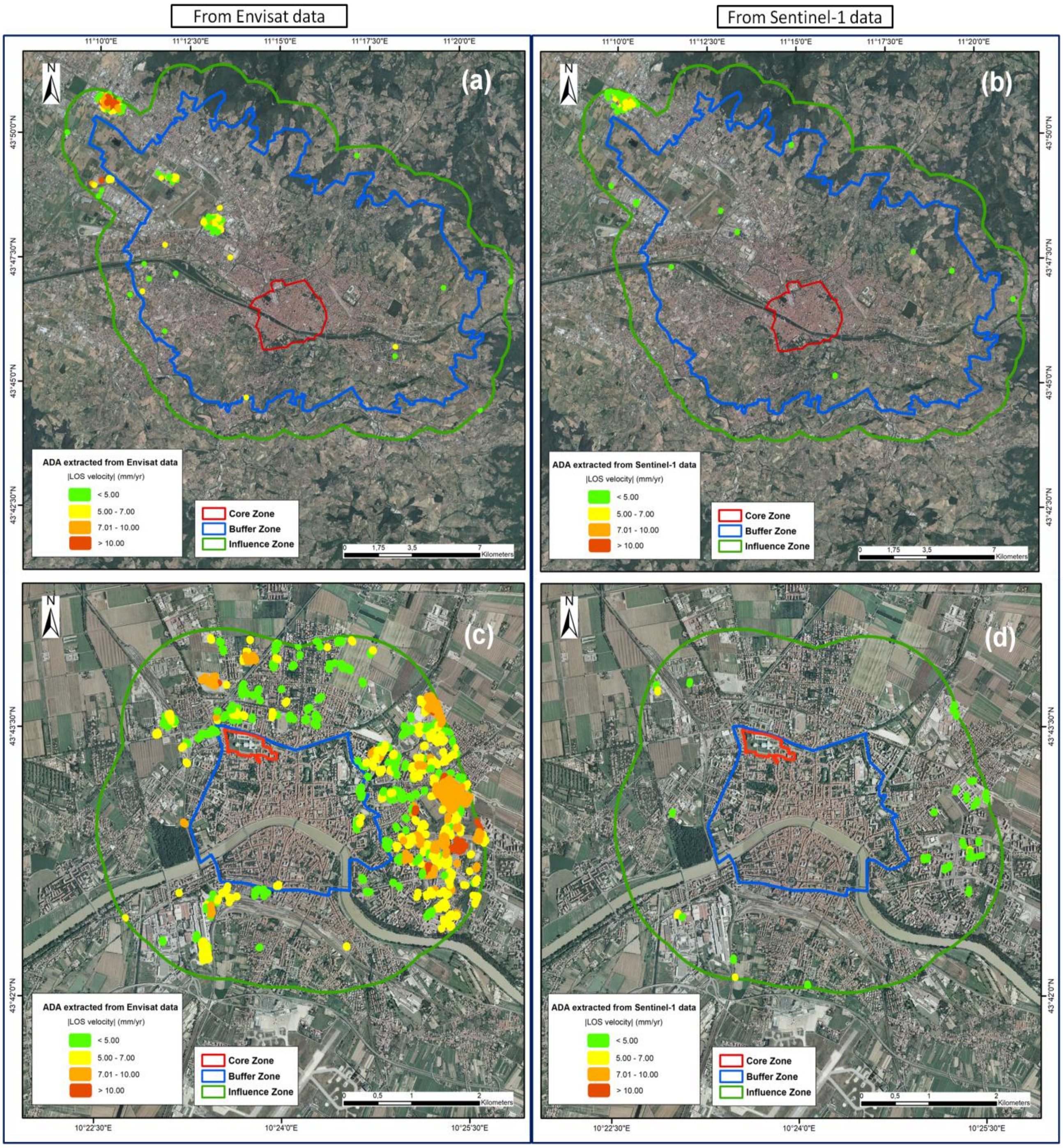

Figure 30. LOS velocities (absolute value) of ADA extracted from Envisat and Sentinel-1 datasets, both in ascending and descending orbit, in the Core, Buffer and Influence Zones of a-b) Historic Center of Florence, and c-d) Piazza del Duomo, Pisa. From Pastonchi et al., 2018.

Among all the ADA, those which have been detected in both datasets, even though some little variations in their position have occurred over time, have been identified. Thus, it was found that in the Core Zone of Val d'Orcia, in the Buffer Zone of the Historic Center of Florence, and in the Influence Zone of Seravezza Palace (Figure 31), Historic Center of Florence and Piazza del Duomo, an intersection between ADA is present (Table 14).

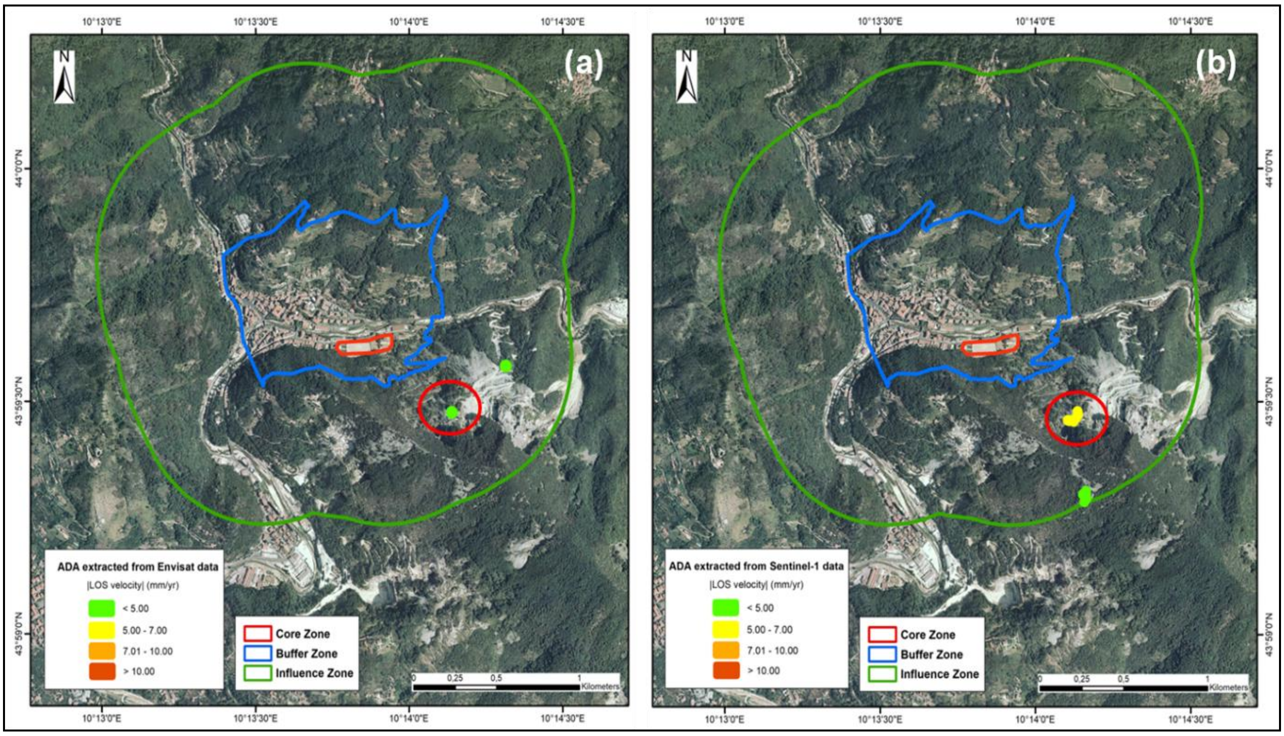

Figure 31. LOS velocities (absolute value) of ADA extracted in the Influence Zone of Seravezza Palace, from a) Envisat data, and b) Sentinel-1 data, both in ascending and descending orbit. The red circle highlights the ADA that, over the years, has remained in the same place (despite some little variations in their area). From Pastonchi et al., 2018.

Table 14. Number of ADA that have been detected in both datasets. From Pastonchi et al., 2018.

UNESCO SITE	INTERSECTIONS BETWEEN ADA		
	CORE ZONE	BUFFER ZONE	TRANSITIONAL ZONE
Historic Center of Florence		1	68
Seravezza Palace			1
Piazza del Duomo, Pisa			69
Val d'Orcia	2		

These movements are probably attributed to the same phenomenon that lasts over time. It is worth noting that also the ADA that do not intersect each other are considered reliable ADA, connected to different geohazards or different behavior of the same phenomenon in different periods.

In addition to this, in the cultural sites where the two ADA datasets intersect the ground-subsidences inventory, i.e. Piazza del Duomo of Pisa and the Historic Center of Florence (see Figure 18 and Figure 19), further analyses were carried out in order to specifically monitor the spatial and temporal evolution of this geohazard. This is the only case where it was possible to monitor a geohazard and this was done because the high number of ADA identified in the aforementioned areas would take a great amount of time for the individual in situ observations. Thus, after having made a cut of all the PS data in the flat areas that fall into subsidence, the LOS velocities of the new Envisat and Sentinel-1 datasets have been interpolated by the Inverse Distance Weighting method (GIS tool), and the ground-subsidence maps of the two cultural sites have been obtained. To enhance the clarity of these maps, the areas not affected by substantial movements have been removed, i.e. only velocity values higher than a threshold that is twice the standard deviation of the map ($\pm 2\sigma_{IDW\ map}$) have been considered (Figure 32).

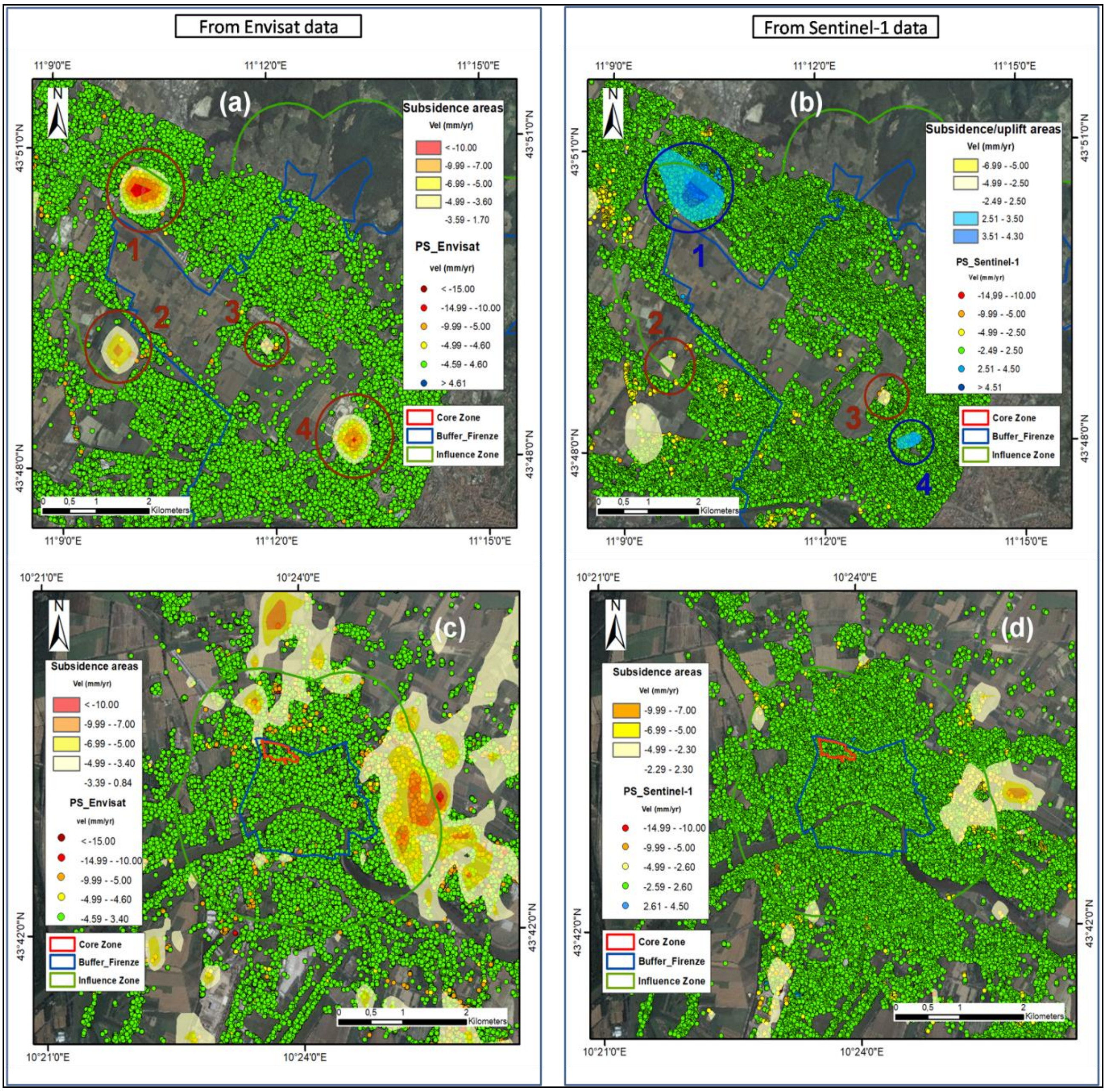

Figure 32. Subsidence maps derived from the interpolation of the Envisat (on the left) and Sentinel-1 (on the right) datasets. a-b) Historic Center of Florence; c-d) Piazza del Duomo, Pisa. Only velocity values > $\pm 2\sigma_{IDW\ map}$ have been considered. The threshold values have been indicated in the map (not-colored value), and in the case of a) and c) maps, the maximum velocity values are lower than + $2\sigma_{IDW\ maps}$ values.

This procedure was performed following a fundamental assumption. For each persistent scatter, the PSI technique provides time series and velocities values of the ground displacements acquired along the LOS of the satellite, tilted about 23° and 35°- 38° from the vertical direction for Envisat and Sentinel-1 data, respectively. Since the difference between movements along the LOS and their vertical component is very small, it has been assume that in flat areas the negative and positive LOS displacement results solely from ground-subsidences and uplifts, respectively (Tosi et al., 2010; Teatini et al., 2012; Tofani et al., 2013; Alfarè et al., 2014).

The obtained results from Envisat data in the Florence area, show the presence of two subsidence areas in the Buffer Zone (subsidences n° 3-4), and two in the Influence Zone (subsidences n°1-2) (Figure 32a), where already indicated by the geohazards inventory (see Figure 18b). The three larger areas are located in industrial areas, whereas the smallest subsidence phenomenon (subsidence n°3) is located at the new headquarters of CNR (National Research Council) of Sesto Fiorentino. The subsidence n°1 shows a large peak of velocity values (v > -10.00 mm/year). In this zone, through Sentinel-1 data, a reversal of movement has been identified (Figure 32b), with uplift values that reach 4.30 mm/yr. The same deformation trend has been detected in a portion of the subsidence area n° 4, where a little uplift (up to 3.5 mm/yr) is visible in Figure 32b. The subsidence phenomenon recorded at the CNR headquarters (area n°3) is not more present in the years 2014-2017, whereas the ground-subsidence n°2 has reduced its areal extension over the years.

Thanks to the approximately ten years of monitoring in the Pisa area, a substantial decrease in the subsidence phenomenon has been observed both in space and in intensity (Figure 32c-d). In fact, in its Buffer Zone, the transition from a subsidence phenomenon that threatened about 7% of its territory, with velocity values up to 5.00 mm/yr, to its current total absence can be observed. In its Influence Zone, instead, this phenomenon has decreased in its extension (from 21.1% to 6.7%) and in its maximum velocity values (from values exceeding 10.00 mm/yr in an area immediately east of the Influence Zone, to values that, through Sentinel-1 data, do not exceed 5.00 mm/yr).

The particular inversion of ground movement from subsidence to uplift recorded in the Influence Zone of Historic Center of Florence can be observed also from the displacement time series of some PS located in one industrial building (Figure 33).

An Envisat PS shows a subsidence of this building of about 110 mm (Figure 33a), while a Sentinel-1 PS shows an uplift up to 15 mm, after a substantial stability until the end of 2015 (Figure 33b).

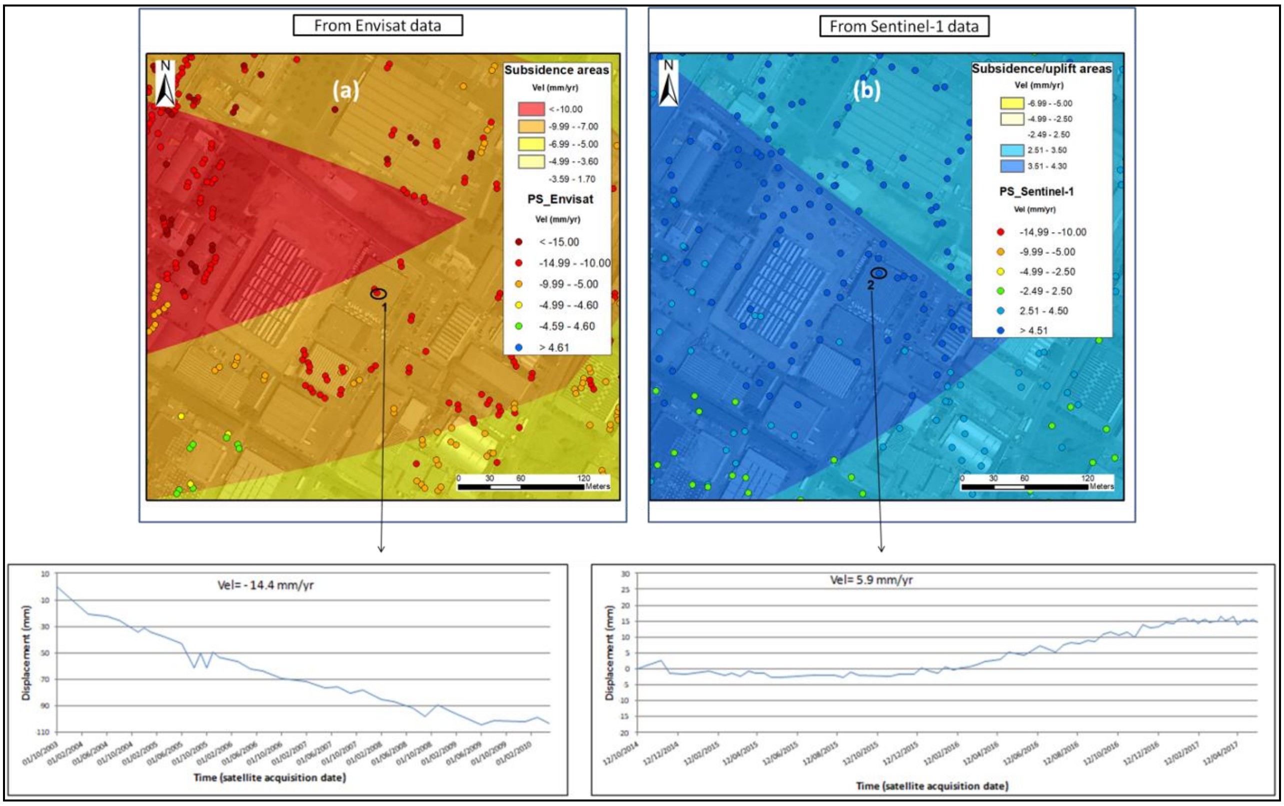

Figure 33. a) Subsidence map obtained from Envisat data and displacement time series of Point 1; b) Uplift map obtained from Sentinel-1 data and displacement time series of Point 2.

3. Analyses at local scale

3.1 GBInSAR for emergency: the case of Lungarno Torrigiani (Florence)

The city of Florence, a symbol of the Renaissance, is exceptionally rich in unique examples of human activity (e.g., churches, cathedrals and historical palaces). This great record of the past is a heritage which requires exceptional measures of conservation. For this reason, in 1982, the Historic Center of Florence has been recorded in the World Heritage List. Despite the care and all the efforts put in place in managing this public good by the UNESCO Agency (as well as for all the other World Heritage Sites), on 25 May 2016, a portion of the artificial riverbank of the Arno River and of the road behind collapsed along Lungarno Torrigiani, just few meters far from the famous "Ponte Vecchio" bridge. Since the event could naturally extend even to areas built all around, increasing the damage to the heritage and endangering the lives of workers involved in the construction sites, an integrated monitoring system was installed for detecting any deformation of the collapsed embankment wall and of all the buildings surrounding it. In this study, a detailed analysis of the past instabilities of this area is presented, considering the special urbanistic context of the involved UNESCO site. Furthermore, the attention has been focused on the potential of the Ground-Based Synthetic Aperture Radar Interferometer (GB-InSAR), here used both as a monitoring tool and as an early warning system.

3.1.1 Geological and geomorphological setting

Florence is crossed by the Arno River, which originates from a source in the southern slopes of Mt. Falterona (1358 a.s.l.) and, after 241 km, flows into the Tyrrhenian Sea near Pisa, covering a total length of 241 km (Billi & Rinaldi, 1997). The Arno River crosses a variety of geomorphological landscapes, sequentially characterized by hilly regions and alluvial plains, such as the “Firenze-Prato-Pistoia Plain”, where the metropolitan area of Florence is located (Figure 34) (Morelli et al., 2012).

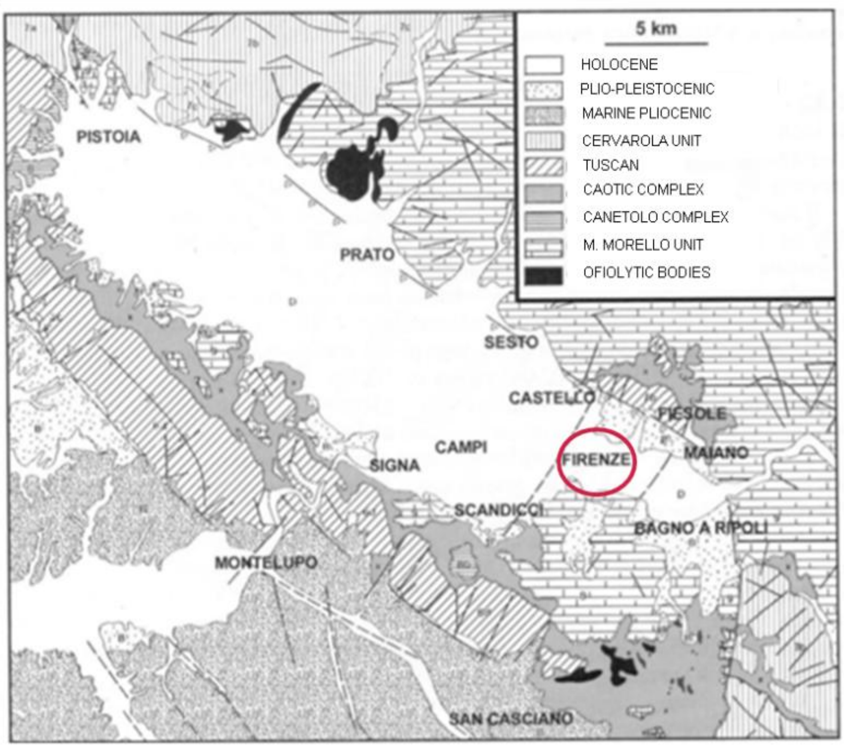

Figure 34. Schematic geological map of the Florence-Prato-Pistoia basin (modified from Coli and Rubellini, 2007). The city of Florence is circled in red.

This is a NW-SE oriented intermontane basin, 45 km long, 10 km wide and with an average altitude of 45 m a.s.l. (Capecchi et al., 1975). It is delimited by two ridges ("Pistoia-Montale-Calvana" — "M.Morello-Fiesole-Settignano" to the north and "M.Albano-Pian dei Cerri-Impruneta" to the south), mainly constituted by calcareous-marly flysch associated with ophiolites and arenaceous flysch (Abbate and Sagri, 1970; Boccaletti and Coli, 1982; Coli and Rubellini, 2007; Pandeli, 2008). The geomorphology of this area is closely connected to the lithology. Gentler slopes (like in the hills south of the Arno River) are mostly associated with flysch of marly-arenaceous composition, while loose lacustrine and fluvial sediments form piedmont areas (Coli and Rubellini, 2007). The genesis of the half-graben is associated with the sedimentation of clay, sandy clay and peat relatable to a lacustrine-swampy environment (Briganti et al., 2003; Capecchi et al., 1975). Between 1.7 and 1.2 My ago, the area of Florence was raised by 50 m by SW-NE faults, as witnessed by the reduced thickness of lacustrine-swampy deposit in this zone (<160m). Between 1.2 and 0.01 My ago, the presence of a marked fluvial environment caused the sedimentation of cobble, gravel, and sand (Pandeli, 2008) above the swampy-lacustrine deposit. The upper layer of sedimentary deposits in the Florence area is constituted by silt (Figure 35), proving that lacustrine-swampy conditions still persisted also in historical time. In fact, the territory around Firenze was reclaimed in the Roman era (I century B.C.), when some watercourses were also channeled and rectified (Marinelli, 1921). This reduced the wandering capability of the rivers and limited the deposition of silt in the floodplain only to exceptional flooding events. During the VI century, the number of inhabitants in Florence had dropped from 50,000 to barely 1000 and a different and less rigorous management of the territory lead to a new swamping of the region (Lopes-Pegna, 1974). The presence of swamps and wandering rivers until recently is still detectable in certain current toponyms of the urbanized area and surroundings, such as Padule street, Pantano street (dialectal forms for “swamp”) or Isolotto district (small island).

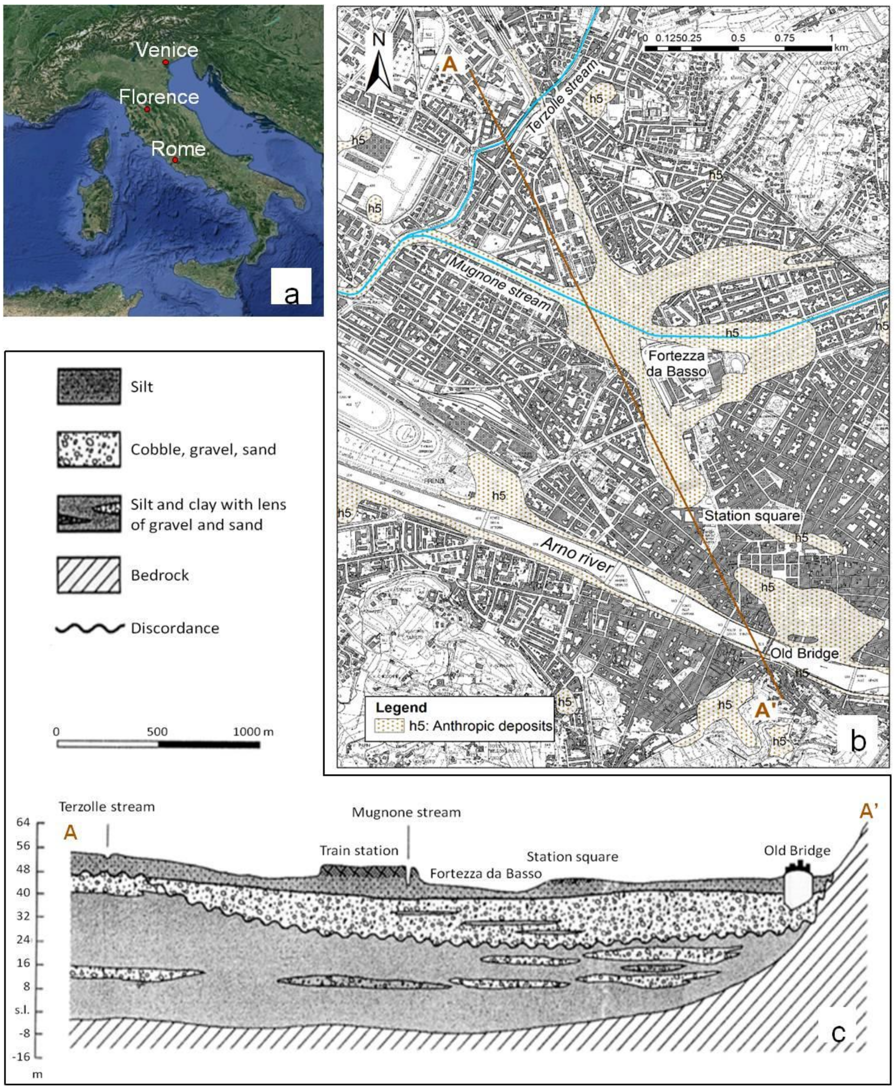

Figure 35. Study area: a) general framing; b) distribution of the current urban structure of Florence with the distribution of the main anthropic deposits and section line where the stratigraphy of the plain is extracted; c) geological reconstruction along section AA' (Morelli et al., 2018).

3.1.2 Evolution of the study area and past instabilities

The Arno riverbank morphology is the result of urbanization typical of centuries-old cities, which have mainly exploited the hydropower of the rivers. Particularly, the current structure of the study area is the product of a specific urban redevelopment approved in 1866 and completed in 1872 (Figure 36a-b) in the overall framework of the reorganization that the city was experiencing during the years in which it was designated as capital of Italy (1865-1871; Poggi, 1882). The recovery plan of Poggi entailed an enlargement of the city through the creation of new districts, new avenues and the main roads alongside the Arno River, currently known as “Lungarni” (Poggi, 1882; Moreno, 2012). The improvements made in the city during this period included also a new water distribution network realized by the designers Raffaele Canevari and Luigi Del Sarto. A system of water supply was constituted by underground filtering galleries, a discharge channel under Lungarno Soderini and Lungarno Torrigiani (Figure 36c-d), and a water-lifting central located at the Pescaia di Santa Rosa (Poggi, 1882; Ottati, 1992).

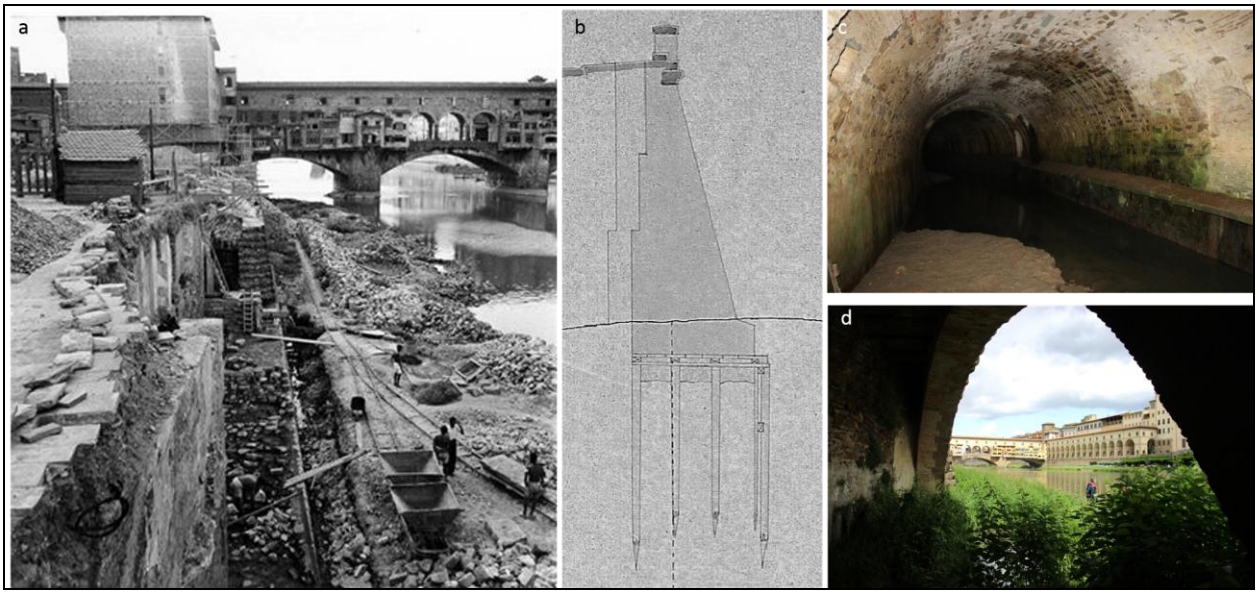

Figure 36. a) Original photo of the Torrigiani riverbank embankment at the beginning of its construction in 1866, (b) the section of the retaining wall from the original design drawings, and the discharge channel inside the Lungarno Torrigiani embankment, as visible in 2017 (c, d). (Morelli et al., 2018).

However, several interventions to the city of Florence began as early as in 1175, when the fifth circle of city walls was completed to encompass and defend some hamlets built on the Arno river left bank, tripling the urbanized area with a secure and stable fortification. Thus, the urban structure migrated its geographical barycentre from a raised and ancient river terrace, which was occupied by the first Roman settlements (about in 59 BC) and permanently inhabited for more than 11 centuries, to the Arno riverbed (Figure 37).

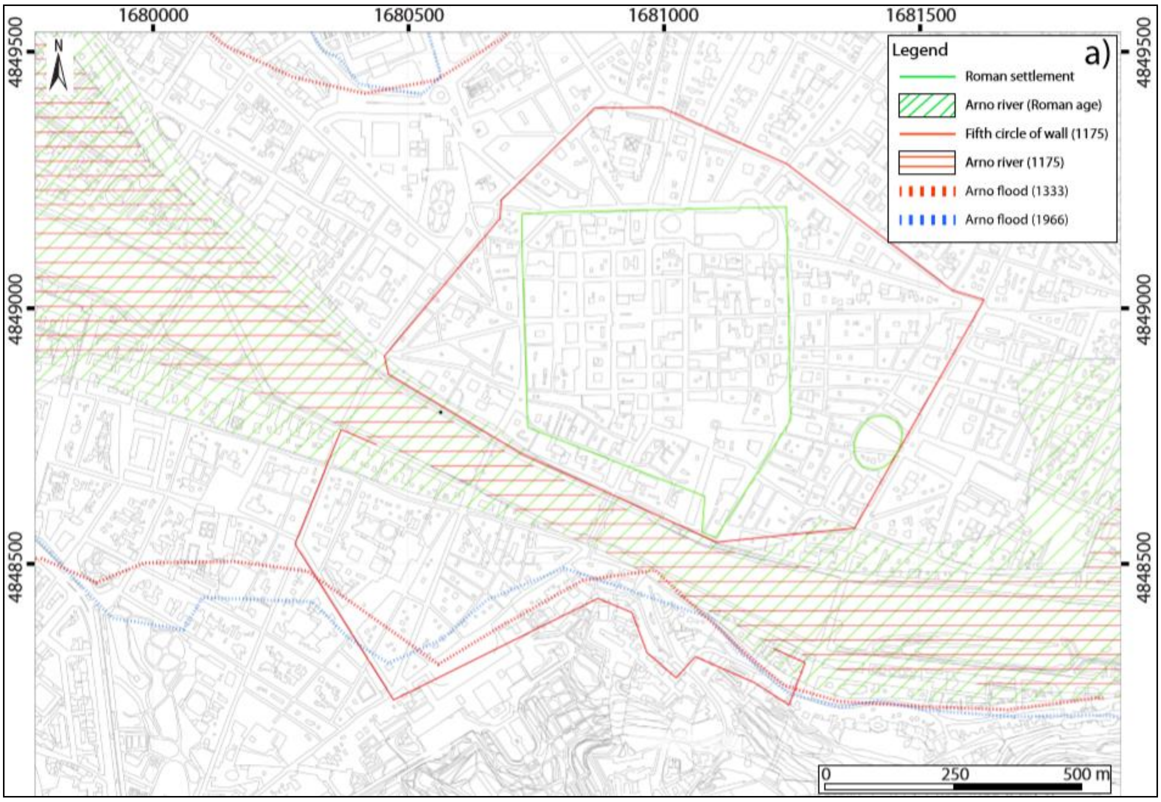

Figure 37. Evolution of the Florence urban structure and Arno flood since 1175: In green the Arno river during the Roman age and the Roman settlement (green line), while in red the Arno river and the wall (red line) in 1175. Dashed red and blue lines represent the extension of the floods in 1333 and 1966, respectively. Modified from Morelli et al., 2018.

So, the hand of man forced the Arno course to flow into narrowest stretch (Francovich et al., 2007; Morelli et al., 2014), and the inhabited area expanded from an alluvial plain less exposed to flooding to a more floodable area. Consequently, in this confined arrangement, the watercourse became a negative actor during flood events (Scampoli, 2003). Eight of these, occurred in 1333, 1547, 1557, 1589, 1740, 1758, 1844, 1966, involved the most considerable damages, such as loss of human lives and destruction of buildings, riverbanks and infrastructure (Morozzi, 1762; Aiazzi, 1845; Canfarini, 1978; Frati, 2015). During the most recent of these events, which took place on 04 November 1966, the Arno River swept the parapets, broke its riverbanks, flooded streets, homes and shops, causing the deaths of several people. On the right riverbank, a portion of Lungarno degli Acciaiuoli embankment collapsed, due to the erosive strength of the river current (Figure 38a). Even the adjacent Lungarno Corsini embankment was affected by slope failures, contributing to the rapid invasion of turbulent waters towards the inner areas of the city (Cenencini F., 1966; Principe and Sica, 1967; Canfarini, 1978; Catenacci, 1992). Regarding the riverbank instability, one year before this event, on 04 July 1965, another portion of the embankment wall, this time along Lungarno Soderini (left riverbank), rapidly collapsed within the Arno River (Figure 38b), after an unquantifiable leakage from the subterranean water supply network that hugely saturated the soil. The resulting landslide had a volume of about 4000-5000 m^3, a length and a width of 40 m and 6 m, respectively, and caused the death of one man (La Nazione, 1965).

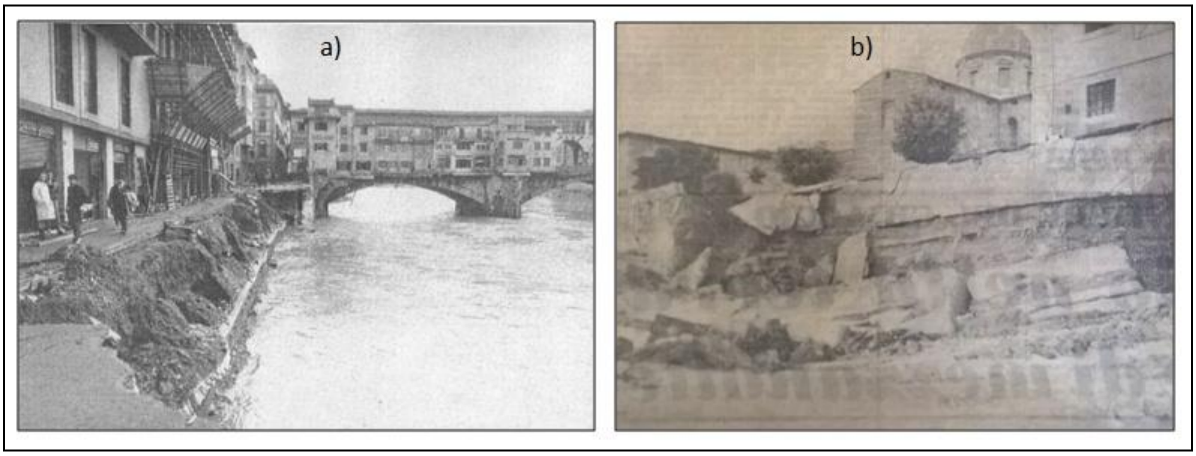

Figure 38. a) Photo of Lungarno Acciaiuoli embankment eroded in 1966 by the violence of the waters (from Principe I. and Sica P., 1967); b) Photo of the embankment wall and the roadway of Lungarno Soderini collapsed on 4 July 1965; from "La Nazione" newspaper of 5 July 1965, Chronicle of Florence.

Following the collapse, the municipality promoted some site inspections to evaluate the stability of the Arno riverbanks and many critical issues emerged both upstream and downstream of the affected area. The maintenance of old structures, in fact, was not always regular and a scarce natural dispersion of pore pressures was increasingly favored by the presence of vertical underground structures (underground passages, buried channels, sewer systems, foundations and riverbank retaining walls) that contributed to impeding the natural groundwater circulation. In the last decades, the maintenance of such complex subterranean system was not always prompt and effective, and sometimes it induced criticalities for the health and security of citizens in different areas of the city (Morelli et al., 2014).

In proximity of the Lungarno Torrigiani riverbank, over the years, not only floods and landslides on riverbanks occurred, but also slope instabilities on the behind hills. The most violent and intense mass movements occurred in the Boboli-Belvedere hill (also known as "Poggio dei Magnoli"), close to Lungarno Torrigiani (Losacco, 1957). First reports of landslides on this hillside date back to 1284 (Frati, 2015) when, after a very intense rainfall, a sudden landslide phenomenon occurred (Villani, 1845). In that occasion, more than 50 buildings collapsed killing many inhabitants (Manni et al., 1733). In 1373, 1490 and 1547 similar injurious events occurred in this area after long periods of rainfall. The latter landslide was highly impacting on the urban layout, and eighteen houses were completely devastated. To solve this problem, the Duke of Florence, in 1565, prohibited constructing new buildings in all the area at risk, and a plate with such ban was affixed on site for future memory (Morozzi, 1762). The last damages to this territory were documented in this area in 1651, when incessant rains triggered local slope deformations and movements. This indicates that a large part of the problem was settled (i.e., the human influence), but the problems at the hydraulic draining system still existed (Bargellini and Guarnieri, 1986; Artusi and Venturi, 2014).

3.1.3 The 2016 riverbank landslide and its management

During the night of 24 May 2016, a large leak of water along the roadway of Lungarno Torrigiani called forth the attention of the population for the unusual circulation of water despite the non-rainy weather. At the same time, a decrease of the water pressure within a pipeline was registered. At about 06:00 a.m., part of Lungarno Torrigiani road surface collapsed of about 4 meters in height and 150 meters in breadth, with the partial sliding of the underlying terrigenous layers towards the riverbed causing a cusp-shaped deformation of the retaining wall without any falling apart (Figure 39a).

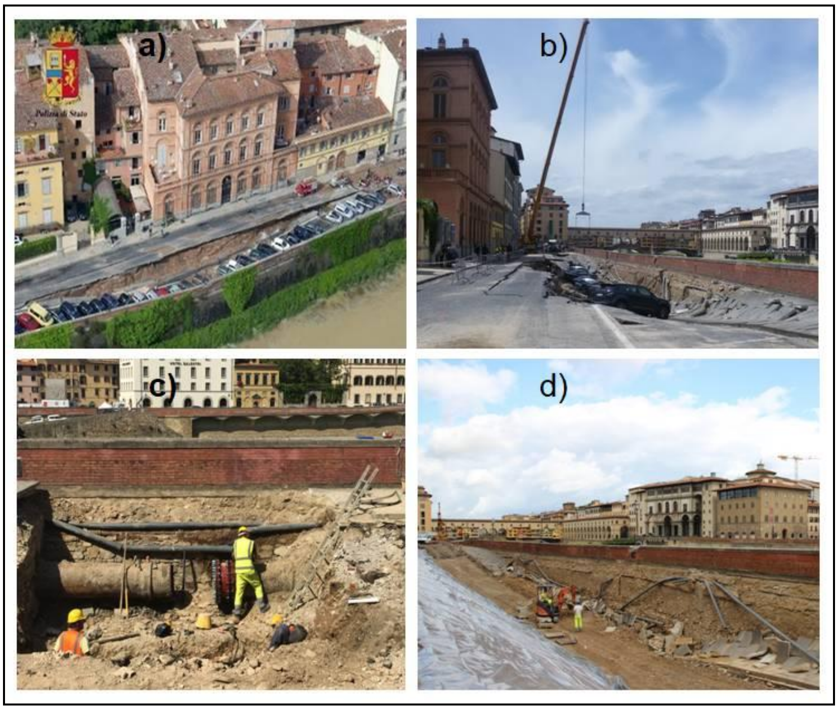

Figure 39. a) Picture from a police helicopter just after the collapse; b) cars removal; c-d) restoration activities.

Luckily there were no victims or injured, but the event caused a great economic loss. After the landslide, the Mayor of the city, as the first responsible authority for civil protection, according to the Italian jurisdiction (Law 225/92), has coordinated the local civil protection organism. Such operating center was immediately activated in the management of restoration activities, in order to protect the involved people and historic assets and to lay the basis for the rapid reconstruction of the embankment wall and the adjacent street. First of all, the stuck cars and the stagnant water have been removed; subsequently, two lines of action have simultaneously followed: i) the construction of a bypass in correspondence of the broken water pipeline and ii) the subsoil investigations, in order to design a reconstruction of the area (Figure 39 b-d). Since the event could naturally also extend to the nearby areas, the Department of Earth Sciences of University of Florence, in coordination with the city authorities, has activated an integrated monitoring system for detecting in real time any deformation of the collapsed area and of the surrounding buildings. This system was composed by the following apparatuses: i) one robotic total station (RTS) with 18 targets; ii) one ground Interferometric radar GB-InSAR; iii) one high performance long-range 3D terrestrial laser scanning (TLS); iv) nine biaxial tiltmeters; v) four crackmeters; and vi) three seismic stations. The information coming from these sensors were saved on a web platform, where all the data were available to be viewed and analyzed.

All the elaborated and interpreted information coming from i, ii, iv and v sensors has been daily sent to the competent authorities through a specific bulletin, in order to guarantee a synergistic coordination between risk managers and the scientific community.

The present research project has focused on the monitoring activity carried out by the GBInSAR, interpreting the data of this instrument and then inserting them in the official bulletin.

3.1.4 GBInSAR technique

The GBInSAR technique exploits the same interferometric principle used in the space-borne InSAR technique to obtain displacement measurements (see Section 2.1), but, having different characteristics and acquisition geometries, it presents further strengths and weaknesses. Generally, the space-borne radars emit pulse signals, while most of the ground-based systems are constituted by a continuous wave stepped-frequency (CW-SF) transceiver. The GBInSAR equipment is portable devices consisting of two antennas (one transmits microwaves and the other receives the backscattered echo from the observed scene), that run with millimetric steps movement along 2-3 m long linear rail. One of these instruments is the linear SAR (LISA) system, developed by the Joint Research Centre (JRC) of the European Commission (Figure 40). This system also includes a network analyzer (NWA) and a control computer (Tarchi et al., 2003; Del Ventisette et al., 2011).

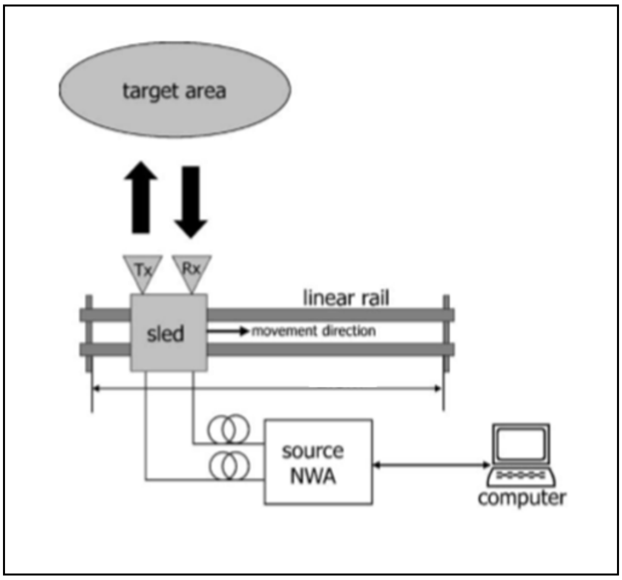

Figure 40. Scheme of the LISA systems (modified from Tarchi et al., 2003).

Through this technique, it is possible to acquire images, called interferograms (see Section 2.1), which are dimensional displacement maps characterized by range (along the direction perpendicular to the rail) and Azimut resolutions (parallel to the synthetic aperture) (Figure 41).

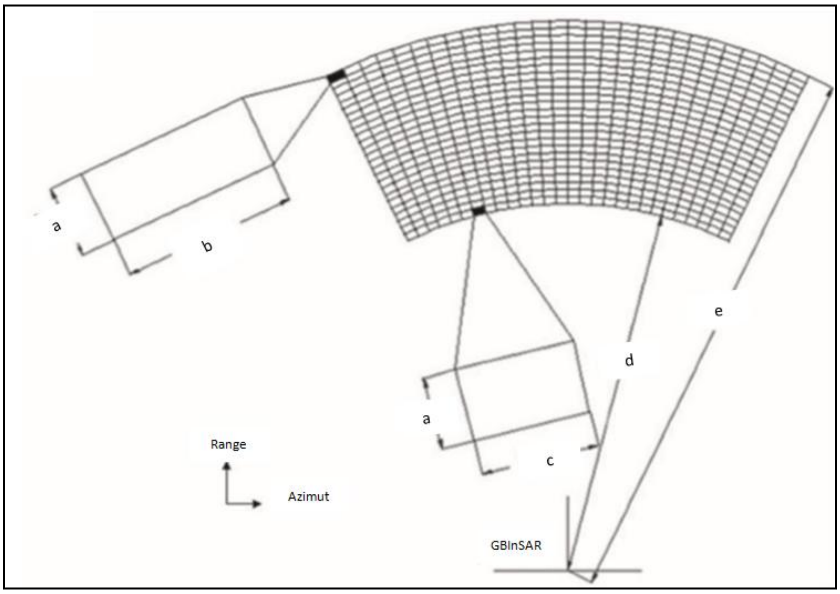

Figure 41. Resolution grid for the GBInSAR system (Modified from Del Ventisette et al., 2011). It is possible to observe that the azimuth resolution is not constant but gets worse as the object distance from the sensor increases.

A specific processing (phase unwrapping) allows switching from these images, that point by point indicate the values of the interferometric phase, to ground displacement maps with metric/sub metric resolution and submillimeter accuracy (Ghiglia and Romero, 1994).
For its instrumental characteristics, the GBInSAR technique guarantees a greater freedom in choosing the position of the radar, allowing to operate even in the presence of steep scenarios (as in the case of Lungarno Torrigiani), where satellites perform unsuccessfully. Furthermore, a high sampling rate (about every 10 minutes, which is a much shorter time than the revisit time of satellites); the possibility to choose the best line of sight (LOS) for the analysis; and a high geometric resolution of the acquired image due to the reduced distance between the radar and the target, are essential characteristics for application in different environmental context, mainly for landslides real-time monitoring and early warning systems (Luzi et al., 2004; Casagli et al. 2009; Casagli et al., 2010; Del Ventisette et al., 2011; Intrieri et al, 2015). The potentialities and the versatility of this instrument have also made it an effective tool for safeguard activities on cultural heritage sites, as it is essential to continuously supervise their stability conditions. In fact, if the investigated scene is a man-made opera, it is not necessary to apply artificial targets to it; this avoids aesthetic and functional impacts on the heritage (Tapete et al., 2013; Montuori et al., 2014; Pratesi et al., 2015; Frodella et al., 2016). However, some limits have been found in this system, such as: the data acquisition obtained only along the LOS (as for the space-borne interferometry); the possibility to monitor only areas of limited extension; the necessity to place the instrument in a stable area, which also has good visibility on the investigated scenario (Tarchi et al., 2003). The main factors that produce noise (decorrelation effects) on the acquired data are, e.g., atmospheric changes; the presence of vegetation, that is subject to strong changes as a function of seasons; and very fast movements on the investigated scene (the GBInSAR is able to monitor displacements from few millimeters per day up to 1 or more meters per day) (Zebker and Villasenor, 1992; Luzi, 2010; Pratesi et al., 2015).

3.1.5 Characteristic of the installed GBInSAR system and data acquisition

The monitoring and early warning activity with GBInSAR on the Lungarno Torrigiani started on 25 May 2016 at 11.00 a.m., and it lasted for the whole duration of the collapsed riverbank restoration works, which ended on 4 November 2016. Unlike the other installed instruments, the GBInSAR continued until 15 January 2017, in order to supervise the stability of reconstruction works.

This instrument has been located in a stable place in the opposite riverbank to the Lungarno Torrigiani, in order to guarantee a fixed observational geometry (zero baseline condition). The stability of the system location has been certified by a PSInSAR analysis of recent satellite data that has been conducted before choosing the site. Furthermore, considering that the radar interferometry provides only the displacement component along the LOS, the viewpoint of the radar has been selected as parallel as possible to the expected direction of the sliding movements (Figure 42a). Later, the instrument has been protected from atmospheric agents through a wooden cabin that was specially built to leave the LOS unobstructed (Figure 42b).

Figure 42. a) GBInSAR instrumentation positioned in the riverbanks opposite to Lungarno Torrigiani, and b) wooden cabin built to protect the GBInSAR.

The GBInSAR, implemented by the Ellegi-LiSALab s.r.l. company, is property of the University of Florence, and it is composed of a 2.0 m long linear rail and a continuous-wave step-frequency (CW-SF) transceiver unit, characterized by a transmitting and receiving antenna, operating in the ku-band (wavelength range of 2.5–1.67 cm; central frequency of 17.2 GHz and 200 MHz bandwidth). This system allows obtaining sub-millimeter sensitivity in the estimation of LOS displacements.

3.1.6 GBInSAR monitoring results

The first step of the GBInSAR monitoring has been the identification of areas on the investigated scene that were suitable for interferometric processing. This action has been performed through the use of a power image, which is related to the amplitude of the backscattered radar signal. As visible in Figure 43, the elements with high reflectivity show high signal in the power image, and they are located in some portions of the collapsed embankment wall and of the buildings behind.

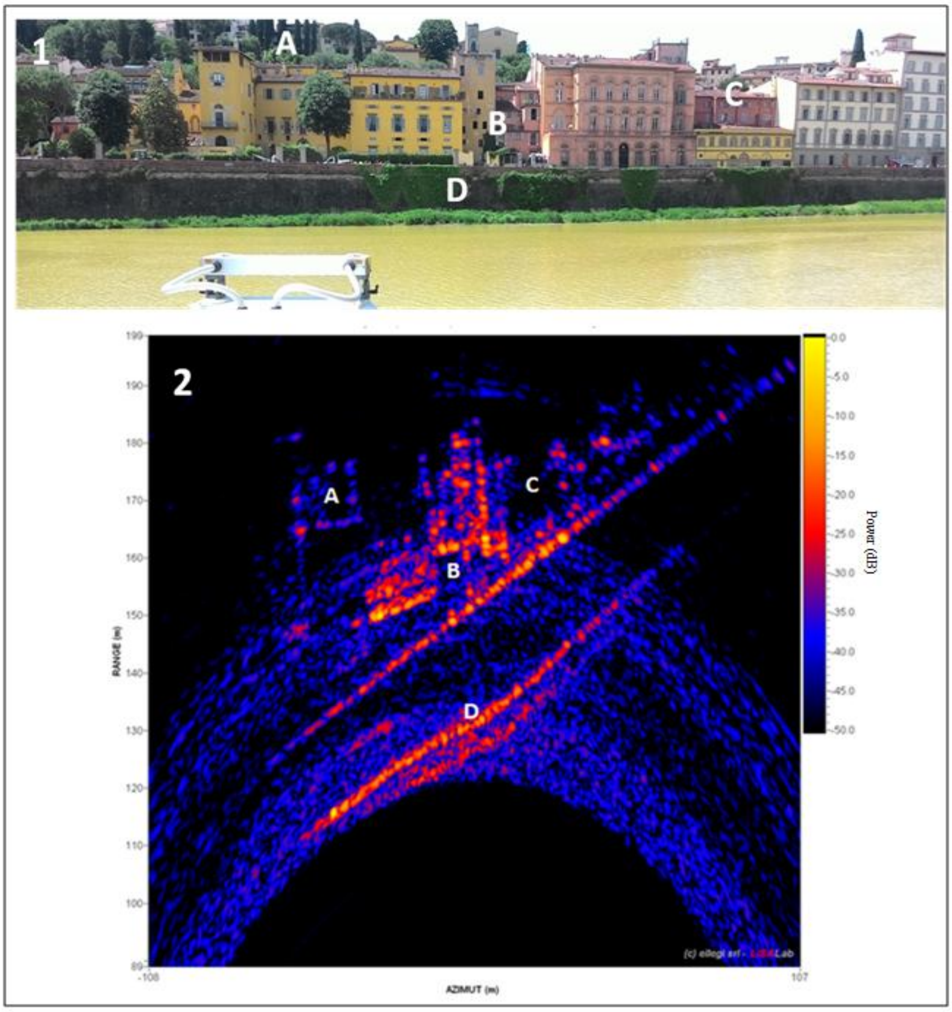

Figure 43. Comparison between 1) optical image and 2) power image of the observed scene, acquired from GBInSAR position on 25 May 2016. Power is expressed in decibels (dB).

The sight from the GBInSAR system has thus offered a fairly suitable coverage for obtaining interferometric maps.

For an optimal deformation analysis of the Lungarno Torrigiani, the cumulative displacement maps have been considered more suitable because they were less affected by atmospheric noise than the single interferograms. These maps are represented with a color scale visualization: stable areas are shown in light green; areas moving toward the GBInSAR feature colors from yellow to purple (maximum cumulative displacement); at last, areas characterized by displacements away from the sensor feature colors from dark green to deep blue (Figure 44).

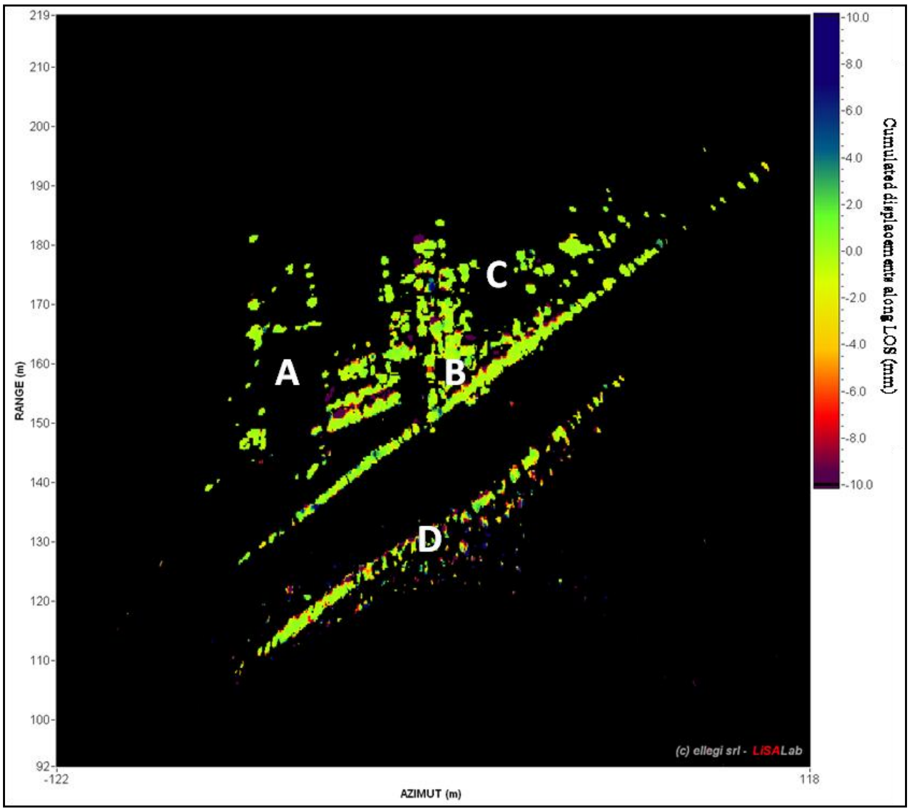

Figure 44. Cumulative LOS displacement measured by the GBInSAR from 11:20 to 17:07 of 25 May 2016.

In this picture, that shows the displacement measured in the early stages of the GBInSAR monitoring, some decorrelated areas (multicolor pixels) are mainly visible on the embankment wall (D area). They are probably due to the removal of the cars that were parked along the Lungarno Torrigiani at the collapsed time and to the climbing vegetation (see Figure 43), which was later removed in order to guarantee a better data analysis. The decorrelated areas on the buildings behind the wall were probably due to atmospheric noise.

In the investigated area, nine control points have been selected in order to monitor the stability of the embankment wall and of the buildings behind also through the time series of their displacements (Figure 45).

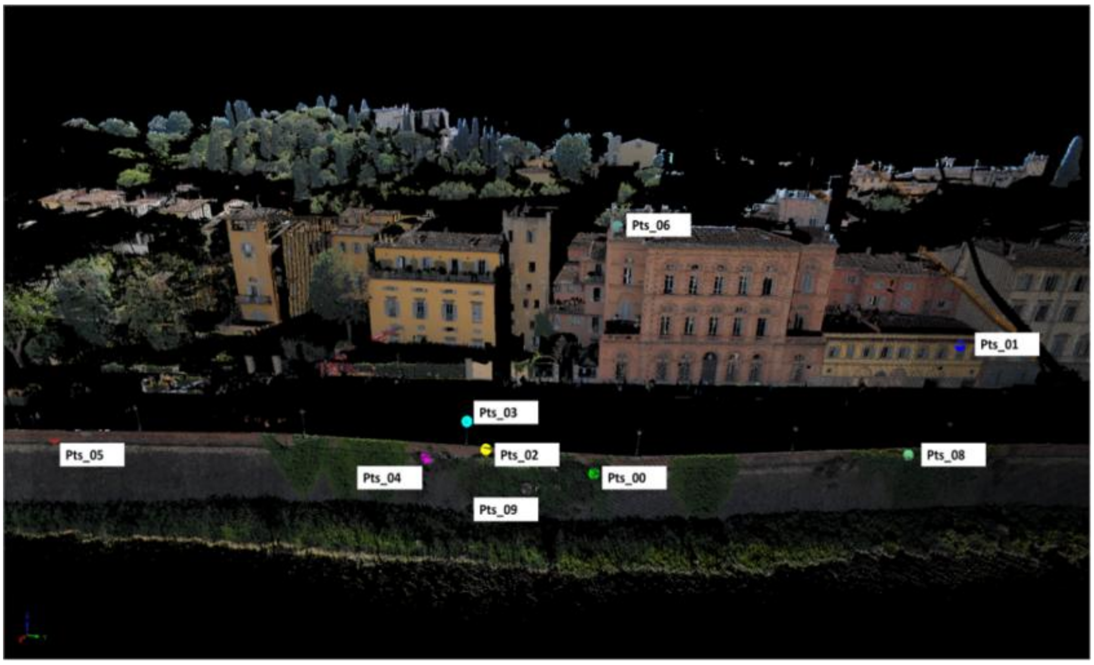

Figure 45. Nine GBInSAR targeted points reported on a coloured point cloud of the whole area obtained with the TLS.

These points have been identified on the basis of high coherent values of the radar signal in their correspondence and for their high representativeness of the main critical issues. Particularly, the points Pts_00, Pts_02, Pts_03, Pts_04, and Pts_09, are located within the cusp-shaped deformation of the retaining wall whereas the points Pts_05 and Pts_08 are located on the fracture systems of the Ponte alle Grazie side and of the Ponte Vecchio side, respectively. The last two points (Pts_01 and Pts_06) were selected in order to be representative of possible movements localized in the buildings behind the landslide.

Furthermore, five criticity levels have been set up by virtue of the expert judgment, in order to discriminate the recorded movement and therefore evaluate the possibility of activating a warning system. These levels are: Low: negligible velocity; Moderate: max. velocity < 0.5 mm/h; Medium: 0.5 mm/h < max. velocity < 1 mm/h; High: max. velocity > 1 mm/h. These assumptions were then validated on the basis of deformation measurements carried out by other instrumentations (RTS, tiltmeters and crackmeters).

The cumulative LOS displacement map (averaged at 24 h and processed with incremental method) of the entire monitoring period, has not shown significant deformation (Figure 46), but some displacement have been localized on the cusp-shaped deformed area of the retaining wall (circled area). They have been mainly attributed to the reconstruction works, whereas the decorrelated areas on the behind buildings were probably due to atmospheric factors.

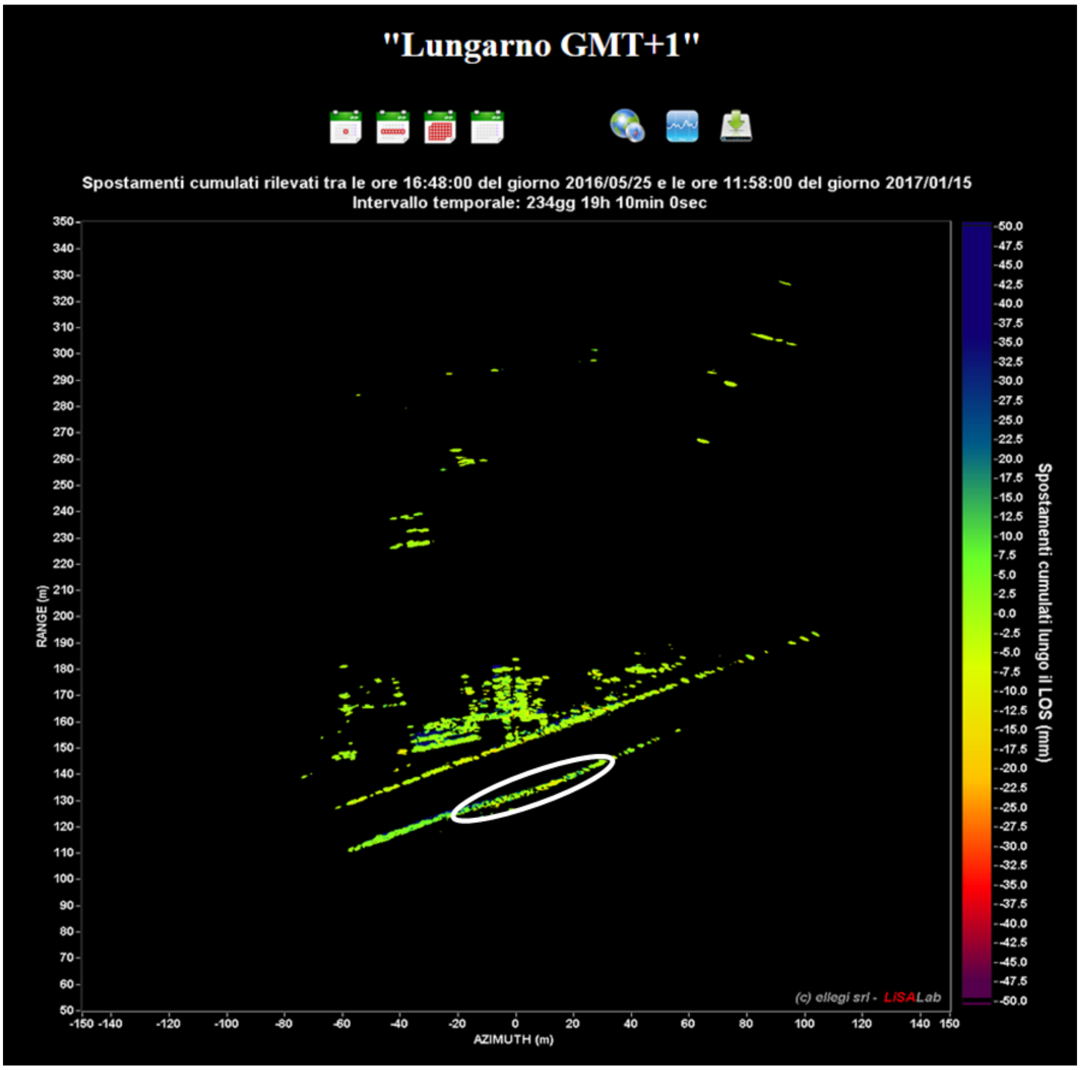

Figure 46. Displacement map covering the entire duration of the GBInSAR campaign. The circle indicates the area of the investigated scene where the greater displacements have been identified.

The daily interpretation of all the data coming from the integrated monitoring has been sent to the competent authorities through the aforementioned bulletin, in order to update them on the degree of the area stability.

The level of criticity detected by the GBInSAR has been always moderated (according to the classification mentioned above), despite some anomalous movements that have been promptly communicated.

For example, starting from the morning of 09 June 2016, a displacement of 5.6 mm towards the Arno River (see Figure 47a,b), in correspondence with the target point n° Pts_02 has been detected by comparing single SAR images. As can be seen from Figure 47a, the monitored area shows a strong decorrelation of the radar datum, and thus, the displacement recorded at the target point has been taken as reference, by virtue of the high coherence value of the radar signal at that point.

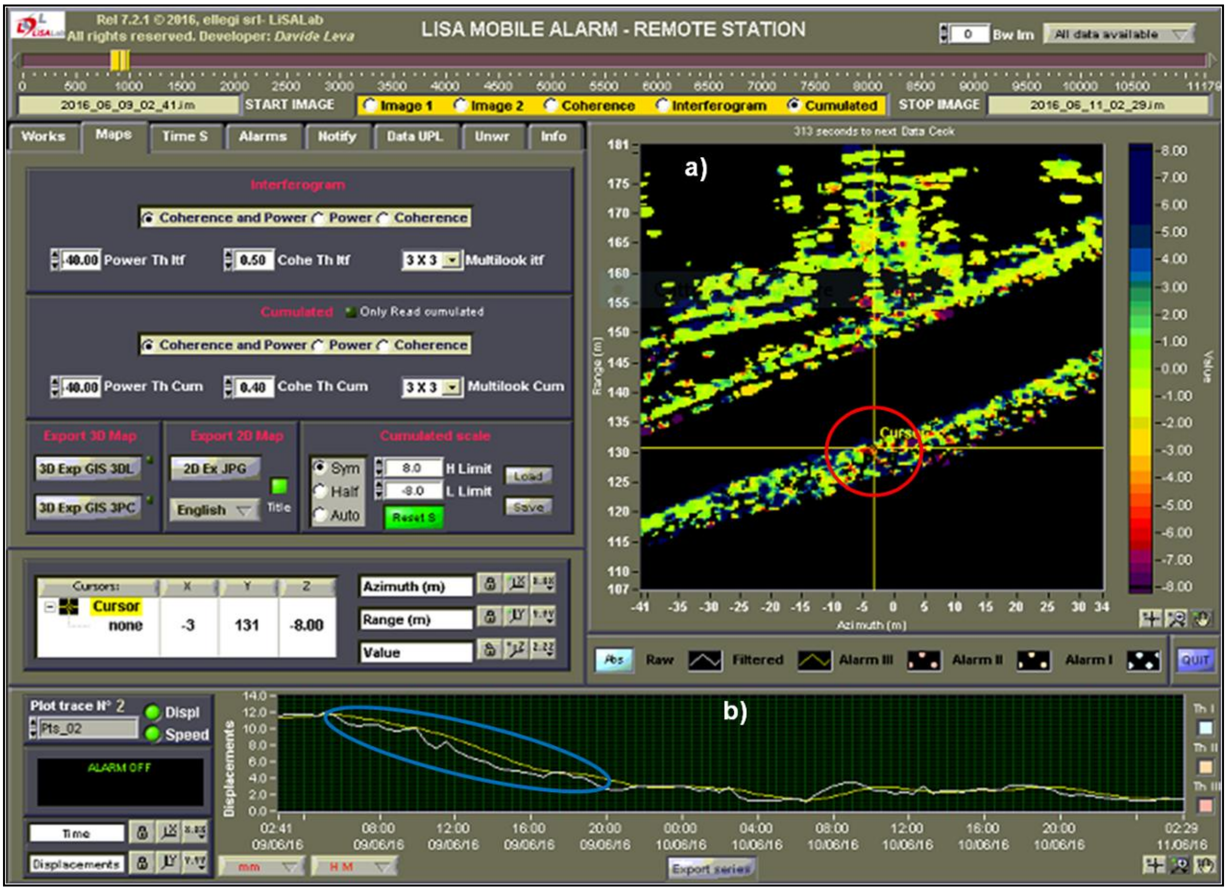

Figure 47. Screenshot of the Lisamobile remote control station. a) 2-D radar map of cumulated displacement recorder from 09 June 2016 at 02:41 a.m. to 11 June 2016 at 02:29 a.m.; the target point n° Pts_02 is circled in red. b) Cumulated displacement time series (the yellow line represents the average of the displacement) relative to control point n° Pts_02: a displacement of about 6.00 mm towards the Arno River is visible and it is circled in blue.

This anomalous movement has been notified on 09 June 2016 through the bulletin of 17.00 p.m. (Figure 48).

In this case, it has been decided to choose a medium criticity level, as such embankment wall displacement has been attributed to the restoration work active in that area.

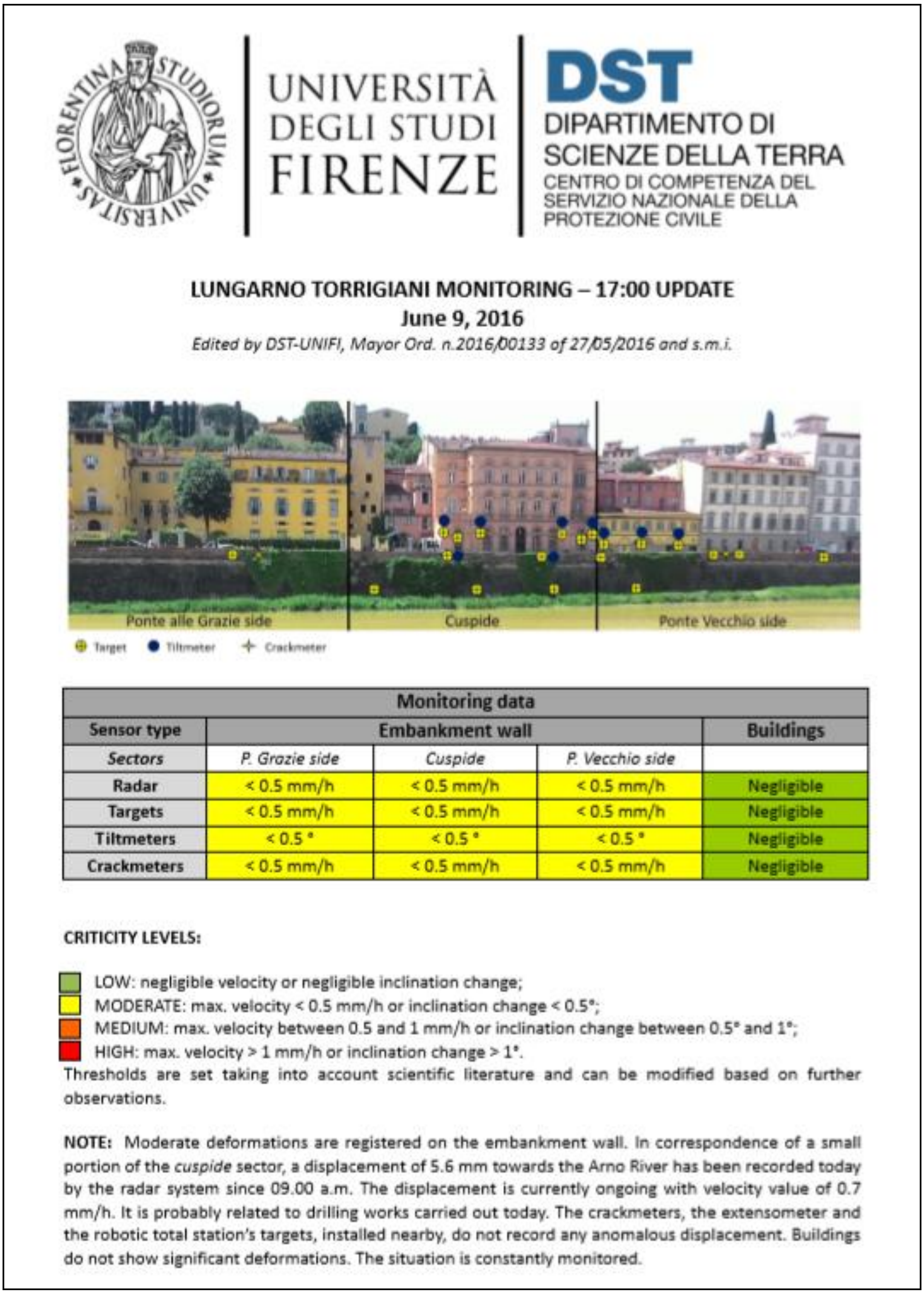

UNIVERSITÀ DEGLI STUDI FIRENZE

DST DIPARTIMENTO DI SCIENZE DELLA TERRA
CENTRO DI COMPETENZA DEL SERVIZIO NAZIONALE DELLA PROTEZIONE CIVILE

LUNGARNO TORRIGIANI MONITORING – 17:00 UPDATE
June 9, 2016
Edited by DST-UNIFI, Mayor Ord. n.2016/00133 of 27/05/2016 and s.m.i.

Monitoring data				
Sensor type	**Embankment wall**			**Buildings**
Sectors	*P. Grazie side*	*Cuspide*	*P. Vecchio side*	
Radar	< 0.5 mm/h	< 0.5 mm/h	< 0.5 mm/h	Negligible
Targets	< 0.5 mm/h	< 0.5 mm/h	< 0.5 mm/h	Negligible
Tiltmeters	< 0.5 °	< 0.5 °	< 0.5 °	Negligible
Crackmeters	< 0.5 mm/h	< 0.5 mm/h	< 0.5 mm/h	Negligible

CRITICITY LEVELS:

- LOW: negligible velocity or negligible inclination change;
- MODERATE: max. velocity < 0.5 mm/h or inclination change < 0.5°;
- MEDIUM: max. velocity between 0.5 and 1 mm/h or inclination change between 0.5° and 1°;
- HIGH: max. velocity > 1 mm/h or inclination change > 1°.

Thresholds are set taking into account scientific literature and can be modified based on further observations.

NOTE: Moderate deformations are registered on the embankment wall. In correspondence of a small portion of the *cuspide* sector, a displacement of 5.6 mm towards the Arno River has been recorded today by the radar system since 09.00 a.m. The displacement is currently ongoing with velocity value of 0.7 mm/h. It is probably related to drilling works carried out today. The crackmeters, the extensometer and the robotic total station's targets, installed nearby, do not record any anomalous displacement. Buildings do not show significant deformations. The situation is constantly monitored.

Figure 48. Bullettin of the 09 June 2016, update of 17.00 p.m. The monitored area has been subdivided in three sectors: Ponte alle Grazie side, Cuspide (Central part of the embankment wall), and Ponte Vecchio side. The criticity levels chosen through all the sensors are showed. Additional information about deformation anomalies are provided in the note section.

The notes of the bulletin, indeed, indicate: "The displacement is currently ongoing with a velocity value of 0.7 mm/h and it is probably related to drilling works carried out today. The other sensors, installed nearby, do not record any anomalous displacement and the buildings behind do not show significant deformations”.

The situation has been constantly monitored in the following hours, in order to understand if the identified displacement would have lasted over time. As expected, the approaching trend of the wall to the Arno River stopped and has been replaced by a substantial stability (Figure 47b).

The GBInSAR system, unlike the other instruments, stopped monitoring on 15 January 2017, in order to supervise the stability of the restoration works. The interferometric data for the period from 4 November 2016 (when the restoration works finished) to 15 January 2017, are summarized in Figure 49, where the displacement time series of the 9 chosen control points are visible. The recorded deformation are between 0.5 mm (Pts_05) and 1.7 mm (Pts_04), and these values show a moving away trend from the radar interferometer (positive values). It is believed that this trend is not due to real displacements of the investigated area but to seasonal variations of temperature. In fact, it has already been demonstrated that displacements values within or close to the stability threshold are not real displacements but they are thermal effects due to sun radiation over the monitored surfaces and seasonal temperature changes (Tapete et al., 2013).

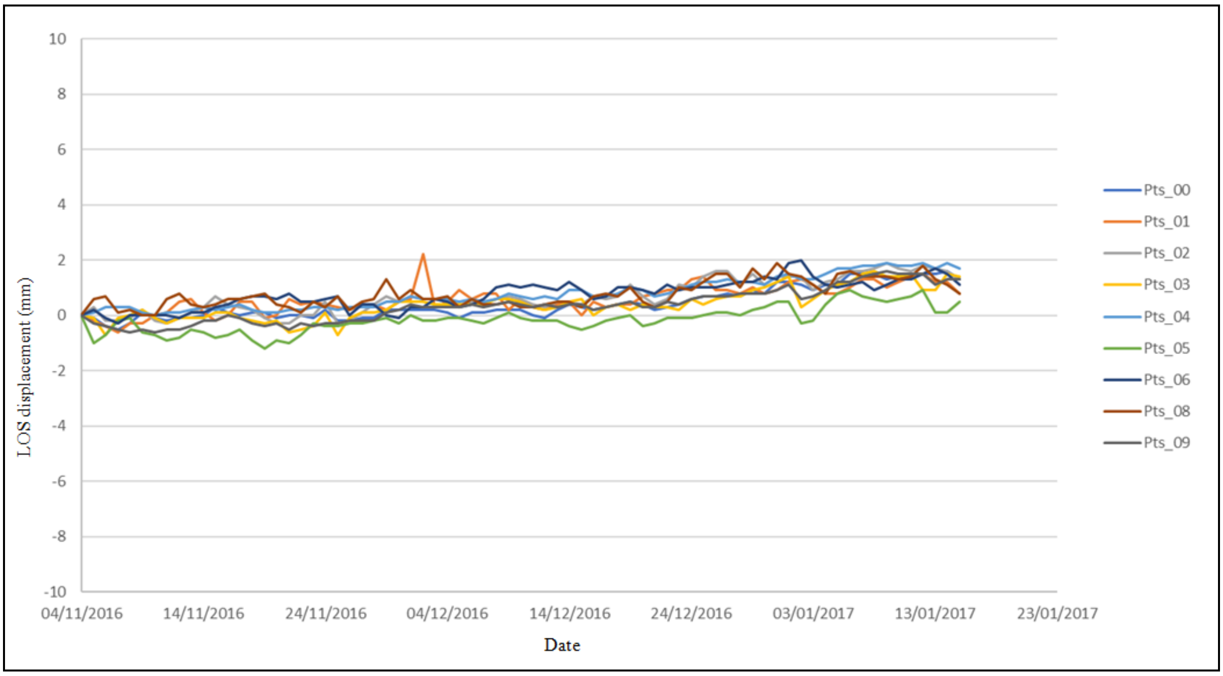

Figure 49. LOS displacement time series of the chosen control points measured by the GBInSAR system for the period from 04 November 2016 to 15 January 2017.

3.2 TLS for monitoring the geological instabilities of Canossa Cliff (Reggio Emilia)

World Heritage properties, unlike cultural sites that are not registered in the World Heritage List, benefit from an international attention that guarantees a large investment of funds in their conservation and management activities. However, each cultural or natural site is characterized by some peculiarities that make it unique and worthy of being preserved over time, regardless of whether it is a UNESCO site or not.

For this reason, the rockfall phenomenon that, over the years, led to the progressive destruction of the Castle and Cliff of Canossa (a cultural asset of high value located in the Emilia Romagna Region, Central Italy), has been analyzed and monitored. By virtue of the characteristics (kinematics and velocities) and the typology of this geological instability, a monitoring was carried out using the Terrestrial Laser Scanner. The TLS is in fact suitable for assessing the magnitude of rockfalls on a cliff, because they are so fast that not even the GBInSAR system can monitor them in real-time. Moreover, the point clouds acquired with the chosen ground-based technique were used to analyze the instabilities observed on the badlands, which constitute the landscape at the foot of the cliff.

3.2.1 Geological and geomorphological setting

The Canossa Cliff is located in the Emilia Romagna Region (Central Italy), few tens kilometers SW of Reggio Emilia, in the pedeappenninic hills between Enza Creek and Secchia River (Figure 50a). This area is characterized by hills, bumps, plains and the typical *calanchi*. This latter is a dialectic term originating exactly from the Emilia Romagna Region, and it is used to describe a type of badland, characterized by a small horse-shoe shaped hydrographic unit formed by clayey bedrock (Farabegoli and Agostini, 2000; Moretti and Rodolfi, 2000).

The Apennines in this area are characterized by average annual rainfall between 2600 mm of the ridge and 900 mm of the hill; the contributions of precipitation have two peaks in autumn (November) and in late spring (April - May), interspersed with two minimums, one more pronounced in summer, and one in winter. At not very high altitudes, the rainfall increases according to the altitude; therefore, also in the Appennine hill, there are notable increases with respect to the plains, even if they have the same seasonal distribution trend (two maxima and two minima). The average annual temperatures vary from 6 ° to 13 ° C; the maximum temperatures are recorded on July whereas the minimum temperatures on January (Castronuovo, 2005).

The outcropping formations are part of the late palaeogeographic domains of the Northern Apennines, and belong entirely to the Epiligurian Domain (Figure 50b; Figure 51). The latter was deposited in some basins on the Ligurian units, following the closure of the Ligurian Ocean that led to the next Apennine Orogenic Phase (Ricci Lucchi and Ori, 1985).

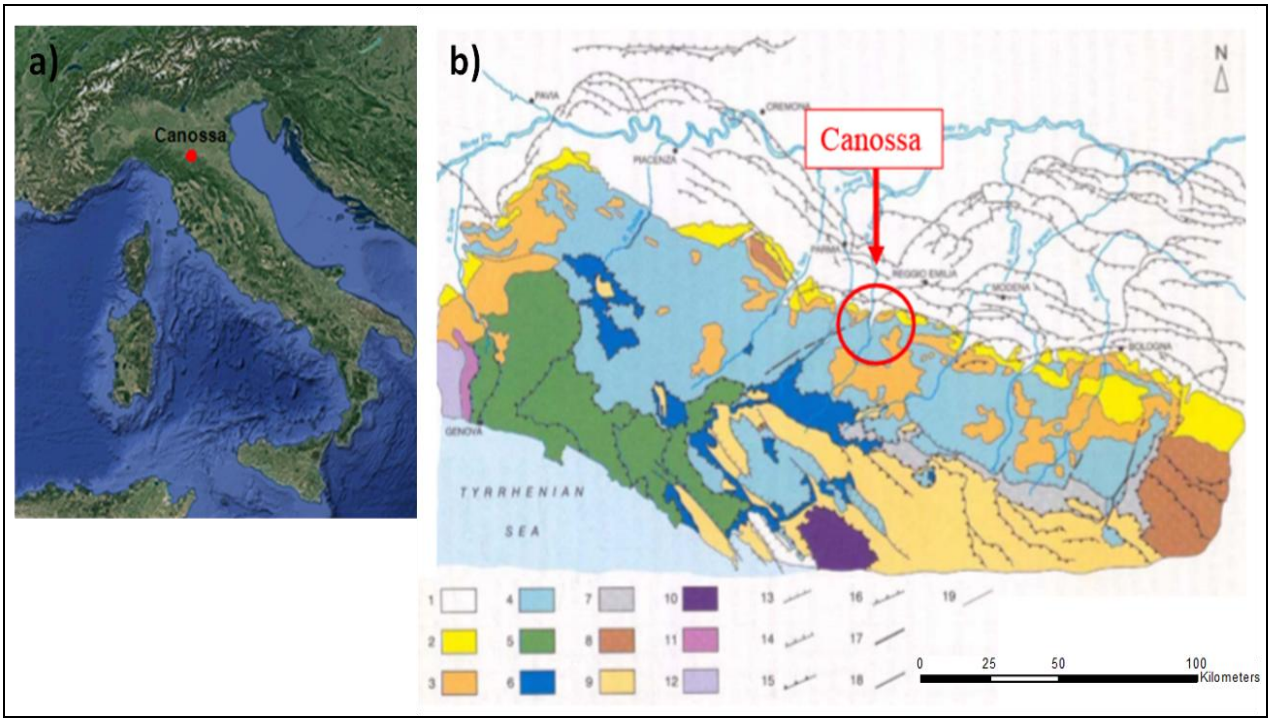

Figure 50. a) Localization of Canossa; b) Geology of the Northern Apennines. 1 Quaternary deposits; 2 Marine deposits of the superior miocene-pleistocene; 3 Epiligurian Succession; 4 Ligurian External Unit; 5 Ligurian Internal Unit; 6 Subligurian Unit; 7 SestolaVidiciatico tectonic Unit and Melange of Fiorenzuola; 8 Umbro-Romagnole Units; 9 Tuscan Units; 10 Tuscan Metamorphic Unit; 11 Sestri-Voltaggio Zone; 12 Voltri Grups; 13 Normal faults; 14 subsoil normal faults; 15 Reverse fault and trusts; 16 subsoil reverse faults; 17 strike-slip faults; 18 high angle faults; 19 lithological limits. Modified from Casagli et al., 2006.

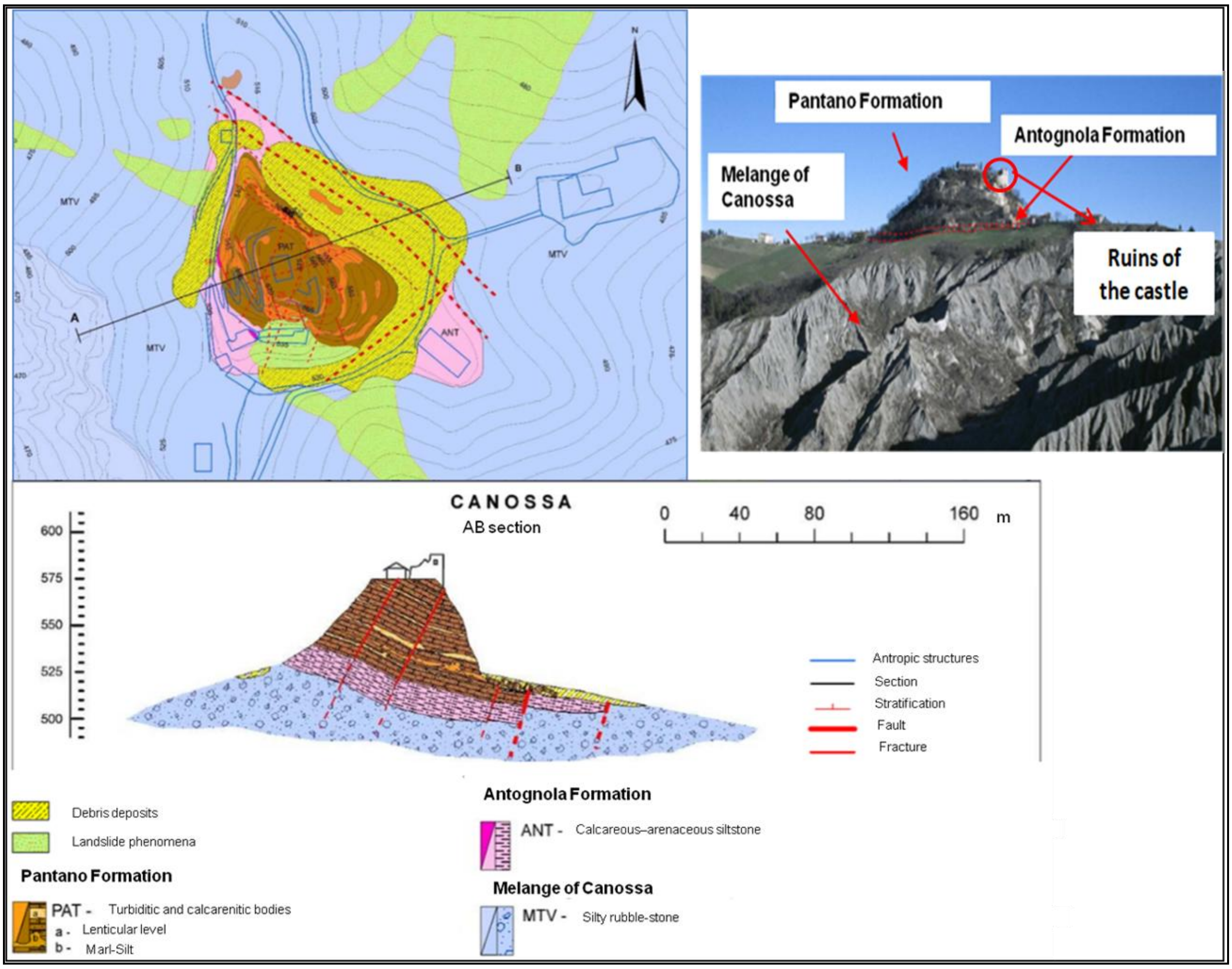

Figure 51. Geological map of Canossa Cliff, modified from Casagli et al., 2006.

This geological setting is structurally referable to the "plate-substratum system" (Figure 52), where several rock and soil slope instabilities are frequent. This structure has often been associated with high risk conditions, because many uplands composed by isolated rock slabs have been sites of historical towns or castles (Gigli et al., 2012, Frodella et al., 2016).

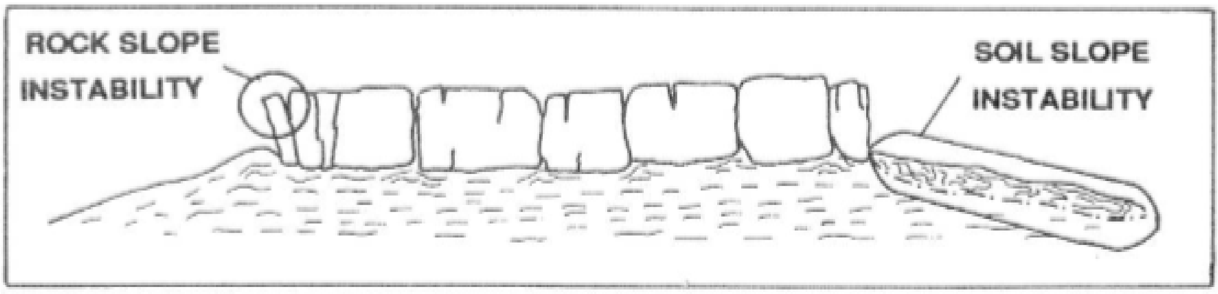

Figure 52. Instability mechanisms of a "plate-substratum system" (Casagli et al., 1992).

In addition to the “plate-substratum system” evolution, that is an extremely slow mechanism, several rapid phenomena such as rockfalls, slips and overturns of rocky blocks represent a serious risk for inhabitants, tourists and the exposed property. These phenomena are mainly due to the several sub-vertical fractures of the “Sandstones of Bismantova” that affect the cliff throughout its thickness (Figure 53), and are the cause of the cracks that currently are present in the castle ruins (Casagli et al., 2006).

Figure 53. Sub-vertical fractures on the rocky wall of Canossa Cliff.

The geomorphological evolution of the area surrounding the cliff is also characterized by two main instability processes: superficial sliding landslides and *calanchi* erosion processes (Casagli, 2006). The first phenomena have threatened in the past the eastern sector, whereas *calanchi*, which are localized exclusively in the western area, are quickly retreating towards the anthropic structures that are present at the foot of the cliff (Figure 54).

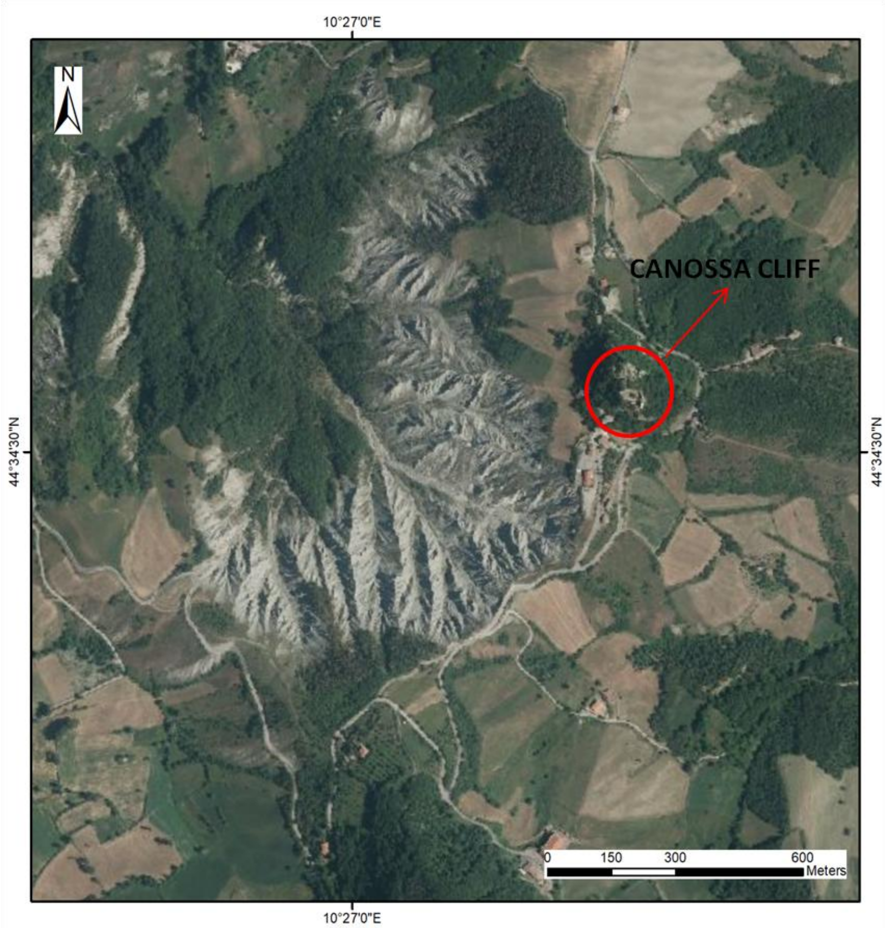

Figure 54. The typical C*alanchi*, located on the left of the Canossa Cliff.

3.2.2 Evolution of the study area and past instabilities

The Apennines near Reggio Emilia are home to a remarkable fortified system, made up of several castles that the Canossa family, beginning with Adalberto Atto, had built in the 10th century on the ridges that naturally played a defense role (Valli, 1987). The Castle of Canossa belongs to this system, and the *calanchi* that surround its cliff, in fact, most likely contributed to the defense of the castle: being inaccessible, they took away much space for action from the enemy troops. This castle, whose architectural structure exploited the natural conformation of the land, at the age of which "Matilde of Tuscany" reigned, was composed of a very large unit made up of towers, walls, courtyards and the church of S. Apollonio (Figure 55).

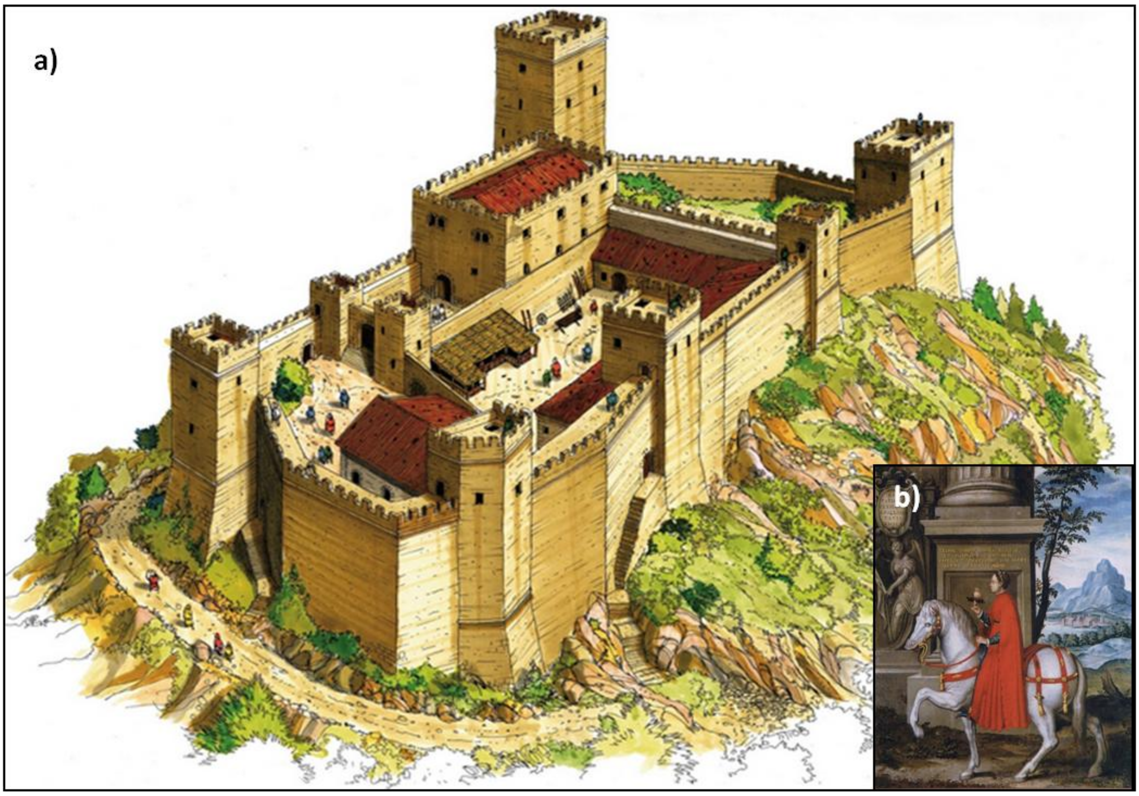

Figure 55. a) The Canossa Castle at the age of “Matilde of Canossa”; b) Matilde on horseback (Modified from Di Cicco, 2015).

Matilde played a very important political role in the 11th century, siding with the Pope during the period of crisis between the Church and the Empire, led, respectively, by Pope Gregory VII and the young Emperor Henry IV. In 1076, the Pope, because of the disagreements known as the "investiture fight", excommunicated the Emperor, depositing him from the throne of Germany and from his rights. Following this action, the Emperor was forced to apologize the Pope, reaching him at the Castle of Canossa, where he was staying as a guest of Matilde. It was this episode that made worldwide famous the Castle of Canossa. Unfortunately, the splendor of the structure was extinguished by the hand of man, through wars and sieges, and by the hand of natural events (Di Cicco, 2015). Thus, in the middle of the 18th century, the castle began its slow decline, until its fall into ruins (Figure 56).

Figure 56. a) The current view of the castle from the street at the foot of the cliff and b) from the current museum.

The news about the past geological instabilities of this area are not very detailed, but landslide phenomena has been recorded starting from XIII-XIV centuries, and it is known that during 1846 a huge boulder collapsed from the cliff. A similar phenomenon occurred recently, on February 2004, when a block of about 80 m^3 collapsed from the North face of the rocky cliff and almost reached the provincial road (Figure 57).

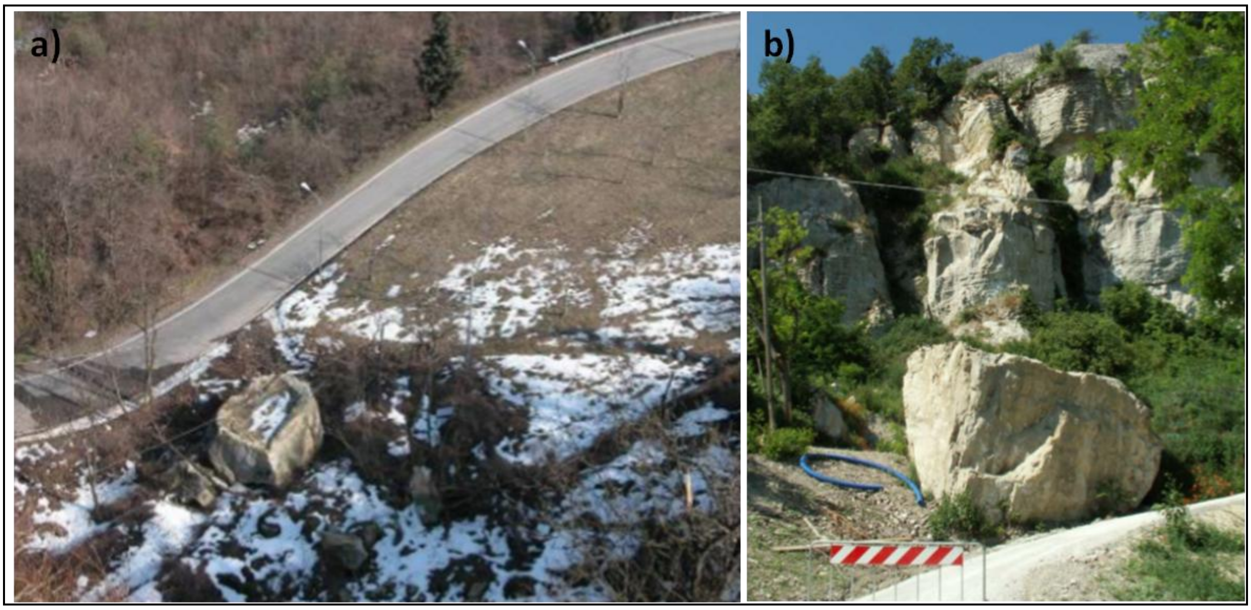

Figure 57. View from a) above and from b) below of the block of about 80 m^3 that collapsed from the rock face on February 2004 (Casagli et al., 2006).

Regarding the landscape adjacent to the cliff, the *calanchi* are the most instable landforms. In the past, they played a defensive role, but recently these morphologies have threatened the safety of this area. In fact, the retreat of the *calanchi*, caused by the erosion phenomenon typical of these forms, has created in the past damages to the road network adjacent to the cliff, as visible in Figure 58, and to the parking area at the foot of the cliff, as visible in Figure 59.

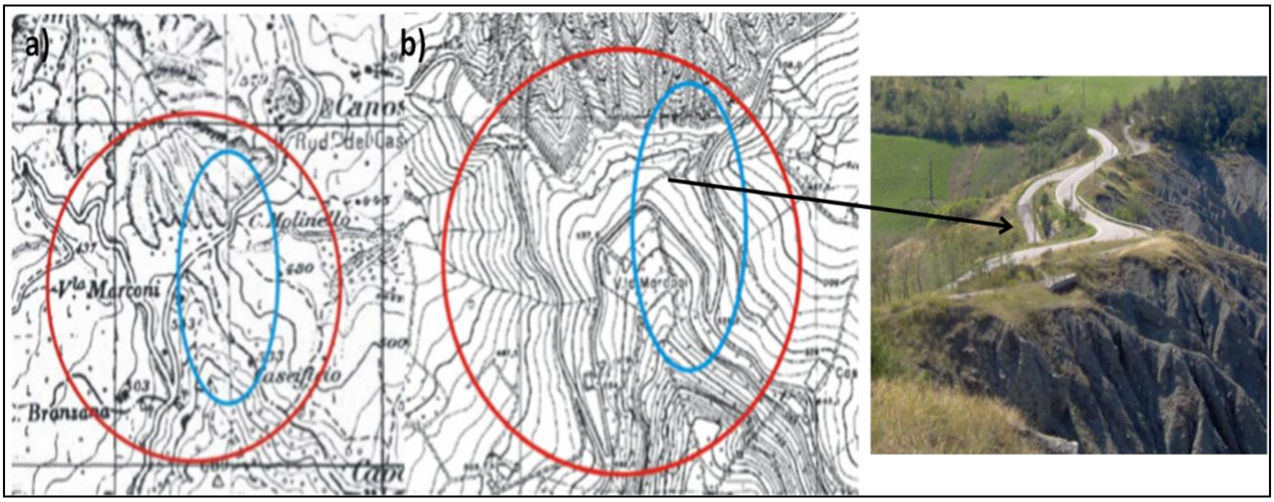

Figure 58. a) IGM map (1: 25000) which shows the old road route. b) CTR map (1: 10000) which shows the new road route. In the picture on the right, a portion of the old road completely surrounded by *calanchi* is visible (Casagli et al., 2006). IGM: Military Geographic Institute; CTR: Regional Technical Card.

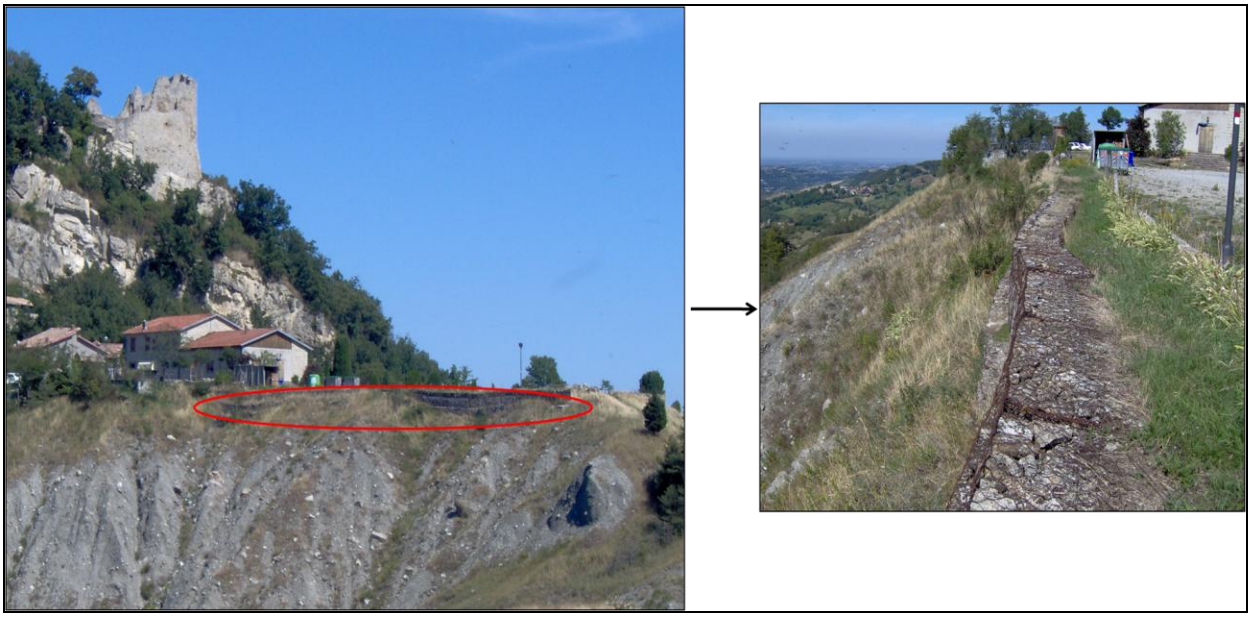

Figure 59. September 2006 photo showing the retreat of the *calanchi* until the parking area protected by a gabion (Casagli et al., 2006).

3.2.3 In situ observations

On 07 February 2017, some field surveys were carried out on the Canossa Cliff and the surrounding landscape, in order to identify any current damages caused by the high instability of this territory.
In proximity of the rocky walls constituted by the "Bismantova Sandstone", no collapsed blocks were identified, probably due to the dense vegetation surrounding this formation (Figure 60).

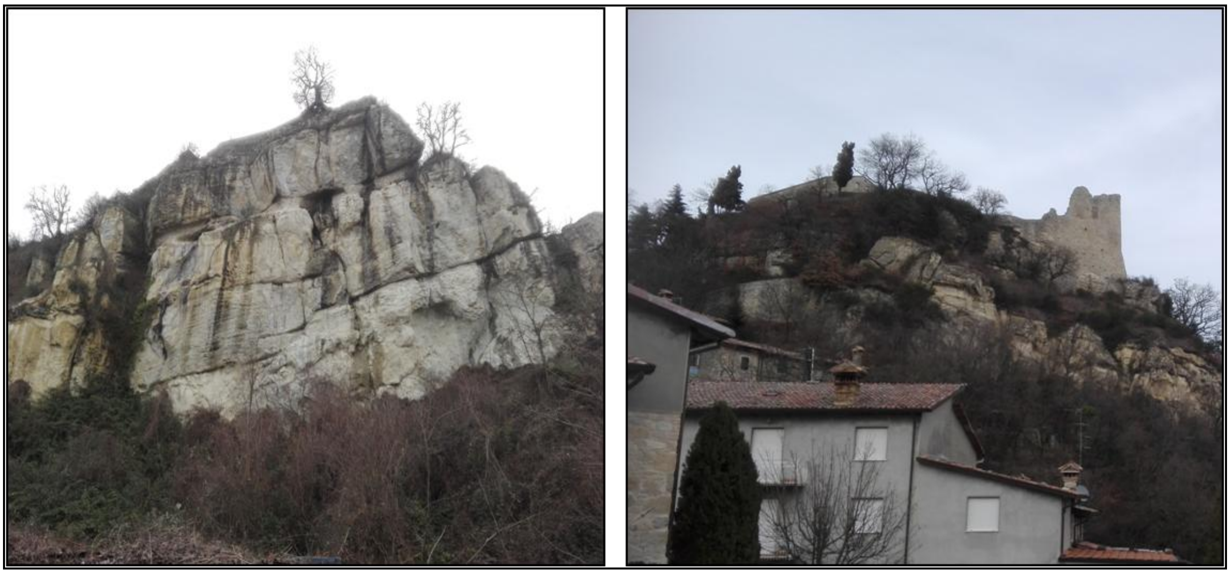

Figure 60. North wall (on the left) and south wall (on the right), located at the base of the Castle ruins.

However, several cracks have been detected on the ruins of the Castle (Figure 61a), whose cause has been attributed to intense fracturing of the rocky mass (see Section 3.2.1). At the foot of the cliff, instead, some damages to the parking area have been identified (Figure 61b-d). Furthermore, in correspondence of the gabion built to protect this area by the retreat of the *calanchi* landscape (see Figure 59), a little collapse have been located (Figure 61e).

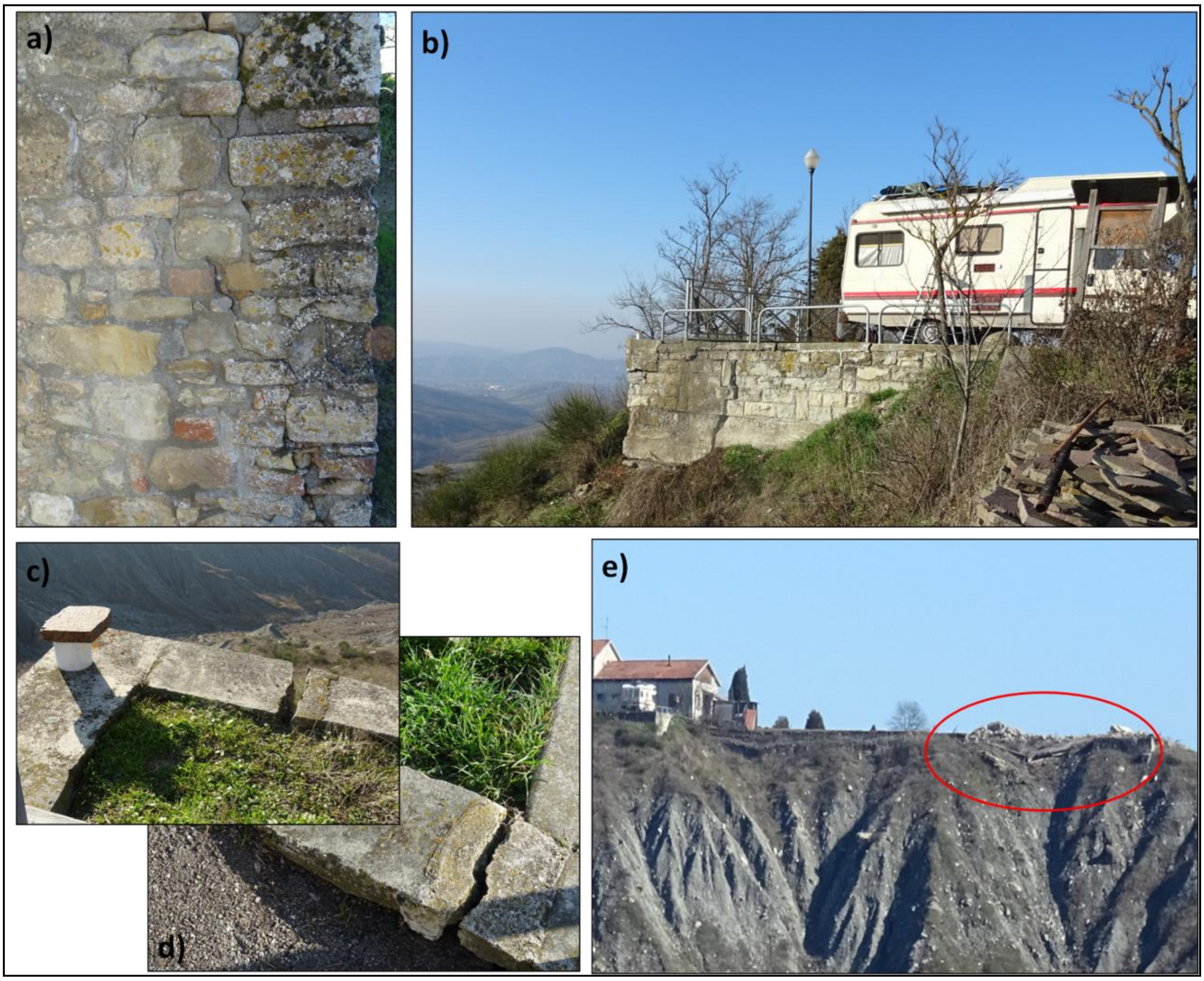

Figure 61. a) One of the cracks identified on the Castle ruins; b-d) damages on the parking area; e) little collapse of a portion of the protection gabion.

3.2.4 TLS technique

The principles of the laser scanning technique, also known as Light Detection and Ranging (LiDAR) technique, were developed since the end of the 1990s. The Airborne Laser Scanning (ALS) system was the first most exploited technique in geosciences applications and it was followed by the Terrestrial Laser Scanning (TLS) technique (Shan and Toth, 2008; Jaboyedoff et al., 2012). The laser scanner is an active remote sensing that, employing a laser beam, allows acquiring, at a very high speed and with a sub-centimetric accuracy, a three-dimensional information of a physical object. Both ALS and TLS send out laser signal and record the returning signal after it has been back-scattered by different objects (ground surface, vegetation, buildings etc.). As regards TLS, the position of the platform is fixed while the scanner moves the beam in vertical and azimuth directions, thus allowing the relief of the investigated object with high resolution (resolution from centimetric to millimetric) (Figure 62). Moreover, some instruments host a digital camera, which, managed and synchronized by the scanning software, allows producing images in real colors directly correlated with the acquired data.

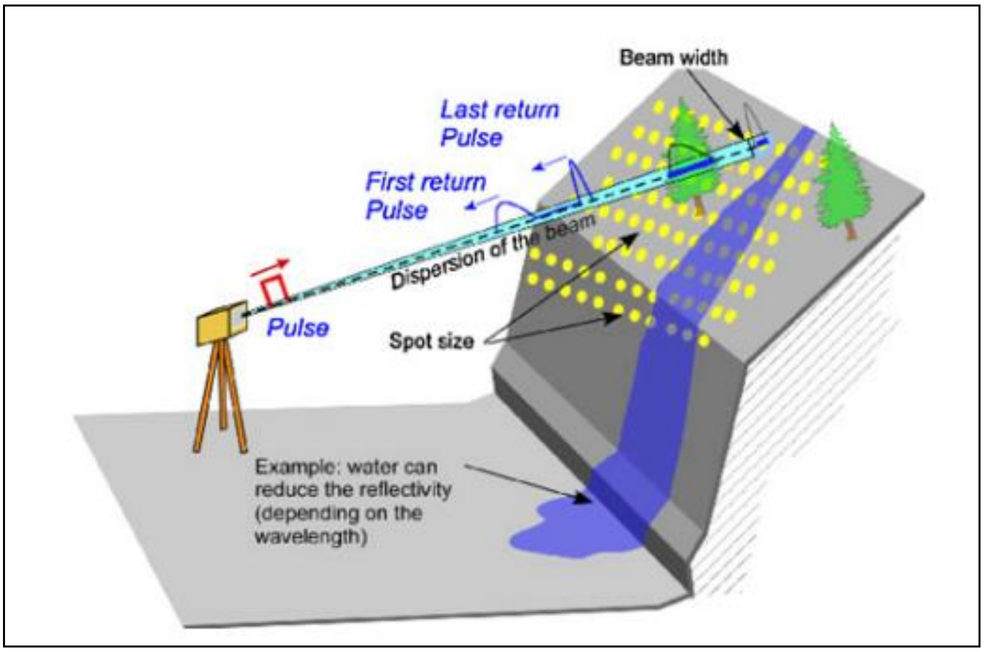

Figure 62. Principles of TLS data acquisition (from Jaboyedoff et al., 2012).

Before scanning, it is necessary to position some optical targets on the investigated element and to determine their coordinates using a high-resolution topographic GPS; the acquisition software is in fact able to recognize the most reflective points and consequently to geo-reference the scan in the chosen reference system.

Two different methods are mainly used in the laser scanning surveying: pulse and phase method (Figure 63). The first one calculates the scanner-object distance by measuring the round-trip time (or time-of-flight, TOF) of a short and intense laser pulse, whereas in the phase method, the distance is calculated by comparing the phase difference between the emitted and received continuous wave (CW) of the laser (Jaboyedoff et al., 2012; Dotta, 2016).

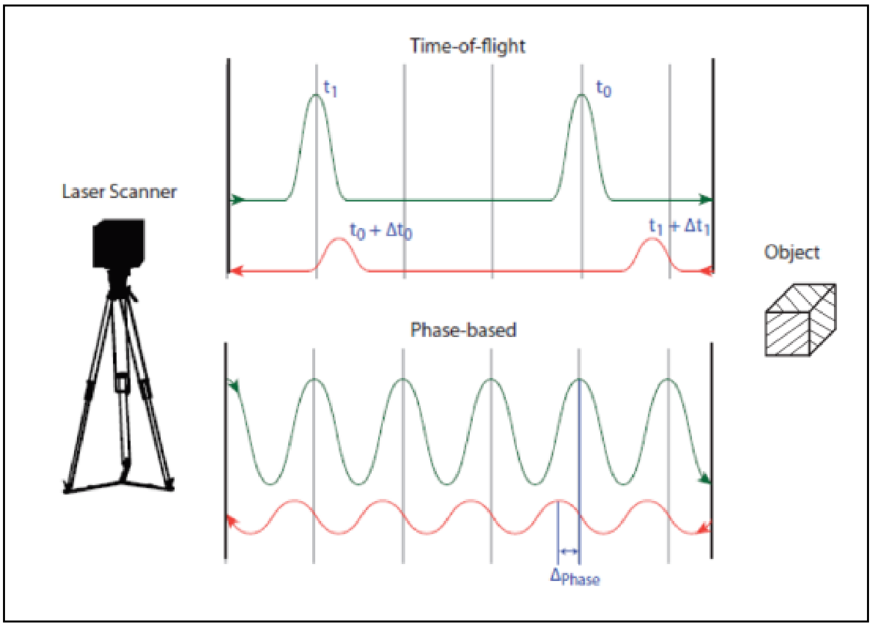

Figure 63. Acquisition principle of pulse (top) and phase method (bottom) (Dotta, 2016).

The result of a laser scanning survey is a 3D reproduction of the investigated scene, consisting of a dense set of points called "point cloud" (Figure 62). This point cloud is characterized by a Cartesian coordinates system (x, y, z) and reflectance values R (x, y, z), and it can be managed with any 3D graphics processing software. Point density depends on: the instrumental resolution, the distance sensor-object, the geometry of the scanned object, and the velocity of the moving platform.

TLS system has been widely exploited in different application such as, for examples, characterization of rockmasses and monitoring campaigns of cliff evolution (Tapete et al., 2013; Dotta, 2016; Frodella et al., 2016).

This device has been also more and more used for instability analysis in cultural heritage sites (urban areas, single monuments or archeological sites), as it is suitable for non accessible or hazardous area and it allows to obtain, in a short time and in a non-invasiveness way, a detailed representation of the investigated asset (Gigli et al., 2012; Fanti et al., 2013; Pratesi et al., 2015). In addition, by comparing point clouds acquired at different times in the same scenario, some volumetric variations can be determined (e.g., the estimation of the material extracted from a quarry, the rate of erosion in a certain area or the volume of detached rocky blocks).

Beyond the several advantages offered by TLS, this technique has some limitations, e.g. the necessity to cover, through more surveys, the shadowed areas due to the presence of some obstacles (e.g., trees and electric lines) between the scanner and the scanned objects, in addition to the amount of time required by (semi-) automatic elaboration of the point clouds during the processing phase (Tapete et al., 2013; Pratesi et al., 2015).

3.2.5. TLS surveys

In the rocky mass of the Canossa Cliff and in the *calanchi* landscape (as explained in Section 3.2.2 and 3.2.3), some of the main threats to the cultural site take place, i.e., the phenomenon of rockfall that has affected in the past the "Sandstones of Bismantova", and the retreat of *calanchi*, that has threatened the areas at the foot of the cliff (see Figure 59, Figure 60 and Figure 61).
The Department of Earth Sciences of the University of Florence, in order to better investigate these critical issues, carried out laser scanner surveys in 2005 and in 2006 (Casagli et al., 2006). From the comparison between the acquired point clouds, no displacements were found that would exceed the accuracy of the methodology, nor in the rocky walls on which the Castle rests, nor in this latter structure. The point clouds of the *calanchi* landscape, until now, has not been used for detailed studies.
At a distance of 11 years, new laser scans were carried out on the same positions of some of the previous TLS campaigns, in order to continue the monitoring and to assess the current state of the evolution of the cliff and of its neighboring territory.
On 07 February 2017, two scans were made in two distinct portion of the cliff: the North wall (S1 in Figure 64) and the South wall (S2 in Figure 64). These are the rocky walls identified as the most sensitive to the rockfalls through the field surveys carried out by the University of Florence in 2005 (on February 2004, a block of about 80 m^3 collapsed from the North face, see Figure 57).
On 15 February 2017, a third scan was carried out along the Provincial Road n° 54 (S3 in Figure 64), in order to monitor the evolution of the *calanchi* near the parking area.

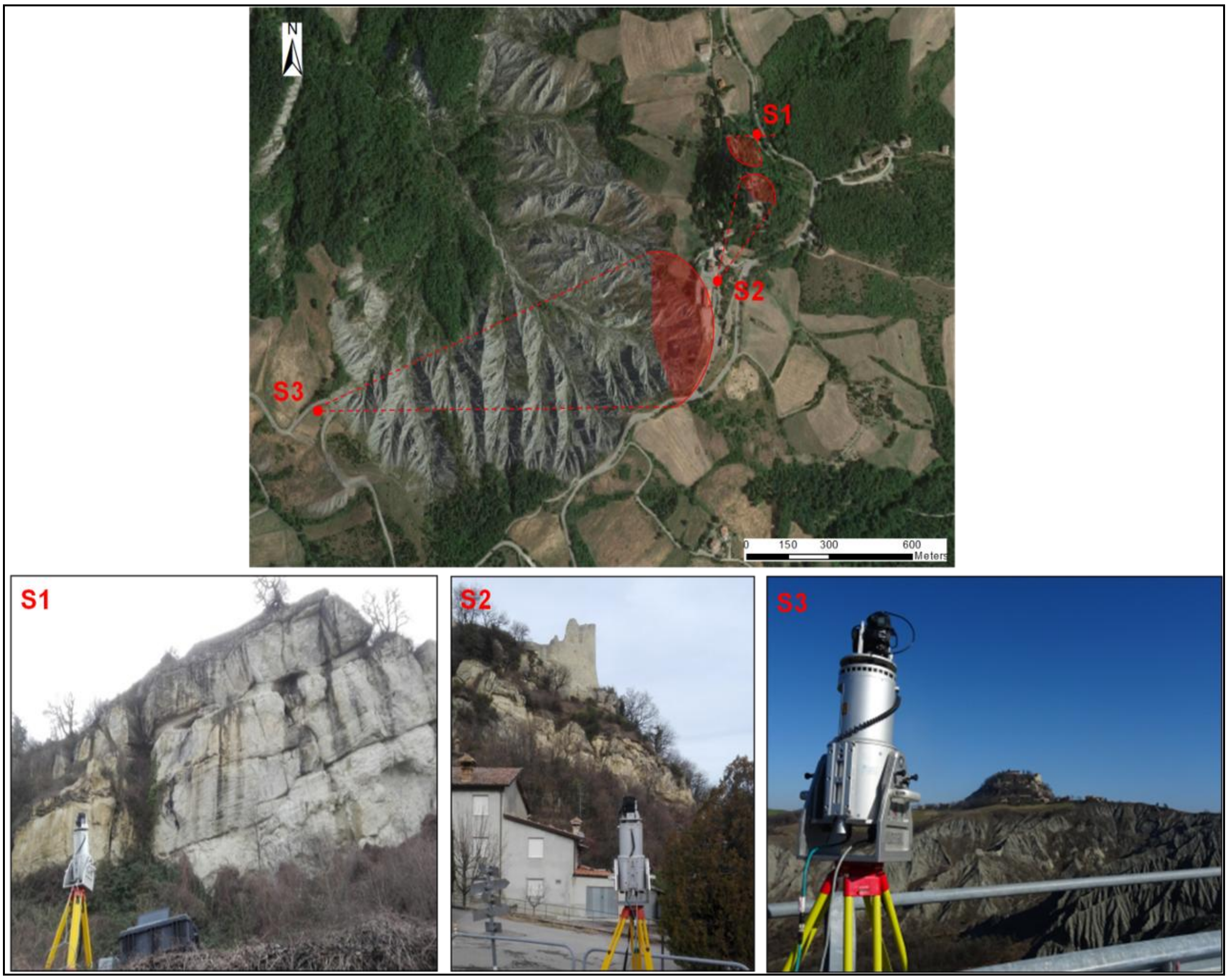

Figure 64. Position of the three scans (S1, S2 and S3) carried out on February 2017.

For an optimal comparison between the different point clouds, the same instrument used by the University of Florence was used (Figure 65): a long range and high accuracy 3D time-of-flight Terrestrial Laser Scanning system, Riegl LMS-Z420i model (RIEGL 2010a), coupled with calibrated digital camera and associated to RiSCAN PRO software package (RIEGL 2010b) for the processing operations. Beying a time of flight (TOF) device, it calculates the scanner-object distance by measuring the round-trip time of a laser pulse.

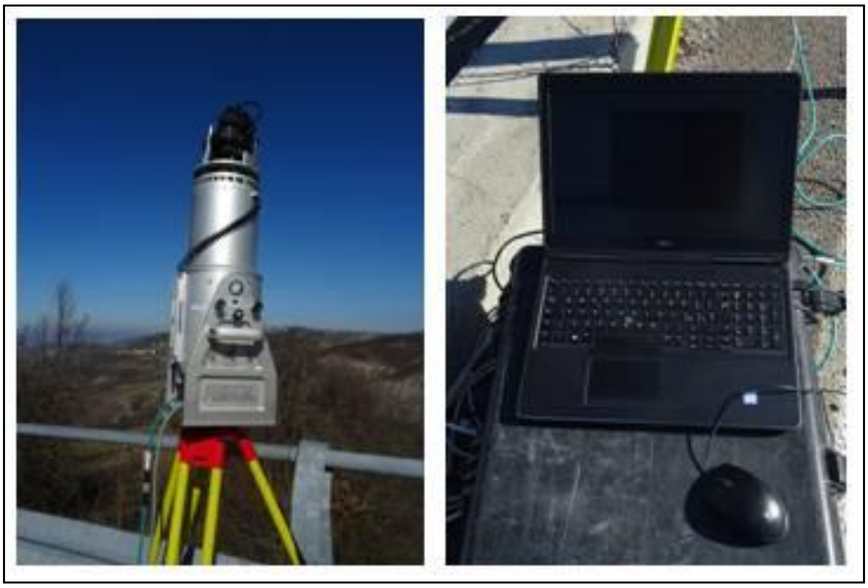

Figure 65. Terrestrial Laser Scanning system, Riegl LMS-Z420i model (on the left) and notebook for its control (on the right).

The main technical characteristics of the used instrument are indicated in the following table (Table 15).

Table 15. Technical characteristic of Riegl LMS-Z420i TLS model.

Measurement of scanner-object distance: up to about 1.000 m
Single point accuracy: ± 5 mm
Minimum vertical scan step: 0.008°
Maximum horizontal scan step: 0.01°
Maximum data acquisition rate: 12.000 points/s.
Wavelength: near-infrared

3.2.6 Data processing and TLS monitoring results

The acquired data during the three surveys are very dense point clouds: the first point cloud is composed by 13.6 millions of points, while the second and the third by 10.1 and 4.1 millions of points, respectively (Figure 66). In Figure 66 n°S2, in addition to the rocky wall, it is also clearly visible a portion of the Canossa Castle ruins, of which was therefore possible to detect the deformation field.

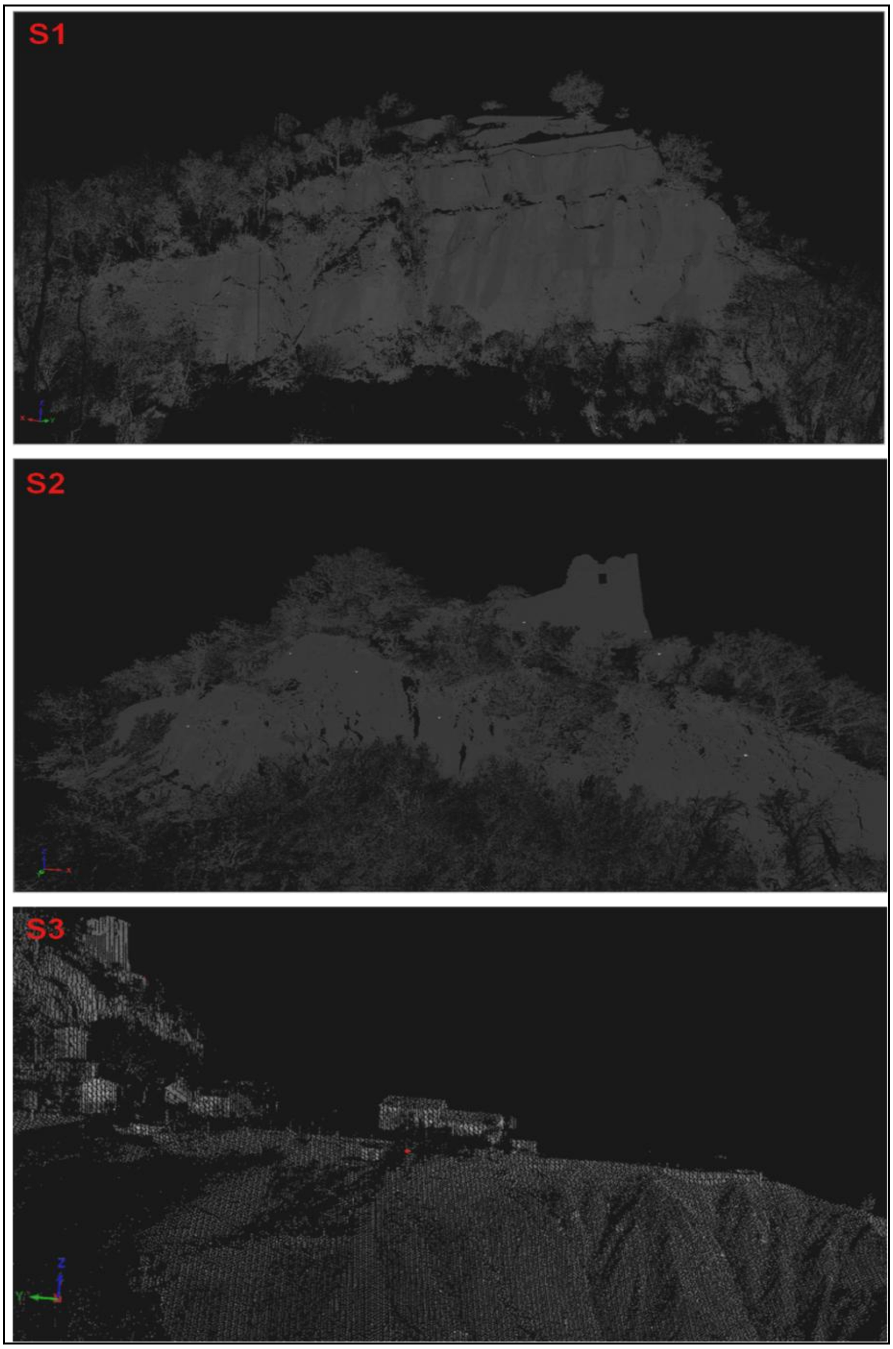

Figure 66. Point clouds acquired at the scan positions S1, S2, S3 (see Figure 64).

After the acquisition phase, the three scans have been managed according to the following workflow (Figure 67): georeferencing, filtering and building of 3D models.

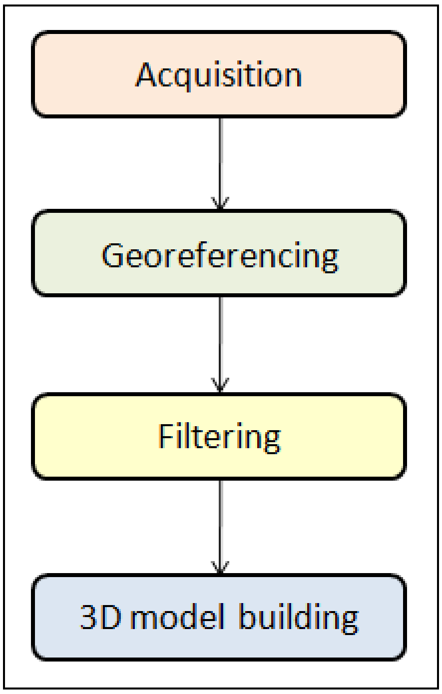

Figure 67. Schematic workflow carried out on the acquired point clouds.

The georeferencing has been carried out aligning the current point clouds with the point clouds acquired on 2006, that were georeferenced in a Global Coordinate System through the acquisition of GPS points.

Georeferencing was then followed by the most demanding part of the entire data processing phase, i.e., the filtering of point clouds from the disturbing effects. As visible from Figure 66, the investigated scenes are rich in vegetation, particularly the two portion of the cliff. A manual removal of both intense vegetation and outliers points was therefore necessary, as the application of automatic filters was not possible on these scenarios.

Once the disturbing elements have been eliminated, it was possible to move from a discrete data, such as the point cloud, to a continuous one, consisting of 3D models (e.g., meshes) of the investigated scenarios obtained by a points triangulation processing (Figure 68). For the calanchi landscape, particularly, a mesh of the collapsed area near the parking zone has been created in order to better analyze this phenomenon.

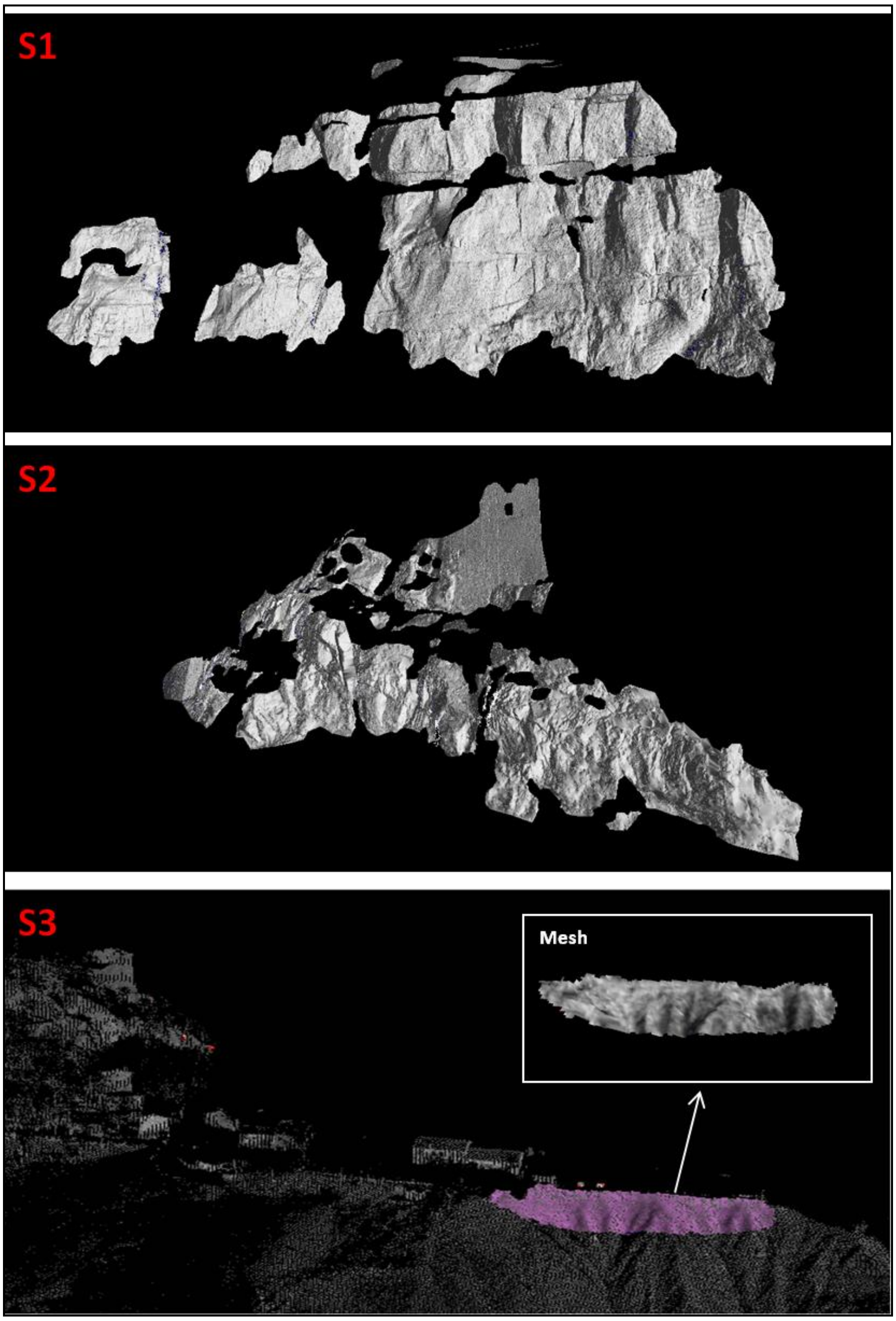

Figure 68. High resolution 3D models (meshes) of the North and South wall of the cliff (S1 and S2, respectively), and of the *calanchi* landscape near the parking area (S3).

From these representation of the investigated scenes, it is possible to appreciate the roughness of the rocky walls of the Canossa cliff, characterized by ledges and niches, and the typical *calanchi* shape.

As aforementioned, TLS surveys have been carried out after 11 years in order to obtain information on the relative movements between the rocky mass constituting the cliff and the possible deformations in correspondence with the ruins of the Canossa Castle, as well as information on the evolution of *calanchi*.

Any changes occurred over time were thus detected by comparing the two acquired datasets (2006 and 2017) through the Surface Comparison tool (RISCAN-PRO, RIEGL, 2010b), which allows comparing a point cloud to a reference mesh. In this study the comparison has been performed taking the 2017 data as point clouds and calculating the displacements through normal vectors mode.

On the North wall of the cliff, through this analysis, five sectors of rocky material detachment have been identified and they are mainly located in the central portion of the rocky mass (Figure 69).

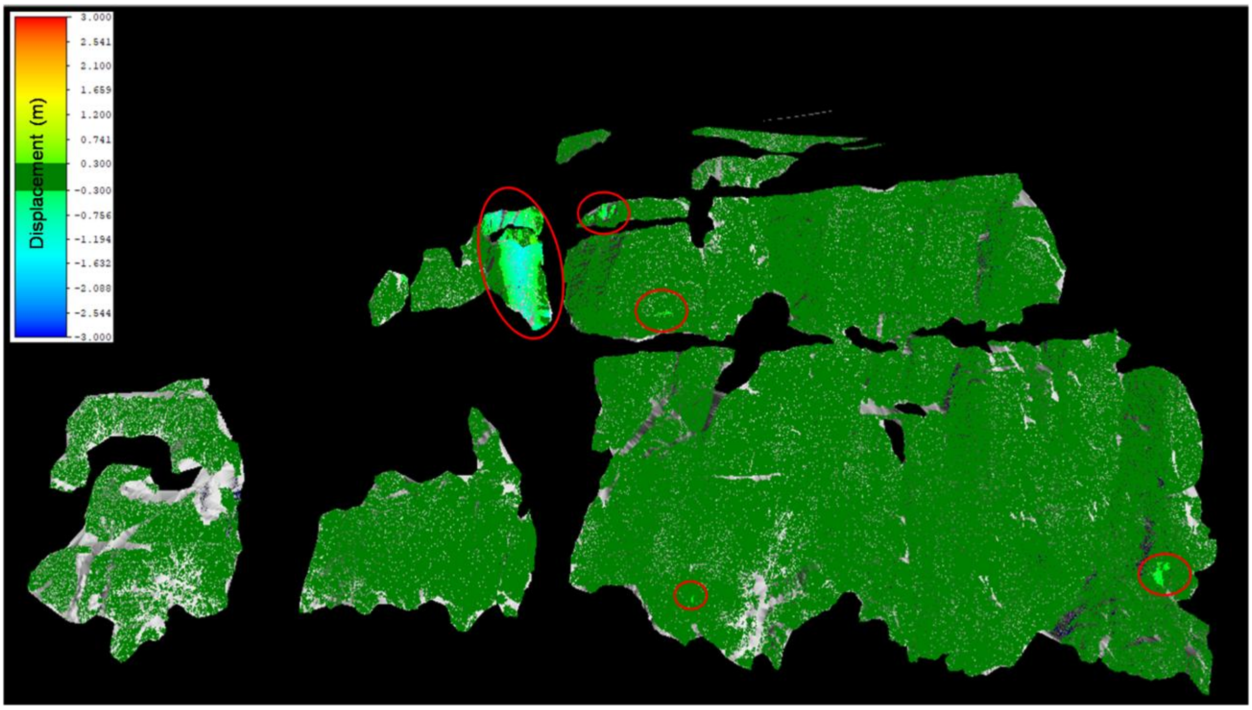

Figure 69. Surface comparison between 2006 scan (visible as mesh) and 2017 scan (visible as colored point cloud) of the North wall, showing detached rock block sectors (highlighted with red circles).

In these five sectors, seven detached blocks have been identified and their volume has been calculated (Figure 70).

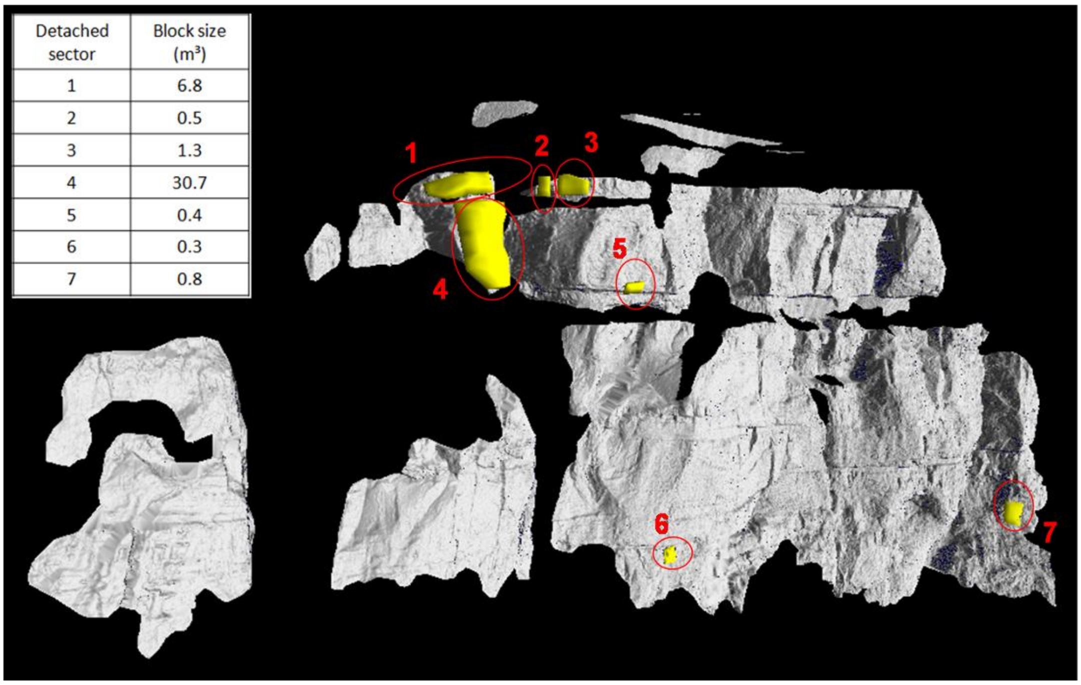

Figure 70. Seven detached blocks from the North wall and their respective volume, displayed together with the 2006 mesh.

The scans comparison carried out on the South wall has allowed identifying two areas of detachment, in which the collapsed blocks turned out to be of 31.6 m^3 and 0.8 m^3 (Figure 71 and Figure 72).

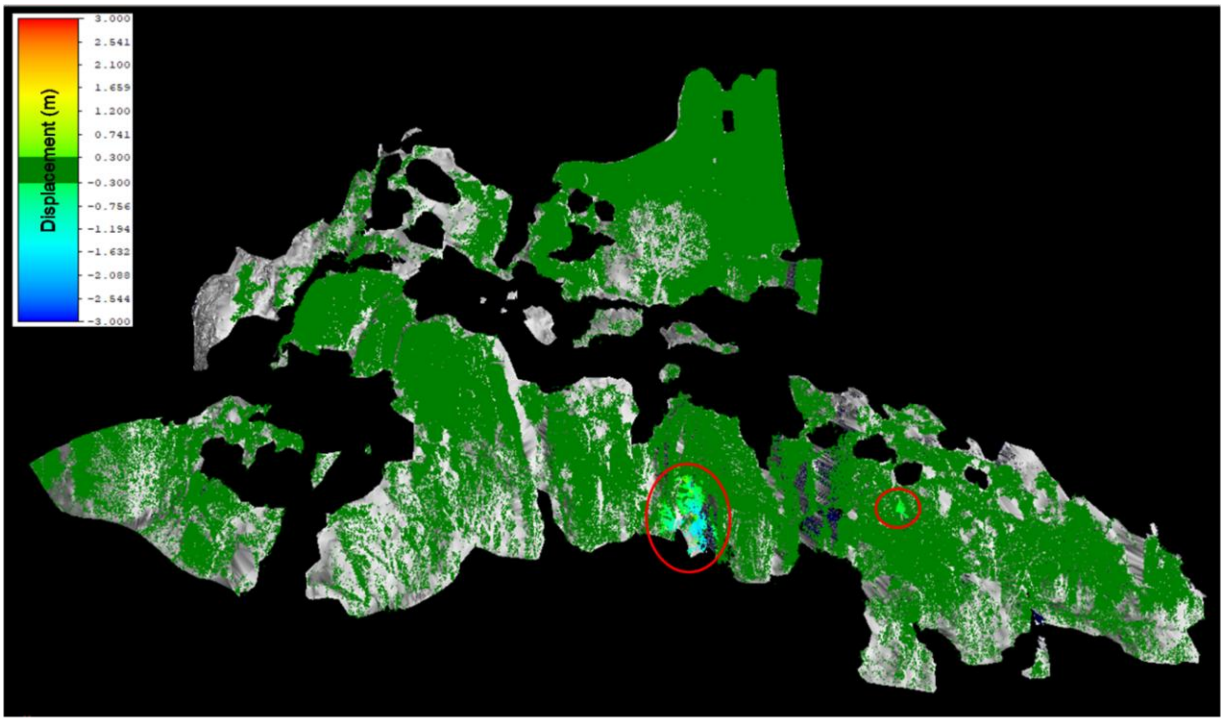

Figure 71. Surface comparison between 2006 scan (visible as mesh) and 2017 scan (visible as colored point cloud) of the South wall, showing the two detachment sectors (highlighted with red circles).

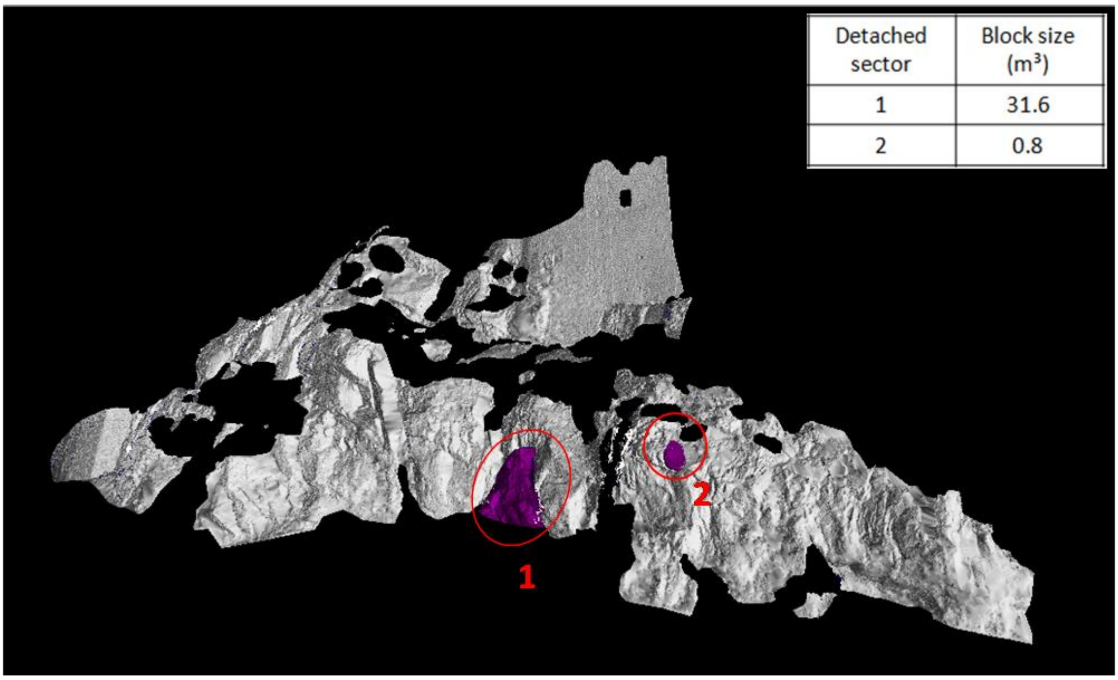

Figure 72. Two blocks detached between 2006 and 2017 from the South wall (displayed as 2006 mesh); on the table their volumes are shown.

A zoom on the Castle ruins shows that this structure, during the 11 years spent between the two scan surveys, did not undergo displacements along the TLS line of sight or that these are less than the TLS instrumental resolution (Figure 73).

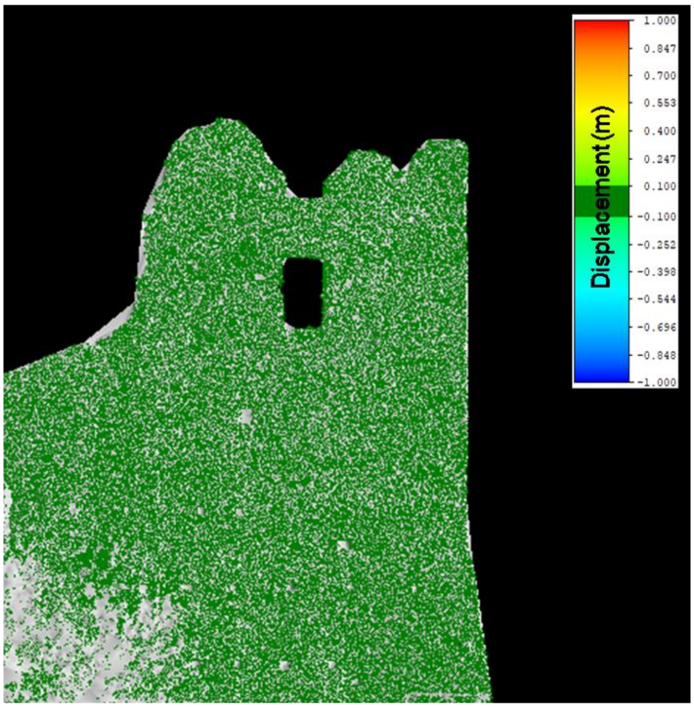

Figure 73. Detail of Figure 71 showing that a displacement is absent at the ruin of the Canossa Castle.

Regarding the *calanchi* area, during the in-situ observation carried out on February 2017, a collapse of the protection gabion positioned near the parking area was located (see Figure 61b-e). Because of the high instability of this area, a detailed surface comparison was therefore carried out between the acquired scans (Figure 74), in order to identify the displacement occurred over the years.

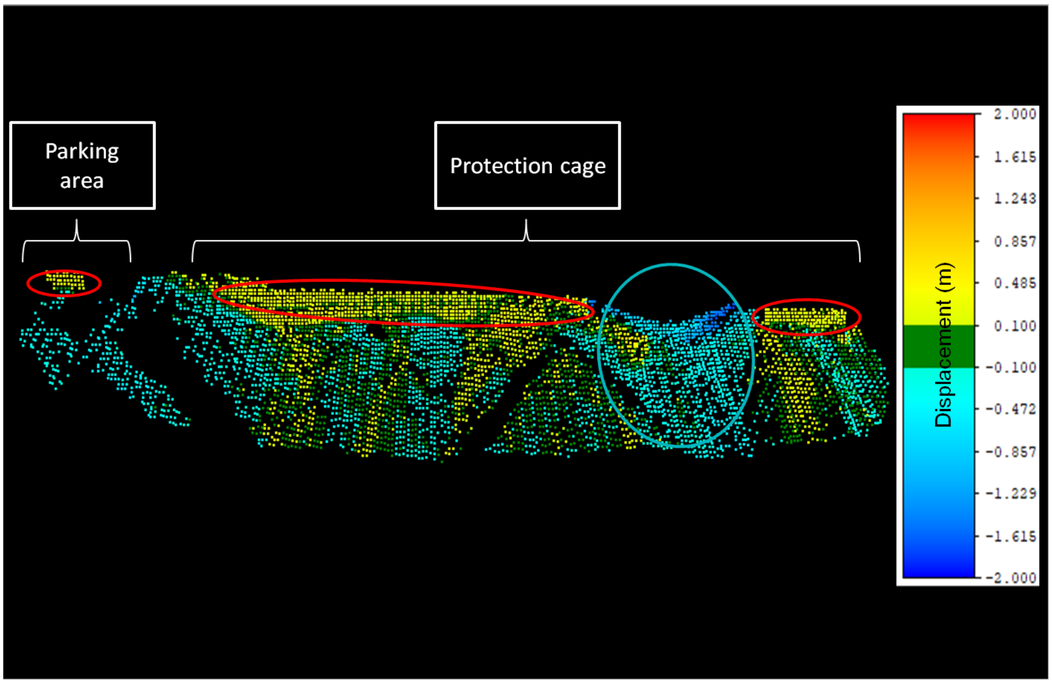

Figure 74. Surface comparison carried out on the collapsed area of the *calanchi* landscape. The result is visible on the 2017 point cloud.

The collapse (circled in blue), which has destroyed part of the protection gabion, has caused a retreat of about 1 m of this *calanchi* portion. In the intact part of the gabion and in a little portion of the parking area, instead, thrusting movements of about 50 cm towards the valley have been detected (areas circled in red).

4. Discussion

The main objective of this thesis work has been to illustrate innovative procedures for assessing geohazards that, more and more frequently, threaten worldwide the cultural assets. Not even international investments (implemented for example by the UNESCO Agency) are able to counter the inestimable damage that natural events cause on sites of cultural interest.

The proposed practices, which exploit the potentiality of the recent technological innovations (both at regional and local scale) together with the knowledge of the past instabilities (at single cultural site scale), can be easily used by local risk managers for the monitoring and the safeguarding of the inestimable cultural heritage guarded by the Earth Planet. In this perspective, the approach of this project has been tested on the Tuscany Region, the Historic Center of Florence and the Canossa Cliff, all located in Italy.

At regional scale, a new procedure for identifying, within the boundaries of the UNESCO sites, the temporal and spatial evolution over time of ADA, which are Active Deformation Areas due to slow-kinematic geohazards (slow-moving landslides or ground-subsidences in this case study) has been proposed. The illustrated methodology, which has shown potential both at regional and detailed scale in other test sites (Barra et al., 2017; Solari et al., 2018), has been specifically adapted for the aims of this work, allowing to derive multitemporal ground deformation measurements for single UNESCO sites starting from PSI regional datasets (Pastonchi et al., 2018).

Although the procedure results are influenced by intrinsic limitations of the space-born InSAR techniques, e.g., slope aspect with respect to the acquisition geometry (no data is acquired in steep slopes or slopes where N-S deformation component occur), and land cover, the proposed workflow allows analyzing, in a fast and frequently updatable way, the huge amount of satellite data of a PSI dataset. The UNESCO sites are sometimes characterized by thousands of PS points (for example the Core Zone of the Historical Center of Florence contains around 5000 PS points), thus, the proposed methodology decreases the time needed to perform single point analysis over wide areas (for example the Core Zone of the Val d'Orcia covers 61,000 ha), that is a strongly time-demanding activity that cannot be frequently repeated. It has to be stressed that the interferometric products have also a great cost-benefit ratio with respect to classical ground measurements such as GPS (Global Positioning Network) networks (Thomas et al., 2014), especially when considering regional scale applications.

The illustrated procedure can be applied to any satellite SAR data but, in this case, in order to build up two different monitored periods similar to the one chosen by the UNESCO Agency to update its reports (every six years), the analysis has been carried out on C-band data, i.e., Envisat (spanning from 2003 to 2010) and Sentinel-1 data (spanning from 2014 and 2018); these latter are the technical evolution of Envisat data. In this way, it was possible to create two different stacks of moving areas, although referred to two sensors. This operative choice is related to (i) the need to create a long-time monitoring period to evaluate possible variation in the spatial distribution of the ADA and in the velocities recorded (as illustrated by the Pisa case study), (ii) the similar characteristics between the two satellites selected, considering that the Sentinel-1 constellation is intended to work in continuity with ESA's (European Space Agency) Envisat (Showstack, 2014). Although the use of two different imaging geometries can lead to misinterpretation of the LOS velocities obtained, the use of both orbits' data as absolute values was considered the best operative choice for an expeditious evaluation of ground deformation affecting a UNESCO site. In flat areas, where subsidence is the main geohazard (such as Florence and Pisa), differences due to the geometry of acquisition are negligible. Therefore, this work wants to be a procedure proposal, aimed at showing preliminary results on a regional test case.

The procedure has aimed at initially creating a priority database of possible hazardous areas (ADA) within the different contours of each UNESCO sites (also within the newly created Influence Zones). This information, as demonstrated in the 2.5 Chapter, can be subsequently easily managed by the competent authorities in order to (i) intersect this database with geohazards inventories, and then (ii) verify on site the effects of the recorded motions, besides better characterize the identified geohazards. The Identity Card of ADA (ICA) has been specially created for this purpose, as not all the ADA have been associated with specific slow-moving geological phenomenon through an office analysis.

The obtained results have shown a general decrease in the number of ADA between Envisat and Sentinel-1 datasets, but in some cases, as at the Val d'Orcia site, an increase in the number of ADA has been identified. The general reduction of ADA is usually connected to a lowering of PS velocities. This mainly depends on the fact that Sentinel-1 data have a lower standard deviation and time series stability, thanks to the high redundancy of data given by the 6-day revisiting time. On the other hand, the evolution of a geological phenomenon is a further cause of both the reduction and the increase of ADA in the investigated sites. For example, the reduction of ADA recorded from Envisat to Sentinel-1 datasets within the Buffer and the Influence Zones of Piazza del Duomo, Pisa (Figure 30), which is the only Tuscan Unesco site where to each ADA has been associated a geohazard, is related to a general slowdown of a well-known subsidence phenomena (Figure 32). This trend has been attributed to the time-dependency of an ongoing consolidation process affecting building built in the last decade (Solari et al., 2017).

The evolution of the ADA detected in the NW area of the Historic Center of Florence, where these main ground deformation intersect the used ground-subsidences inventory, has been better analyzed through a PS interpolation (Figure 32), as it was done also for the Pisa area (already discussed). In this territory, during the years 2003-2010, four ground-subsidences have been detected: those localized in industrial zones (areas n°1, 2 and 4 in Figure 32) could be due to a significant demand of groundwater from local aquifers, whereas, that which in the past threatened the CNR buildings (area n°3 in Figure 32) could be associated to the load that these constructions, being new at that time, have applied on the ground (Pratesi et al., 2016). This latter hypothesis can be corroborated by the fact that in the CNR complex a ground-subsidence is no longer recorded. At the industrial zone, instead, in recent years (2014-2017), in addition to a decrease both in extension and in intensity (velocity values) of the subsidence phenomenon recorded in the area n° 2 and partially in the area n° 4, there has been an inversion of movement. The uplifts identified in the areas n° 1 and n° 4 in Figure 32, could be due to a decrease of the groundwater abstraction rate (Pratesi et al., 2016).

Always by way of example, the increase in the number of ADA identified in the hilly landscape of the Val d'Orcia UNESCO site through the Sentinel-1 dataset (Figure 29 and Table 6) is probably related to (i) a higher density of points in partially vegetated areas because of the type of processing (SqueeSAR) and the temporal repeatability of the sensor and (ii) the evolution of the typical clayey landscape of the Val d'Orcia, including slope denudation and landslide phenomena (Della Seta et al., 2009; Vergari et al., 2011; Aucelli et al., 2016). The high instability of this site identified by a satellite analysis was also found through in situ investigations carried out on some ADA. The record of the main information in the Identity Card of ADA has allowed cataloging several damages both on buildings, infrastructures and ground surface. Through these investigations, it has been possible to identify landslides and damages even in places where landslide inventory does not indicate any movement of the ground (see Figure 23 and Figure 28).

The results finally show that only one Core Zone of Tuscany (Val d'Orcia) is affected by some Active Deformation Areas (ADA), whereas the greatest number of ADA has been extracted within the Influence Zones. This indicates how fundamental the investigations in these newly created zones are, which should be included in the UNESCO management system in order to guarantee better site conservation. In addition to the aforementioned results, by comparing the past deformations with the current ones, it has been possible to identify the areas in which the movements persist in time and in the same place. These areas could be attributed to the same phenomenon (slow-moving landslides or ground-subsidence for Tuscany Region) that lasts over time. Focusing on these phenomena would avoid damages that could, in the long-term, compromise the integrity of UNESCO sites.

In the first local scale case study of this thesis work, the emergence of the Lungarno Torrigiani (Florence) caused by a riverbank landslide has been managed. Thanks to rapid interventions based on several innovative technologies, on several technical means and experiences in the field of cultural heritage and the safeguarding of human life, a return to normality has been put in place in the collapsed area. In fact, only five months after the event, the restoration works were completed, leaving the wall with its post-event geometry, since the residual conditions of the structure have been deemed stable and safe. Therefore, the reaction of the city alert system was quick and effective, allowing a consistent limitation of damages up to the final positive results. In particular, the crux of the emergency management was certainly the prompt activation of all the operational units and skills existing in its territory.

In this framework, after few hours from the collapse, the Department of Earth Sciences was activated and, based on its experiences in the field of monitoring of collapsing structures (anthropic and natural), an advanced control system was immediately organized. All the data analyzed and interpreted were promptly communicated to the competent authorities through a bulletin, specially created to be as explicit as possible. Particularly, the GBInSAR system (already successfully tested during other landslide monitoring and early warning systems, Casagli et al., 2003; Barbieri et al., 2004; Luzi et al., 2006; Casagli et al., 2010), by virtue of its high accuracy and resolution, has identified millimetric movements of the embankment wall, even when the other instruments have not detected any deformation (see Figure 48). Despite some limitations of this technique, among which the decorrelation effects that made complex the interpretation of the data, the GBInSAR has been the only tool able to guarantee a real-time landslide monitoring, by virtue of its high sampling rate (about every ten minutes). This frequent information has allowed operating in safety and planning time to time the redevelopment of the area. Moreover, the GBInSAR instrumentation, being the only one among those used which not require the installation of targets or devices in the analyzed good, has allowed a "*post-operam*" monitoring of the area, in order to verify the stability over time of the restoration works.

The historical research of past instabilities conducted in this thesis work, together with further investigations carried out by the University of Florence (geotechnical characterization; TLS; geophysical and bathymetric surveys; riverbank stability analysis), allowed characterizing the landslide that occurred on 25 May 2016 (Morelli et al., 2018). It was therefore understood that the evolution of the studied collapse has been the result of the combination and interaction of two different dynamics. The first one is the riverbank failure, a typical destructive phenomenon during extreme hydraulic conditions like the highly concentrated water circulation on the slope behind or high-water levels in the riverbed after exceptional rainfalls. These critical conditions, sometimes intensified and worsened by landslides and debris floods, are well known throughout the history of the city, especially after the intense urbanization starting from 1175 (see Section 3.1.2). The second one is the continuous loss of water from the subterranean pipes of the aqueduct, a more contemporary phenomenon, which developed starting from the capillary diffusion of the modern structure in every part of the city (completed with the nineteenth-century works). In recent decades, this dense network has undergone minimal maintenance and has suffered sudden localized breakages and abundant leakages up to repercussions on daily city life. In some circumstances, also the safety and health of most of the citizens have been put at risk (Morelli et al., 2014). The evolution of the studied landslide encompasses both the aforementioned dynamics, and the occurred chain of circumstances is quite new for the city history. At first, a significant breakage of the aqueduct located along the riverbank has occurred, and an abundant flow of water has dispersed in the surrounding soil until its complete saturation. Then, it has reached the road level and only few hours after the structural damage at the main pipe the embankment has collapsed (Morelli et al., 2018).

In the second case study carried out at local scale, the analysis of 3D meshes obtained from the laser scanning allowed analyzing and monitoring the main instability mechanisms that have threatened and still threaten the Castle and the Cliff of Canossa (Emilia Romagna Region). Despite some limitations of the TLS technique (shadow areas in the point clouds due to, e.g., rugged topography or scanned surfaces parallel to the LOS of the instrument; the huge amount of acquired information; and the data filtering that dilates the times of the post-acquisition phase; Jaboiedoff et al., 2012), it has been possible to identify that the North face of the cliff is the one most subject to the rockfalls (see Figure 70). In fact, through the estimate conducted excellently with the TLS technique, the number and the volume of the rocky blocks detached from the North face of the cliff are resulted greater than those detected on the Southern rocky face. In this portion of the rocky wall, already in 2004, the detachment of a huge block of rock occurred, creating damages to the neighboring provincial road. The overlap of a rocky mass, characterized by elastic deformations and fragile ruptures, on soils characterized by a marked tendency to the plastic and viscous flow, is one of the most unfavorable conditions for the slope stability. In the case of Canossa Cliff, the overlap of sandstone on a clayey substratum induces deep gravitational deformation that affect and feed the “plate-substratum” system of this area, causing, as consequence, the rockfall phenomenon (Casagli et al., 2006). It is important to underline that, among the factors that trigger and accelerate the instability processes of the Canossa Cliff, there are not only the geomechanical properties of the outcrops on which the cliff rests, but also the effects of atmospheric agents such as, e.g., the concentration of rainy and snowy events in limited periods of time, and the harsh temperatures of the winter months (Bertolini, 2001; Castronuovo, 2005). In fact, a persistent presence of fluids in the sub-vertical cracking system of the rocky plate can trigger hydrostatic and cryostatic thrust processes.

The monitoring carried out on the cliff allowed also detecting that the ruins of the old castle are currently stable: no deformations has been indeed identified through the surface comparison tool of the used software to manage the acquired point clouds.

The geological instabilities of the Canossa cultural site are due also to the changing reality of the *calanchi* that are localized on the clayey landscape at the foot of the cliff. In this environment context, it has been observed, both by means of on-site investigations and by a research of the past instability, that the retreat of this type of badlands creates damages to the neighboring structures. Not even the gabion, built in the past just to prevent this phenomenon, has been useful to protect the parking area upstream of the *calanchi*. In this zone, through a surface comparison carried out on the point clouds acquired in 2006 and in 2017, a collapse has been identified, besides the thrusting movements towards the valley that affect the remaining part of the gabion and a portion of the parking area. All this is not surprising since *calanchi* are particular erosional landforms where slope denudation and landslide phenomena are frequent (Fantoni, 2005).

5. Conclusion

In recent years, the development of innovative and useful technologies for geological processes monitoring and mapping has provided to the scientific community additional tools for geohazards management and reduction. Between these, the remote sensing systems showed the best features to improve the preservation of cultural heritage threaten by geological processes. Therefore, in a reality where economic resources are scarce and the authorities responsible for the risks tend to underestimate the damages that geohazards create on cultural sites, one of the action that has to be done is to enhance good cultural heritage management practices and reinforce institutional support through the innovation and the knowledge of the past instabilities. This was, in fact, the main objective of this thesis work, developed during a three years-long activity both at the Department of Earth Sciences of the University of Florence (Italy), and at the Centre Tecnològic Telecomunicacions Catalunya (CTTC) of Castelldefels (Barcelona). The project approach includes a regional-scale analysis and two analyses carried out on a local scale.
At regional scale, the proposed satellite InSAR-based procedure allows mapping, characterizing and monitoring the temporal and spatial evolution of slow-kinematic phenomena (slow-moving landslides and ground-subsidences) affecting UNESCO sites, considered as Core, Buffer, and Influence Zones, the latter defined for the first time for the aims of this research. The greatest number of ADA extracted within the Influence Zones highlights the importance of these boundaries in the preservation of the Outstanding Universal Value of UNESCO sites over times. These areas should be taken into consideration within the UNESCO management system, because a territory is a continuously changing reality, in which it is necessary to extend the monitoring. This can be corroborated by the fact that some ADA which do not match with the official geohazards inventories has been identified and characterized. Therefore, include the monitoring of slow-kinematic phenomena within the procedures of the periodical UNESCO reports can be a useful tool to better define management and protection strategies. The developed methodology has been applied for the first time in the test area of the Tuscany Region, where several UNESCO heritage sites are present. The obtained results are preliminary but they represent useful information to plan potential on-site actions (e.g., consolidation and drainage works or periodic monitoring campaigns through the use of some instruments such as tiltmeters or crackmeters), or to define specific times (shorter than every 6 years) for processing satellite data according to the severity of the damages found during the in situ observations.

Thanks to the free availability, the regularity of acquisition, and the worldwide coverage of the Sentinel-1 data, the procedures proposed in this thesis could be easily and quickly exploited by decision makers in order to safeguard each World Heritage Site.

The Lungarno Torrigiani (Florence, Tuscany Region) case study has illustrated the potentialities of the GBInSAR during the management of the emergency within the Historic Center of Florence, and the usefulness of researching the past instabilities in order to characterize the occurred riverbank landslide. The ground-based radar technique, by virtue of its high accuracy, high scan rate and the capability to operate in every weather or illumination condition, has demonstrated the importance of its use during an early warning system for near to fail buildings and infrastructures. Moreover, from this case study it emerged that only through the aware synergistic coordination between the public administrators in charge and the scientific community, an optimal policy for the protection and conservation of a cultural asset can be effectively sustained. This kind of management meets also the increasingly pressing needs of the economic systems that must rapidly support the emergency costs, and, thus, it can be exploited by the UNESCO system for its future challenges of disaster risk reduction (Sendai Framework 2015-2030) within cultural and historic urban landscapes.

The last case study concerning the Canossa cultural site (Emilia Romagna Region) has showed how, through an historical research of the past geological instability events combined with in situ observations, the main critical issues on which carry out new surveys can be well localized. In this case, the monitoring with a TLS system has been fundamental, because the non accessible and dangerous areas on which carry out the investigations request mandatorily a remote sensing technique. Moreover, the surface comparison between point clouds acquired by TLS at different times has been necessary to determine the volumetric variations occurred on the rocky walls of the cliff, since the rockfall is the phenomenon that most frequently threatens this cultural site. A permanent monitoring could be one of the best choices to reduce the instability processes, especially when consolidation works do not guarantee excellent results, as it has been observed in a *calanchi* portion. In the future it is planned to acquire point clouds on the whole *calanchi* scenario in order to define the rate of erosion of these ephemeral landforms. All the Canossa work has been mainly carried out in order to promote good geological risk management practices in cultural realities that are out of international attention (e.g., UNESCO), and that therefore are devoid of substantial economic subsidies. It is on these sites that the community should pay the most attention, in order to prevent their future and inevitable disappearance.

The proposed case studies are intended as useful examples to illustrate how to effectively assess geological risks that threaten cultural heritage both at regional and local scale. In future, the satellite analysis that have been carried out on the seven UNESCO cultural sites of Tuscany could be expanded to the sites present throughout all the Italian territory, in order to promote good management practices also at national level. Furthermore, it is expected to exploit further remote sensing techniques at local scale (e.g., the Infrared Thermographic (IRT) technique and Unmanned Aerial Vehicles-UAVs), in order to show all the new technologies potential for an improvement of the safeguard of cultural heritage threatened by geological processes.

Works derived from this PhD Thesis

Publication:

- Pastonchi, L.; Barra, A.; Monserrat, O.; Luzi, G.; Solari, L.; & Tofani, V. (2018). Satellite Data to Improve the Knowledge of Geohazards in World Heritage Sites. Remote Sensing, 10(7), 992.

Conference Paper:

- Morelli, S.; Pazzi, P.; Bandecchi, A. E.; Valori, L.; Gambacciani L.; Ceccatelli, M.; Gracchi, T.; Marini, F.; Masi, E.B.; Pastonchi, L.; Lotti, A.; Fontanelli, K.; Casagli, N. - *A multidimensional and interdisciplinary strategy for geo-hydrological risk reduction oriented towards minors*- EGU General Assembly, April 2018.

Posters:

- Pastonchi L., Pazzi V., Morelli S., Marini F., Valori L., Gambacciani L., Casagli N. - *Testing the awareness of landslide risk in some schools in Tuscany (Italy)* – 4th World Landslide Forum 2017, Ljubljana (Slovenia) – 29 May-2 June 2017.

- Pastonchi, L.; Barra, A.; Montserrat, O.; Luzi, G.; Solari, L.; Tofani, V. - Procedure for the identification and monitoring of ground deformations through satellite data in UNESCO World Heritage Sites; XIII Convegno Nazionale delle Sezioni della Società Geologica Italiana di Geoscience and Information Technologies, Idrogeologia; Sarzana (SP) – 11-13/06/2018.

References

Abbate, E., Sagri M., 1970. The Eugeosynclinal sequences. Sediment. geol. 4 (3-4), 251-340. Doi: https://doi.org/10.1016/0037-0738(70)90018-7

Aiazzi, G. (1845). Narrazioni istoriche delle più considerevoli inondazioni dell'Arno, e notizie scientifiche sul medesimo. Raccolte ed insieme riunite da GA. Tip. Piatti. (In Italian).

Alexander D. (1993) - Natural Disasters. Chapman and Hall, New York, pp 621.

Alfarè, L.; Donnici, S.; Marini, M.; Moscatelli, M.; Tosi, L.; Vallone, R. (2014). The Impact of Land Subsidence on Preservation of Cultural Heritage Sites: The Case Study of Aquileia (Venetian-Friulian Coastland, North-Eastern Italy). In Engin. Geology for Soc. and Terr., 4, 179-182.

Allen, R. E. (2016). Financial crises and recession in the global economy, Edward Elgar Publishing, Cheltenham, UK.

Antonello, G.; Casagli, N.; Farina, P.; Leva, D.; Nico, G.; Sieber, AJ.; Tarchi, D. (2004). Ground-based SAR interferometry for monitoring mass movements. Landslides 1:21 – 28

Artusi, L., Venturi, M. (2014). Chiassi e vicoli dimenticati di Firenze, Ab Edizioni, Empoli, Italy (in Italian).

Aucelli, P. P.; Conforti, M.; Della Seta, M.; Del Monte, M.; D'uva, L.; Rosskopf, C. M.; Vergari, F. (2016). Multi-temporal digital photogrammetric analysis for quantitative assessment of soil erosion rates in the Landola catchment of the upper Orcia valley (Tuscany, Italy). Land Degradation & Development, 27(4), 1075-1092.

Bamler, R., and Hartl, P. (1998). Synthetic aperture radar interferometry. Inverse problems, 14(4), R1.

Barbieri, M.; Corsini, A.; Casagli, N.; Farina, P.; Coren, F.; Sterzai, P.; Leva, D.; Tarchi, D. (2004). Space-borne and ground-based SAR interferometry for landslide activity analysis and monitoring in the appennines of Emilia Romagna (Italy): Review of methods and preliminary results, review of methods and preliminary results. Special Publication) ESA SP (550), 463-470.

Bargellini, P. and Guarnieri, E. (1986). Le strade di Firenze. Bonechi, Firenze, Italy (in Italian).

Barra, A.; Monserrat, O.; Mazzanti, P.; Esposito, C.; Crosetto, M.; Scarascia Mugnozza, G. (2016) First insights on the potential of Sentinel-1 for landslides detection. Geomat. Nat. Hazards Risk. 7, 1874–1883.

Barra, A.; Solari, L.; Bejar-Pizarro, M.; Monserrat, O.; Bianchini, S.; Herrera, G.; Crosetto, M.; Sarro, R.; Gonzalez-Alonso, E.; Mateos, R.M.; Ligüerzana, S.; López, C.; Moretti, S. (2017). A methodology to detect and update Active Deformation Areas based on Sentinel-1 SAR images. Remote Sens. 9, 1002.

Bertolini, G. (2001). Modalità di riattivazione, interventi, caratteri geotecnici e mineralogici di una frana di argilla a struttura caotica (argille scagliose, Auctt): la frana di Casoletta com. Vezzano sul Crostolo (RE) – Quaderni di geologia Applicata, 8-1. (In Italian).

Bianchini, S.; Pratesi, F.; Nolesini, T.; Casagli, N. (2015). Building deformation assessment by means of Persistent Scatterer Interferometry analysis on a Landslide-affected area: The Volterra (Italy) case study. Remote Sens., 7, 4678-4701.

Billi, P., and Rinaldi, M. (1997). Human impact on sediment yield and channel dynamics in the Arno River basin (central Italy). IAHS Publications-Series of Proceedings and Reports-Intern Assoc Hydrological Sciences, 245, 301.

Boccaletti, M. and Coli, M. (1982). Carta geologico-strutturale dell'Appennino settentrionale, 1:250.000 scale geological map, Prog. Fin. Geodinamica, Publication n. 429-1982, C.N.R. and SELCA, Firenze, Italy.

Bonforte, A; Guglielmino, F.; Coltelli, M.; Ferretti, A.; Puglisi, G. (2011). Structural assessment of Mount Etna volcano from permanent scatterers analysis. Geochem. Geophy. Geosy. 12, 1–19. DOI:10.1029/2010GC003213.

Bortolotti, V (1992). The Tuscany–Emilian Apennine. Regional geological guidebook, Vol. 4, S.G.I. BEMA Editrice, 329pp.

Briganti, R.; Ciufegni, G.; Coli, M.; Polimeni, S.; Pranzini, G. (2003). Underground Florence: Plio-Quaternary geological evolution of the Florence area. Boll. Soc. Geol. It. 122, 435-445.

Bromhead, E. N.; Canuti, P.; Ibsen, M. L. (2006). Landslides and cultural heritage. Landslides, 3(4), 273-274.

Canfarini, A. (1978). Sistemazione dell'Arno in Firenze mediante l'abbassamento delle platee in muratura dei ponti Vecchio e a Santa Trinita, Ispettorato Superiore del Genio Civile per l'Arno - Firenze, pp 3-16 (in Italian).

Canuti, P.; Margottini, C.; Fanti, R.; Bromhead, E.N. (2009). Cultural Heritage and Landslides: Research for Risk Prevention and Conservation. In Landslides—Disaster Risk Reduction; Sassa, K., Canuti, P., Eds.; Springer: Berlin/Heidelberg, Germany; pp. 401–433.

Capecchi, F.; Guazzone, G.; Pranzini, G. (1975). Il bacino di Firenze-Prato-Pistoia. Geologia del sottosuolo e ricostruzione evolutiva. Boll. Soc. Geol. It. 94, 637-660 (in Italian).

Capitanio, C.; Bini, M.; Francini, C. (2017). The safeguarding area for the Historic Center of Florence, UNESCO site, DIDA Dipartimento di Architettura Università degli Studi di Firenze, ISBN 978889608032.

Cardinali M.; Reichenbach P.; Guzzetti F.; Ardizzone F.; Antonini G.; Galli M.; Cacciano M.; Castellani M.; Salvati P. (2002) – A geomorphological approach to estimate landslide hazard and risk in urban and rural areas in Umbria, central Italy. Natural Hazards and Earth System Science, Vol. 2, 57-72.

Carmignani, L.; Conti, P.; Cornamusini, G.; Pirro, A. (2013). Geological map of Tuscany (Italy). J. Maps, 9, 487–497.

Carmignani, L.; Decandia, F. A.; Disperati, L.; Fantozzi, P. L.; Kligfield, R.; Lazzarotto, A.; Liotta, D.; Meccheri, M. (2001). Inner Northern Apennines. In Anatomy of an Orogen: the Apennines and adjacent Mediterranean Basins, Springer Netherlands 2001, 197-213.

Casagli, N. (1992). Slope instability in rock masses overlying a soft substratum: some analyses in the Italian Northern Apennine. unpublished Master thesis, Master of Science in Engennering Rock Mechanics, Imperial College, London.

Casagli, N.; Catani, F.; Del Ventisette, C. and Luzi, G. (2010). Monitoring, prediction, and early warning using ground-based radar interferometry. Landslides, 7(3), 291-301.

Casagli, N.; Catani, F.; Tofani, V.; Righini, G.; Fanti, F. (2009a). DIANA: Dati interferometrici per l'analisi ambientale: frane e subsidenza – Progetto esecutivo. Firenze. Unpublished work (In Italian).

Casagli, N.; Catani, F.; Tofani, V.; Rosi, A.; Tanteri, L.; Agostini, A.; Stefanelli, C. T. (2013). DIANA: Dati interferometrici per l'analisi ambientale: frane e subsidenza – Prodotto 1-Rapporto finale. Firenze, maggio. Unpublished work (In Italian).

Casagli, N.; Farina, P.; Leva, D.; Tarchi, D. (2003). Application of ground-based radar interferometry to monitor an active rockslide and implications for emergency management. In: Hermanss R, Evans S, Scarascia Mugnozza G, Strom A (Eds) Massive Rock Slope Failure. NATO Science Series Book. Kluwer

Casagli, N.; Gigli, G.; Lombardi, L.; Mugnai, F. (2006). Studio e monitoraggio delle condizioni di instabilità della Rupe di Canossa (RE); ENTE COMMITTENTE: Servizio Tecnico Bacini Enza e Sinistra Secchia di Reggio Emilia, Regione Emilia Romagna. FIRENZE, DICEMBRE 2006. Unpublished work. (In Italian).

Casagli, N.; Tibaldi, A.; Merri, A.; Del Ventisette, C.; Apuani, T.; Guerri, L; Guash, J. F.; Tarchi, D. (2009b). Deformation of Stromboli Volcano (Italy) during the 2007 eruption revealed by radar interferometry, numerical modelling and structural geological field data. Journal of Volcanology and Geothermal Research, 182(3-4), 182-200.

Castronuovo, A. (2005). Predisposizione al dissesto per frane superficiali del medio e basso appennino della provincia di Reggio Emilia. Master Science Thesis, University of Modena and Reggio Emilia. (In Italian).

Catenacci, V. (1992). Il dissesto geologico e geoambientale in Italia dal dopoguerra al 1990. Istituto Poligrafico e Zecca dello Stato, Roma (in Italian).

Ciampalini, A.; Raspini, F.; Frodella, W.; Bardi, F.; Bianchini, S.; Moretti, S. (2016). The effectiveness of high-resolution LiDAR data combined with PSInSAR data in landslide study. Landslides, 13, 399-410.

Cigna, F.; Osmanoğlu, B.; Cabral-Cano, E.; Dixon, T. H.; Ávila-Olivera, J. A.; Garduño-Monroy, V. H.; DeMets, C.; Wdowinski, S. (2012). Monitoring land subsidence and its induced geological hazard with Synthetic Aperture Radar Interferometry: A case study in Morelia, Mexico. Remote Sens. of Env., 117, 146-161. DOI. Available online: https://doi.org/10.1016/j.rse.2011.09.005

Cigna, F.; Tapete, D.; Lee, K. (2018). Geological hazards in the UNESCO World Heritage sites of the UK: From the global to the local scale perspective. Earth-Sci. Rev., 176, 166–194.

Colesanti, C., and Wasowski, J. (2006). Investigating landslides with space-borne Synthetic Aperture Radar (SAR) interferometry. Engineering geology, 88(3-4), 173-199.

Coli, M., Rubellini, P., 2007. Note di Geologia Fiorentina. SELCA, Firenze, Italy (in Italian).

Cooper, A. H. (2008). The classification, recording, databasing and use of information about building damage caused by subsidence and landslides. Quarterly Journal of Engineering Geology and Hydrogeology, 41(3), 409-424.

Costantini, M.; Ferretti, A.; Minati, F.; Falco, S.; Trillo, F.; Colombo, D.; Novali, F.; Malvarosa, F.; Mammone, C.; Vecchioli, F.; Rucci, A.; Fumagalli, A.; Allievi, J.; Ciminelli, M. G.; Costabile, S. (2017). Analysis of surface deformations over the whole Italian territory by interferometric processing of ERS, Envisat and COSMO-SkyMed radar data. Remote Sens. Environ., 202, 250-275.

Crosetto, M.; Monserrat, O.; Cuevas-González, M.; Devanthéry, N.; Crippa, B. (2016a). Persistent scatterer interferometry: a review. ISPRS J. of Photogr. and Remote Sens., 115, 78-89.

Crosetto, M.; Monserrat O., Devanthéry, N.; Cuevas-González, M.; Barra, A.; Crippa, B. (2016b). Persistent Scatterer Interferometry using Sentinel-1 data. The International Archives of the Photogrammetry, Remote Sensing and Spatial Information Sciences, Volume XLI-B7, XXIII ISPRS Congress, 12–19 July 2016, Prague, Czech Republic.

Crosetto, M.; Monserrat, O.; Cuevas, M.; Crippa, B. (2011). Spaceborne differential SAR interferometry: Data analysis tools for deformation measurement. Remote Sensing, 3(2), 305-318.

Cruden, D.M.; Varnes, D.J. (1996). Landslide Types and Processes. In Landslides: Investigation and Mitigation, Special Report 247-Transportation Research Board, National Research Council; Turner, A.K., Schuster, R.L., Eds.; National Academy Press: Washington, DC, USA; pp. 36–75.

Cuca, B. (2017). The contribution of earth observation technologies to monitoring strategies of cultural landscapes and sites. International Archives of the Photogrammetry, Remote Sensing & Spatial Information Sciences, 42.

Dai, F. C.; Lee, C. F.; and Ngai, Y. Y. (2002). Landslide risk assessment and management: an overview. Engineering geology, 64(1), 65-87.

Del Soldato, M.; Bianchini, S.; Calcaterra, D.; De Vita, P.; Martire, D. D.; Tomás, R.; Casagli, N. (2017). A new approach for landslide-induced damage assessment. Geomatics, Natural Hazards and Risk, 8(2), 1524-1537.

Del Ventisette, C.; Intrieri, E.; Luzi, G.; Casagli, N.; Fanti, R.: Leva, D. (2011). Using ground based radar interferometry during emergency: the case of the A3 motorway (Calabria Region, Italy) threatened by a landslide. Natural Hazards and Earth System Sciences, 11(9), 2483.

Della Seta, M.; Del Monte, M.; Fredi, P.; Palmieri, E.L. (2009). Space–time variability of denudation rates at the catchment and hillslope scales on the Tyrrhenian side of Central Italy. Geomorphology, 107, 161–177.

Delmonaco, G.; Margottini, C.; Spizzichino, D. (2009). Low-impact interventions for the preservation of Cultural Heritage: the dying town of Civita di Bagnoregio (Central Italy) and the killer landslide. Protection of Historical Buildings–PROHITEC, 9, 1455-1459.

Devanthéry, N.; Crosetto, M.; Cuevas-González, M.; Monserrat, O.; Barra, A.; Crippa, B. (2016). Deformation monitoring using Persistent Scatterer Interferometry and Sentinel-1 SAR data. Procedia Comp. Scie, 100, 1121-1126, ISSN 1877-0509

Di Cicco, I. (2015). Il Castello di Canossa. http://misteriestoria.blogspot.com/2015/11/il-castello-di-canossa.html (In Italian).

Dotta, G. (2016). Semi-automatic analysis of landslide spatio-temporal evolution. unpublished PhD thesis, University of Florence, Italy.

Evans, D. L., and Farr, T. G. (2006). The use of interferometric synthetic aperture radar (InSAR) in archaeological investigations and cultural heritage preservation. In Remote sensing in archaeology (pp. 89-102). Springer, New York, NY.

Fanti, R.; Gigli, G.; Lombardi, L.; Tapete, D.; Canuti, P. (2013). Terrestrial laser scanning for rockfall stability analysis in the cultural heritage site of Pitigliano (Italy). Landslides, 10(4), 409-420.

Fantoni, L. (2005). Studio Geologico tecnico della Rupe di Canossa (Appennino Reggiano). Thesis, University of Modena, (In Italian).

Farabegoli, E. and Agostini, C. (2000). Identification of calanco, a badland landform in the northern Apennines, Italy. Earth surface processes and Landforms, 25(3), 307-318.

Farina, P.; Casagli, N.; Ferretti, A. (2007). Radar-interpretation of InSAR measurements for landslide investigations in civil protection practices. In Proceedings of the First North American Landslide Conference, Vail, CO, USA, 3–8 June; pp. 272–283.

Fell R, Corominas J, Bonnard C, Cascini L, Leroi E, Savage WZ. (2008). Guidelines for landslide susceptibility, hazard and risk zoning for land-use planning. Eng Geol. 102:99–111.

Fell, R.; Ho K.K.S.; Lacasse S.; Leroi, E. (2005). A framework for landslide risk assessment and management. In: Hungr O, Fell P, Couture R, Eberhardt E, editors. Landslide risk management. London: Taylor & Francis Group; p. 3–25.

Ferretti, A.; Fumagalli, A.; Novali, F.; Prati, C.; Rocca, F.; Rucci, A. (2011). A new algorithm for processing interferometric data-stacks: SqueeSAR. IEEE Transactions on Geosci. Remote Sens., 49, 3460-3470.

Ferretti, A.; Prati, C.; Rocca, F. (2001). Permanent Scatterers in SAR interferometry. IEEE Trans. on Geosci. Remote Sens. 39, 8–20.

Figueroa-Miranda, S.; Vargas, J.T.; Ramos-Leal, J.A.; Hernández-Madrigal, V. M.; Villaseñor-Reyes, C.I. (2018). Land subsidence by groundwater over-exploitation from aquifers in tectonic valleys of Central Mexico: A review. Engineering Geology.

Franceschetti, G., Lanari, R. (1999). Synthetic Aperture Radar Processing. CRC Press, New York.

Francovich, R.; Cantini, F.; Scampoli, E.; Bruttini, J. (2007). La storia di Firenze tra tarda antichità e medioevo. Nuovi dati dallo scavo di via de’ Castellani. Annali di Storia di Firenze, 2, 9-48 (in Italian).

Frati, M. (2015). "Questo diluvio fece alla città e contado di Firenze infinito danno". Danni, cause e rimedi nell'alluvione del 1333. Città e Storia, 10 (1), 41-60 (in Italian).

Fratini, F., and Rescic, S. (2014). The stone materials of the historical architecture of Tuscany, Italy. Geological Society, London, Special Publications, 391(1), 71-92.

Frodella, W.; Ciampalini, A.; Gigli, G.; Lombardi, L.; Raspini, F.; Nocentini, M.; Scardigli, C.; Casagli, N. (2016). Synergic use of satellite and ground based remote sensing methods for monitoring the San Leo rock cliff (Northern Italy). Geomorphology, 264, 80-94.

Galland, P.; Lisitzin, K.; Oudaille-Diethardt, A.; Young, C. (2016). World Heritage in Europe Today. Publisher: United Nations Educational, Scientific and Cultural Organization, Paris, France, 123; ISBN 978-92-3-100143-7.

Ghiglia, D. C. and Romero, L. A. (1994). Robust two-dimensional weighted and unweighted phase unwrapping that uses fast transforms and iterative methods. JOSA A, 11(1), 107-117.

Gigli, G.; Frodella, W.; Mugnai, F.; Tapete, D.; Cigna, F.; Fanti, R.; Intrieri E.; Lombardi, L. (2012). Instability mechanisms affecting cultural heritage sites in the Maltese Archipelago. Natural hazards and earth system sciences., 12(6), 1883-1903.

Gizzi, F. T. and Lazzari, M. (2012). Geological risks and cultural heritage safeguard. Disaster Adv, 5, 3-4.

Hanssen, R.F. (2001). Radar Interferometry: Data Interpretation and Error Analysis. Kluwer Academic Publishers, Dordrecht. 326 pp.

Henderson, F.M., Lewis, A.J. (1998). Principles and Applications of Imaging Radar, 3rd edition. Vol. 2 of Manual of Remote Sensing. John Wiley & Sons, Inc., New York.

http://tre-altamira.com/technology/#sar-imagery. (Accessed on April 2018).

https://site.tre-altamira.com/company/our-technology/#insar-and-dinsar (Accessed on April 2018).

http://whc.unesco.org/en/factors/ (Accessed on December 2018).

http://whc.unesco.org/en/periodicreporting/ (Accessed on December 2018).

http://tre-altamira.com/technology/#insar-and-dinsar. (Accessed on April 2018).

http://www502.regione.toscana.it/geoscopio/cartoteca.html (Accessed on April 2018).

https://site.tre-altamira.com/company/our-technology/#insar-and-dinsar. (Accessed on April 2018).

http://tre-altamira.com/technology/#insar-and-dinsar. (Accessed on April 2018).

https://whc.unesco.org/en/criteria/ (Accessed on February 2018).

http://whc.unesco.org/en/list/stat (Accessed on April 2018).

http://whc.unesco.org/en/list (Accessed on April 2018).

Intrieri, E.; Gigli, G.; Nocentini, M.; Lombardi, L.; Mugnai, F.; Fidolini, F.; Casagli, N. (2015). Sinkhole monitoring and early warning: An experimental and successful GB-InSAR application. Geomorphology, 241, 304-314.

Jaboyedoff, M., Oppikofer, T., Abellán, A., Derron, M. H., Loye, A., Metzger, R., & Pedrazzini, A. (2012). Use of LIDAR in landslide investigations: a review. Natural hazards, 61(1), 5-28.

Jamiolkowski, M.; Lancellotta, R.; Pepe, C. (1993). Leaning Tower of Pisa—Updated Information.

Kriesi, H. (2012). The political consequences of the financial and economic crisis in Europe: Electoral punishment and popular protest. Swiss Polit. Sci. Rev. 18 (4), 518-522. Doi: https://doi.org/10.1111/spsr.12006.

La Nazione (1965). Historical archive of the newspaper – Exstracts of the newspaper “La Nazione” from July 1965 to December 1965 (in Italian).

Lollino, G., and Audisio, C. (2006). UNESCO World Heritage sites in Italy affected by geological problems, specifically landslide and flood hazard. Lands., 3(4), , 311-321. DOI. Available online: https://doi.org/10.1007/s10346-006-0059-7

Lopes-Pegna, M. (1974). Firenze, dalle origini al medioevo. Del Re, Firenze (in Italian).

Losacco, U. (1957). Costituzione geologica e franosità dei colli fiorentini a sud dell'Arno - Pubblicazioni del Centro di studi per la geologia dell'Appennino / Consiglio nazionale delle ricerche, 46. Estr. da: Bollettino della Società geologica italiana, vol. 76; pp. 29-36 (in Italian).

Lu, P.; Casagli, N.; Catani, F. and Tofani, V. (2012). Persistent Scatterers Interferometry Hotspot and Cluster Analysis (PSI-HCA) for detection of extremely slow-moving landslides. International journal of remote sensing, 33(2), 466-489.

Luzi, G. (2010). Ground based SAR interferometry: a novel tool for geoscience. INTECH Open Access Publisher.

Luzi, G.; Pieraccini, M.; Mecatti, D.; Noferini, L.; Macaluso, G.; Galgaro, A.; Atzeni, C. (2006). Advances in ground based microwave interferometry for landslide survey: a case study. Int J Remote Sens 27(12):2331 – 2350.

Luzi, G.; Pieraccini, M.; Mecatti, D.; Noferini. L.; Guidi, G.; Moia, F.; Atzeni, C. (2004). Ground-based radar interferometry for landslides monitoring: atmospheric and instrumental decorrelation sources on experimental data. IEEE Trans Geosci Remote Sens 42(11):2454–2466.

Manni, D.M.; Mannelli, A.; Della Tosa, S.; Capponi, G.; Capponi, N. (1733). Cronichette antiche di vari scrittori del buon secolo della lingua toscana. Manni, D.M., (Ed.), Firenze (In Italian).

Mansour, M. F.; Morgenstern, N. R.; Martin, C. D. (2011). Expected damage from displacement of slow-moving slides. Landslides, 8(1), 117-131.

Margottini, C., and Vilímek, V. (2014). The ICL network on "landslides and cultural & natural heritage (LACUNHEN)". Landslides, 11(5), 933-938.

Marinelli, O. (1921). La carta topografica e lo sviluppo di Firenze. Rivista geografica italiana 28, 18-38 (in Italian).

Martin, O. and Piatti,G. (2009). World Heritage and Buffer Zones. In Proceedings of the International Expert Meeting on World Heritage and Buffer Zones, Davos, Switzerland, 11–14 March 2008; UNESCO World Heritage Center: Paris, France. Available online: http://whc.unesco.org/en/series/25/ (accessed on 29 January 2018).

Massonnet, D., and Feigl, K. L. (1998). Radar interferometry and its application to changes in the Earth's surface. Reviews of geophysics, 36(4), 441-500.

Montuori, A.; Luzi, G.; Stramondo, S.; Casula, G.; Bignami, C.; Bonali, E.; Bianchi, M. G.; Crosetto, M. (2014). Combined use of ground-based systems for Cultural Heritage conservation monitoring. In Geoscience and Remote Sensing Symposium (IGARSS), IEEE International (pp. 4086-4089).

Morelli, S.; Battistini, A.; Catani, F. (2014). Rapid assessment of flood susceptibility in urbanized rivers using digital terrain data: Application to the Arno river case study (Firenze, northern Italy). Appl. Geogr. 54, 913, 35-53. Doi: https://doi.org/10.1016/j.apgeog.2014.06.032.

Morelli, S.; Segoni, S.; Manzo, G.; Ermini, L.; Catani, F. (2012). Urban planning, flood risk and public policy: the case of the Arno River, Firenze, Italy. Appl. Geogr. 34, 205-218. Doi: http://dx.doi.org/10.1016/j.apgeog.2011.10.020.

Morelli, S.; Pazzi, V.; Tanteri, E.; Nocentini, M.; Lombardi, L.; Gigli, G; Casagli. N. (2018). UNESCO World Heritage Sites coexisting with riverbank landslides: the challenge of conservation from past to future. (In preparation).

Moretti, S. and Rodolfi, G. (2000). A typical "calanchi" landscape on the Eastern Apennine margin (Atri, Central Italy): geomorphological features and evolution. Catena, 40(2), 217-228.

Morozzi, F. (1762). Dello Stato antico e moderno dell'Arno e delle cause e de' rimedi delle sue inondazioni. Ragionamento istorico-matematico, G.B. Stecchi, Firenze, Italy (in Italian).

Navrud, S. and Ready, R. C. (2002). Valuing cultural heritage: Applying environmental valuation techniques to historic buildings, monuments and artifacts. Edward Elgar Publishing.

Nencini, F. (1966). Firenze i giorni del diluvio, Sansoni Editore, Firenze, pp. 9-19 (in Italian).

Nolesini, T.; Frodella, W.; Bianchini, S.; Casagli, N. (2016). Detecting slope and urban potential unstable areas by means of multi-platform remote sensing techniques: The Volterra (Italy) case study. Remote Sens., 8, 1-18.

Ottati, D. (1992) - L'acquedotto di Firenze dal 1860 ad oggi –Edizioni Il Vantaggio; pp71-98. (In Italian).

Pandeli, E. (2008). La pianura di Firenze-Prato-Pistoia nel quadro dell'evoluzione geologica dell'Appennino settentrionale. Conference Proceedings "Un piano per la Piana: idee e progetti per un parco", 9-10 May 2008, Scientific and Technological Pole of Sesto Fiorentino, University of Firenze (in Italian).

Pastonchi, L.; Barra, A.; Monserrat, O.; Luzi, G.; Solari, L.; & Tofani, V. (2018). Satellite Data to Improve the Knowledge of Geohazards in World Heritage Sites. Remote Sensing, 10(7), 992.

Pavlova, I.; Makarigakis, A.; Depret, T.; Jomelli, V. (2017). Global overview of the geological hazard exposure and disaster risk awareness at World Heritage Sites. J. Cult. Her., 28, 151-157, ISSN 1296-2074, DOI. Available online: https://doi.org/10.1016/j.culher.2015.11.001.

Pedersen A. (2002). Managing Tourism at World Heritage Sites: a Practical Manual for World Heritage Site Managers. UNESCO, World Heritage Center, Paris.

Peduto, D.; Cascini, L.; Arena, L.; Ferlisi, S.; Fornaro, G.; Reale, D. (2015). A general framework and related procedures for multiscale analyses of DInSAR data in subsiding urban areas. ISPRS J. Photogr. Remote Sens., 105, 186-210.

Poggi, G. (1882). Sui lavori per l'ingrandimento di Firenze. Relazione (1864-1877), Barbera Edizioni, Firenze, Italy (In Italian).

Pratesi, F.; Nolesini, T.; Bianchini, S.; Leva, D.; Lombardi, L.; Fanti, R.; Casagli, N. (2015a). Early warning GBInSAR-based method for monitoring Volterra (Tuscany, Italy) city walls. IEEE Journal of Selected Topics in Applied Earth Observations and Remote Sensing, 8(4), 1753-1762.

Pratesi, F.; Tapete, D.; Del Ventisette, C.; Moretti, S. (2016). Mapping interactions between geology, subsurface resource exploitation and urban development in transforming cities using InSAR Persistent Scatterers: Two decades of change in Florence, Italy. Appl. Geogr. 77, 20–37.

Pratesi, F.; Tapete, D.; Terenzi, G.; Del Ventisette, C.; Moretti, S. (2015b). Rating health and stability of engineering structures via classification indexes of InSAR Persistent Scatterers. Int. J. App. Earth Obs.Geoinf., 40, 81-90.

Principe I. and Sica P. (1967). L'inondazione di Firenze del 4 Novembre 1966, l'Universo n°2, pp. 192-211 (in Italian).

Raspini, F.; Bardi, F.; Bianchini, S.; Ciampalini, A.; Del Ventisette, C.; Farina, P., Ferrigno, F.; Solari, L.; Casagli, N. (2016). The contribution of satellite SAR-derived displacement measurements in landslide risk management practices. Nat. Haz., 86, 327-351.

Raspini, F.; Bianchini, S.; Ciampalini, A.; Del Soldato, M.; Solari, L.; Novali, F.; Del Conte, S.; Rucci, A.; Ferretti, A.; Casagli, N. (2018). Continuous, semi-automatic monitoring of ground deformation using Sentinel-1 satellites. Sci. Rep. 8, 7253.

Ricci Lucchi F. and Ori G.G. (1985). Field excursion D: Synorogenic deposits of a migratine basin system in the NW adriatic foreland: Examples from Emilia-Romagna region, Northern Appennines. In international Symposum on Foreland Basins. Fribourg Guidebook. Edited by Ph. Allen, P. Homewood & G. Williams, 137 – 176.

RIEGL (2010a). Data sheet of long range & high accuracy 3D terrestrial laser scanner LMS-Z420i. http://www.riegl.com/uploads/tx_pxpriegldownloads/10_DataSheet_Z420i_03-05-2010.pdf

RIEGL (2010b). Operating & processing software RiSCAN PRO for RIEGL 3D laser scanners. Available from: http://www.riegl.com/products/software-packages/riscan-pro/

Rosen P.A.; Hensley S.; Joughin I.R.; Li F.K., Madsen S.N.; Rodriguez E.; Goldstein R.M. (2000) - Synthetic aperture radar interferometry. Proc. I.E.E.E. 88 (3). 333-382.

Rosi, A.; Segoni, S.; Catani, F.; Casagli, N. (2012). Statistical and environmental analyses for the definition of a regional rainfall threshold system for landslide triggering in Tuscany (Italy). J. Geograph. Scie., 22, 617-629.

Rosi, A.; Tofani, V.; Agostini, A.; Tanteri, L.; Tacconi Stefanelli, C.; Catani, F.; Casagli, N. (2016). Subsidence mapping at regional scale using persistent scatters interferometry (PSI): The case of Tuscany region (Italy). Int. J. App. Earth Obs. and Geoinf.,52, 328-337.

Rosi, A.; Tofani, V.; Tanteri, L.; Tacconi Stefanelli, C.; Agostini, A.; Catani, F.; Casagli, N. (2018). The new landslide inventory of Tuscany (Italy) updated with PS-InSAR: geomorphological features and landslide distribution. Lands., 15, 1-15. DOI Available at: https://doi.org/10.1007/s10346-017-0861-4

Scampoli, E. (2003). Evoluzione urbanistica di Firenze nel Medioevo. La realizzazione di un GIS per lo studio di Firenze medievale (In Italian).

Shan J. and Toth K. (2008) Topographic laser ranging and scanning: principles and processing. CRC Press, Taylor & Francis Group, LLC, UK.

Showstack, R. (2014). Sentinel satellites initiate new era in earth observation. Eos Trans. Am. Geophys. Union, 95, 239–240.

Solari L. (2017). Spaceborne radar remote sensing: hydrogeological events monitoring and future developments. Unpublished PhD thesis, University of Pisa, Italy.

Solari, L.; Barra, A.; Herrera, G.; Bianchini, S.; Monserrat, O.; Béjar-Pizarro, M.; Crosetto, M.; Sarro, R.; Moretti, S. (2018). Fast detection of ground motions on vulnerable elements using Sentinel-1 InSAR data. Geom., Nat. Haz. and Risk, 9, 152-174.

Solari, L.; Ciampalini, A.; Raspini, F.; Bianchini, S.; Zinno, I.; Bonano, M.; Manunta, M.; Moretti, S.; Casagli, N. (2017). Combined use of C-and X-Band SAR data for subsidence monitoring in an urban area. Geosciences, 7, 21.

Spennemann, D. H. and Graham, K. (2007). The importance of heritage preservation in natural disaster situations. International Journal of Risk Assessment and Management, 7(6-7), 993-1001.

Spizzichino, D.; Leoni, G.; Comerci, V.; Brustia, E.; Guerrieri, L.; Dessi, B.; Trigila, A.; Iadanza, C. (2016). PROTHEGO Deliverable D.01.01: UNESCO Cultural Heritage Vs Natural hazards at European scale, Version 1.0. JPICH Heritage Plus PROTHEGO project, Open Report, pp. 30. Available at: http://www.prothego.eu/

Taboroff, J. (2000). Cultural heritage and natural disasters: incentives for risk management and mitigation. Managing Disaster Risk in Emerging Economies. New York: World Bank. Disaster Management Risk, 2, 71-79.

Tang, P.; Chen, F.; Zhu, X.; Zhou, W. (2016). Monitoring cultural heritage sites with advanced multi-temporal InSAR technique: The case study of the Summer Palace. Remote Sensing, 8, 1-15.

Tapete, D. and Cigna, F. (2017b). InSAR data for geohazard assessment in UNESCO World Heritage sites: State-of-the-art and perspectives in the Copernicus era. Int. J. of App. Earth Obs. and Geoinf., 63, 24-32.

Tapete, D., and Cigna, F. (2012). Rapid mapping and deformation analysis over cultural heritage and rural sites based on Persistent Scatterer Interferometry. International Journal of Geophysics.

Tapete, D., and Cigna, F. (2017a). Trends and perspectives of space-borne SAR remote sensing for archaeological landscape and cultural heritage applications. Journal of Archaeological Science: Reports, 14, 716-726.

Tapete, D.; Casagli, N.; Luzi, G.; Fanti, R.; Gigli, G.; Leva, D. (2013). Integrating radar and laser-based remote sensing techniques for monitoring structural deformation of archaeological monuments. Journal of Archaeological Science, 40(1), 176-189.

Tapete, D.; Fanti, R.; Cecchi, R.; Petrangeli, P.; Casagli, N. (2012). Satellite radar interferometry for monitoring and early-stage warning of structural instability in archaeological sites. J. Geophys. Eng, 9, 10-25.

Tarchi, D.; Casagli, N.; Fanti, R.; Leva, D.; Luzi, G.; Pasuto, A.; Pieraccini, M.; Silvano, S. (2003) Landslide monitoring by using ground-based SAR interferometry: an example of application to the Tessina landslide in Italy. Eng Geology 68(1 – 2).

Tarchi, D.; Rudolf, H.; Pieraccini, M; Atzeni, C. (2000). Remote monitoring of buildings using a ground-based SAR: application to cultural heritage survey. International Journal of Remote Sensing, 21(18), 3545-3551.

Teatini, P.; Tosi, L.; Strozzi, T.; Carbognin, L.; Cecconi, G.; Rosselli, R.; Libardo, S. (2012). Resolving land subsidence within the Venice Lagoon by persistent scatterer SAR interferometry. Phys Chem Earth Parts A/B/C 40–41:72–79. doi:10.1016/j.pce.2010.01.002

Themistocleous, K.; Cuca, B.; Agapiou, A.; Lysandrou, V.; Tzouvaras, M.; Hadjimitsis, D. G.; Kyriakides, P.; Kouhartsiouk, D.; Margottini, C.; Spizzichino, D.; Cigna, F.; Crosta, G.; Frattini, P.; Fernandez Merodo, J. A. (2016). The protection of cultural heritage sites from geo-Hazards: the PROTHEGO project. In Euro-Mediterranean Conference (pp. 91-98). Springer, Cham.

Tofani, V.; Raspini, F.; Catani, F.; Casagli, N. (2013). Persistent Scatterer Interferometry (PSI) technique for landslide characterization and monitoring. Remote Sens., 5, 1045-1065. DOI:10.3390/rs5031045

Tomás, R.; Romero, R.; Mulas, J.; Marturià, J.J.; Mallorquí, J.J.; Lopez-Sanchez, J.M.; Herrera, G.; Gutiérrez, F.; González, P.J.; Fernández, J.; et al. (2014). Radar interferometry techniques for the study of ground subsidence phenomena: A review of practical issues through cases in Spain. Environ. Earth Sci., 71, 163–181.

Tosi, L.; Teatini, P.; Strozzi, T.; Carbognin, L.; Brancolini, G.; Rizzetto, F. (2010). Ground surface dynamics in the northern Adriatic coastland over the last two decades. Rend Fis Acc Lincei 21(Suppl 1):S115–S129. doi:10.1007/s12210-010-0084-2182

UNESCO (1972). Convention concerning the protection of the world cultural and natural heritage: adopted by the General conference at its seventeenth session, Paris, 16 November 1972. Available online: https://whc.unesco.org/en/conventiontext/.

UNESCO (2010). UNESCO at a galance. UNESCO, World Heritage Center, Paris. Available online: http://www.unesco.org/new/en/unesco/about-us/who-we-are/history/milestones/.

UNESCO (2013). Managing Cultural World Heritage. World Heritage Center, Paris. ISBN 978-92-3-001223-6

UNESCO (2017). Operational Guidelines for the Implementation of the World Heritage Convention. Update of 12 July 2017. UNESCO, World Heritage Centre, Paris. Available online: https://whc.unesco.org/en/guidelines/

Vacca, G.; Deidda, M.; Dessi, A.; Marras, M. (2012). Laser scanner survey to cultural heritage conservation and restoration. International Archives of the Photogrammetry, Remote Sensing and Spatial Information Sciences, 39(B5), 589-594.

Vai, G.B. and Martini, I.P. (2001). Anatomy of an Orogen: the Apennines and adjacent Mediterranean basins. Kluver Academic Publishers, Dortdrecht, 2001, 632pp.

Valli, F. M. (1987). Architettura di castelli nell'Appennino reggiano. Aedes Muratoriana. (In Italian).

Vergari, F.; Della Seta, M.; Del Monte, M.; Fredi, P.; Palmieri, E. L. (2011). Landslide susceptibility assessment in the Upper Orcia Valley (Southern Tuscany, Italy) through conditional analysis: a contribution to the unbiased selection of causal factors. Natural Hazards and Earth System Sciences, 11(5), 1475.

Villani, G (1845). Cronica – a cura di Gherardi Dragomanni, Vol I, Firenze, Coen; pp 430 (in Italian).

Vlcko, J. (2004). Extremely slow slope movements influencing the stability of Spis Castle, UNESCO site. Landslides, 1(1), 67-71. DOI. Available online: https://doi.org/10.1007/s10346-003-0007-8

Will, T. and Meier, H. R. (2007). Cultural heritage and natural disasters: risk preparedness and the limits of prevention. Cultural Heritage and Natural Disasters Risk Preparedness and the Limits of Prevention: Heritage at Risk, Special Edition, 9-20.

Zebker, H. A. and Villasenor, J. (1992). Decorrelation in interferometric radar echoes. IEEE Transactions on geoscience and remote sensing, 30(5), 950-959.

Zhou, W.; Chen, F.; Guo, H. (2015). Differential radar interferometry for structural and ground deformation monitoring: a new tool for the conservation and sustainability of cultural heritage sites. Sustainability, 7(2), 1712-1729.